

Cooperative agreement

No. DTFH61-99-X-00104

Intelligent Vehicle Initiative (IVI) Field Operational Test Program

Final Report

Volume 3 of 4

**Freightliner Trucks Field Operational Test: The
Freightliner/Meritor Wabco Roll Stability
Advisor and Control at Praxair**

By

**Chris Kirn, Steve Wreggit, Thomas Connolly, Jamie Gertsch, Andrew
McLandress, Seth Rogers, and Markus Spitzer
Vehicle Systems Technology Center**

For

**U.S. Department of Transportation
Federal Highway Administration
Washington, D.C.**

September 25, 2002



Table of Contents

1	THE VSTC ROLE IN THE RA&C PROJECT	1
1.1	Human Factors Aspects of the Roll Stability Advisor & Control System	1
1.2	Theoretical Rollover Warning Effectiveness – Task 20	1
1.3	Evaluation of the Lane Guidance™ System – Task 21	2
1.4	The Vehicle Systems Technology Center, a division of DaimlerChrysler Research and Technology North America.....	2
2	HUMAN FACTORS ASPECTS OF THE ROLL STABILITY ADVISOR & CONTROL (RA&C) SYSTEM	4
2.1	General RA&C System Description and Background	4
2.2	Roll Stability Advisor Characteristics	5
2.3	Hard Braking Event Detection Characteristics	10
2.4	Roll Stability Control Characteristics.....	11
2.5	Leg and Trip Related Information.....	12
2.6	System Startup and Fault Messaging.....	13
3	THEORETICAL ROLLOVER WARNING EFFECTIVENESS – TASK 20 ...	15
3.1	A Predictive Rollover Warning System	15
3.2	Average Velocity Histories for Hotspots 1 and 2	16
3.3	Multi-body Dynamics Analysis of the FOT Vehicles.....	22
3.3.1	<i>Physical Vehicle</i>	<i>22</i>
3.3.2	<i>Simulation Models and Inputs.....</i>	<i>24</i>
3.3.3	<i>Simulation Model Correlation and Validation.....</i>	<i>34</i>
3.3.4	<i>Results and Analysis.....</i>	<i>41</i>
3.3.5	<i>Summary and Conclusions.....</i>	<i>59</i>
3.3.6	<i>Further Work and Recommendations</i>	<i>60</i>
3.4	Evaluation of a Rollover Warning Capability	60
3.4.1	<i>Statistical Analysis</i>	<i>60</i>
3.4.2	<i>Rollover Warning Components</i>	<i>64</i>
3.4.3	<i>Vehicle Velocity Prediction.....</i>	<i>70</i>
3.4.4	<i>Intervention Timing.....</i>	<i>70</i>
3.4.5	<i>Rollover Warning Theoretical Results.....</i>	<i>71</i>
3.4.6	<i>Vehicle Velocity Prediction Evaluation</i>	<i>75</i>
3.4.7	<i>Complete System Evaluation.....</i>	<i>78</i>
3.4.8	<i>Conclusions</i>	<i>79</i>
4	EVALUATION OF THE LANE GUIDANCE™ SYSTEM	81
4.1	Introduction.....	81
4.2	The Lane Guidance™ System.....	82
4.3	Data Structure.....	83
4.4	Performance Evaluation.....	84
4.4.1	<i>Overall tracking performance.....</i>	<i>84</i>
4.4.2	<i>Performance Dependent upon Daytime</i>	<i>84</i>

4.4.3	<i>Performance dependent upon weather conditions</i>	87
4.4.4	<i>Performance dependent upon vehicle speed</i>	88
4.4.5	<i>Performance dependent upon cruise control state</i>	88
4.4.6	<i>Performance during lane change maneuvers</i>	89
4.5	Warning Situations	93
4.6	Summary and Conclusions	94
5	REFERENCES	96

List of Figures

Figure 2-1: Centrally Located Message Center	4
Figure 2-2: Message Center location, message center keys and the RSC indicator lamp location and telltale symbol	5
Figure 2-3: RSA System Operation - Desired Driving Range.....	6
Figure 2-4: RSA System Operation - Level One Event.....	7
Figure 2-5: RSA System Operation - Level Two Event	8
Figure 2-6: RSA System Operation - Level Three Event	9
Figure 2-7: Hard Braking Event Detector (HBED) Messages and Tone.....	10
Figure 2-8: Roll Stability Control (RSC) and Automatic Traction Control (ATC) messaging and activation event explanation	11
Figure 2-9: Leg and Trip Displays.....	12
Figure 2-10: RA&C System Startup and System Description.....	13
Figure 2-11: RA&C System Fault Message with Operating Characteristics	14
Figure 3-1: Average Vehicle Speed through Hotspot 1 for both Phases 1 and 2 with the location of the RSA Advisories (Warnings), entire length of the curve	18
Figure 3-2: Average Vehicle Speed through Hotspot 1 for both Phases 1 and 2 with the location of the RSA Advisories (Warnings), curve between 690 & 730 meters	19
Figure 3-3: Average Vehicle Speed through Hotspot 1 for both Phases 1 and 2 with the location of the RSA Advisories (Warnings), curve between 950 & 1000 meters	19
Figure 3-4: Average Vehicle Speed through Hotspot 2 for both Phases 1 and 2 with the location of the RSA Advisories (Warnings), entire length of the curve	20
Figure 3-5: Average Vehicle Speed through Hotspot 2 for both Phases 1 and 2 with the location of the RSA Advisories (Warnings), curve between 660 & 720 meters	21
Figure 3-6: Average Vehicle Speed through Hotspot 2 for both Phases 1 and 2 with the location of the RSA Advisories (Warnings), curve between 900 & 960 meters	21
Figure 3-7: Oblique view of the UMTRI test vehicle.....	23
Figure 3-8: Side view of the UMTRI test vehicle.....	23
Figure 3-9: Example speed profile comparing the vehicle speed sensor data with GPS speed data	27
Figure 3-10: Aerial photograph of hotspot 1	29
Figure 3-11: Hotspot 1 road data	31
Figure 3-12: Three dimensional road reproduction of hotspot 1	31
Figure 3-13: Aerial photograph of hotspot 2	32
Figure 3-14: Hotspot 2 road data	33
Figure 3-15: Three dimensional road reproduction of hotspot 2	33
Figure 3-16: Input deviations of the simulation models for the hotspot 1 example trip..	35

Figure 3-17: Input deviations of the simulation models for the hotspot 2 example trip..	35
Figure 3-18: Sensor comparisons of the simulation models for the hotspot 1 example trip	36
Figure 3-19: Sensor comparisons of the simulation models for the hotspot 2 example trip	36
Figure 3-20: Axle wheel loads comparisons of the simulation models for the hotspot 1 example trip.....	37
Figure 3-21: Axle wheel loads comparisons of the simulation models for the hotspot 2 example trip.....	37
Figure 3-22: Path of the FOT vehicle and simulation models for the hotspot 1 example trip	39
Figure 3-23: Truncated path of the FOT vehicle and simulation models for the hotspot 2 example trip.....	39
Figure 3-24: Sensor comparisons of the FOT vehicle and simulation models for the hotspot 1 example trip.....	40
Figure 3-25: Sensor comparisons of the FOT vehicle and simulation models for the hotspot 2 example trip.....	40
Figure 3-26: Nonlinear relationship between payload percentage and center of gravity height for the tanker semitrailer	42
Figure 3-27: DADS tilt table tests of a vehicle with fixed and sloshing payloads and with different liftoff criteria	44
Figure 3-28: Comparison of tilt table test results for axle liftoff conditions	44
Figure 3-29: An example of speed scaling	45
Figure 3-30: Locations of wheel liftoff for all payloads for hotspot 1 example.....	47
Figure 3-31: Locations of wheel liftoff for all payloads for hotspot 2 example.....	47
Figure 3-32: Critical curvature and speed as a function of payload for hotspot 1 example	49
Figure 3-33: Critical curvature and speed as a function of payload for hotspot 2 example	49
Figure 3-34: Critical accelerations as a function of payload for hotspot 1 example	50
Figure 3-35: Critical accelerations as a function of payload for hotspot 2 example	50
Figure 3-36: Critical accelerations as a function of center of gravity height for hotspot 1 example	51
Figure 3-37: Critical accelerations as a function of center of gravity height for hotspot 2 example	51
Figure 3-38: Critical accelerations as a function of center of gravity height for all hotspot 1 trips.....	53
Figure 3-39: Critical accelerations as a function of center of gravity height for all hotspot 2 trips.....	53

Figure 3-40: Critical vehicle speeds as a function of center of gravity height for all hotspot 1 and 2 trips	54
Figure 3-41: Critical accelerations as a function of center of gravity height for static and dynamic rollover simulation results	55
Figure 3-42. Axle wheel load transfer of trip 939 (hotspot 2) with fixed and sloshing loads.	56
Figure 3-43. Semitrailer center of gravity roll angle with fixed and sloshing loads (hotspot 2).	57
Figure 3-44. Semitrailer center of gravity roll angle for a fixed load, flat road case and a sloshing load, banked road case compared to the road bank angle.....	58
Figure 3-45. Semitrailer axle loads of the most realistic model and the flat road, bracket load model.	59
Figure 3-46: RSA frequency by road class. High RSA scores are much more common for ramps.	61
Figure 3-47: RSA score for Hotspot 1. 100% means a likely rollover. 75% leads to an RSA warning.	62
Figure 3-48: Speed for Hotspot 1. The traces that got a warning are towards the top of the distribution all the way through the segment	63
Figure 3-49: Mass distribution. The traces that got a warning are towards the top of the mass distribution as well.	63
Figure 3-50: Safe Velocity curve Calculation using only current road information based on the instantaneous safe speed approach	65
Figure 3-51: Hotspot 1 road information. Top plot shows overhead view and bottom plot shows curvature.....	68
Figure 3-52: The desired velocity and individual cost function terms for each point during the maneuver. Four sets of data are shown from the 15 performed iterations. The legend indicates the color of each iteration.....	69
Figure 3-53: Total cost for the maneuver through hotspot 1 at each iteration.....	69
Figure 3-54: Predictive Safe Speed simulation results for hotspot 1. $a_{max} = 2.0 \text{ m/(s*s)}$, $v_{des} = 20 \text{ m/s}$, low K_{fuel} value.	72
Figure 3-55: Predictive Safe Speed simulation results for hotspot 1 $a_{max}=2.0 \text{ m/(s*s)}$, $v_{des}=20 \text{ m/s}$, high K_{fuel} value.	72
Figure 3-56: Predictive Safe Speed simulation results for hotspot 1. $a_{max}=2.25 \text{ m/(s*s)}$, $v_{des} = 20 \text{ m/s}$, high K_{fuel} value.	74
Figure 3-57: Overhead view of hotspot 2.	75
Figure 3-58: Predictive Safe Speed simulation results for hotspot 2. $a_{max} = 2.0 \text{ m/(s*s)}$, $v_{des} = 20 \text{ m/s}$, high K_{fuel} value.	75
Figure 3-59: Speed predictions from all 4 models on a pass over hotspot 1.	76
Figure 3-60: Performance on hotspot 1.	77
Figure 3-61: Performance on hotspot 2	77

Figure 4-1: The Lane Guidance™ windshield mounted camera and additional CPU (both shown in corner) process forward viewing images of the lane markings to detect if the vehicle is drifting out of the lane of travel	82
Figure 4-2: Total number of recorded status bytes on an hourly basis for all tractors from February 1, 2001 to May 18, 2001	83
Figure 4-3: Total number of tracking events for all tractors on an hourly basis in February 2001	85
Figure 4-4: Daily average percentage of tracking for tractors 1, 2, 3, and 5 on an hourly basis in February 2001	85
Figure 4-5: Monthly average percentage of improved tracking during night period compared to day period.....	86
Figure 4-6: Comparison of daily average tracking performance on an hourly basis in February 2001 and May 2001	87
Figure 4-7: Average cruise control usage dependent upon 24-hour day period, only considering Tractor 1 Vehicle Speeds > 90 kph (November 2000 – June 2001)	89
Figure 4-8: Typical Lane Change Maneuver Data History, Tractor 1, Trip 16.....	90
Figure 4-9: Lane Change Maneuver with detection delay, Tractor 1, Trip 552	91
Figure 4-10: Double Lane Change Maneuver, Tractor 3, Trip 43.....	92
Figure 4-11: Typical Lane Departure Situation, Tractor 1, Trip 135	93
Figure 4-12: Daily Average Warning Situations on an hourly basis, all tractors, from February 2001 to June 2001	94

List of Tables

Table 3-1: Vehicle geometric properties.....	24
Table 3-2: Vehicle inertial properties of the STARCAT and DADS models.....	25
Table 3-3: List of selected trips	28
Table 3-4: Hotspot 1 road data (Wolfe, 2002).....	29
Table 3-5: Summary of tilt table tests.....	45
Table 3-6: Relationship between critical lateral accelerations and semitrailer center of gravity height	52
Table 4-1: Lane Tracker Status Bits	83
Table 4-2: Average Percentage of Tracking Performance per Day Reported on a Monthly Basis	84
Table 4-3: Weather-Dependent Tracking Performance for Tractors 1 & 2.....	88
Table 4-4: Tracking Performance dependent upon Vehicle Speed in kilometers per hour (kph).....	88
Table 4-5: Status Byte Combinations describing a Warning Situation	93

1 The VSTC Role in the RA&C Project

The Vehicle Systems Technology Center (VSTC), a division of DaimlerChrysler Research and Technology North America (DCRTNA), has contributed to Freightliner's Field Operational Test (FOT) on the Rollover Stability Advisor and Control (RA&C) system. This project has been performed as part of the United States Department of Transportation's (USDOT) Intelligent Vehicle Initiative (IVI). The VSTC has benefited from this project in many ways throughout the course of the three-year FOT. The main contributions can be grouped into three general areas: in-vehicle human factors, vehicle rollover and lane guidance. This report describes the outcome of the VSTC's participation in the RA&C project with regards to the three topic areas. This report is separated into chapters with each chapter being devoted exclusively to the different individual topics.

1.1 Human Factors Aspects of the Roll Stability Advisor & Control System

This chapter summarizes the human factors aspects for the Roll Stability Advisor & Control system. It describes the driver messaging and tones for the Roll Stability Advisor (RSA), the Roll Stability Control (RSC) and the Hard Braking Event Detection (HBED) systems. Each portion of the RA&C system is defined and the methodology for developing the associated message center text is explained.

1.2 Theoretical Rollover Warning Effectiveness – Task 20

In this chapter, the concept of a predictive rollover warning system is introduced. First, a vehicle speed analysis is presented based on the FOT data for the two geographical locations that produced the most RSA advisories during Phase 2, referred to as Hotspots and originally identified by UMTRI. Next, a detailed dynamic analysis of these two hotspots is performed. This is achieved by applying multi-body dynamics simulations to the Praxair tractor-semitrailer combination to better understand the physical behavior of the combination vehicle as well as the driver input that produced each maneuver within the limits of the road geometry. The simulation results are then used to produce vehicle specific and maneuver specific dynamic rollover characteristics that accurately capture the essential elements of vehicle rollover. The intention of this study is to answer the question: What information is necessary to accurately predict combination vehicle rollover? Information gained through this analysis is used to better understand the requirements for a predictive system.

Next, the concept of extending the Rollover Stability Advisor to a proactive Rollover Warning System is described. It discusses results from a preliminary statistical analysis to understand the characteristics of rollover events as well as addresses the methodology and requirements of a Rollover Warning System. A demonstration of the predictive rollover-warning algorithm is performed for hotspots 1 and 2 as a proof of concept, based on data collected during the FOT. Finally the chapter closes with prospects for deployment of a Rollover Warning System.

1.3 Evaluation of the Lane Guidance™ System – Task 21

This chapter addresses the analysis of the data collected by the Lane Guidance™ system as part of Task 21 of the Field Operational Test. The goal of this investigation was to understand the performance of the system under different environmental conditions such as rain, snow and nighttime/daytime. Additionally, the data were used to identify characteristics for potential warning scenarios, as well as lane change maneuvers in order to better understand the overall system capabilities and performance.

Data collected by the Praxair tractors from November 2000 to June 2001 relevant to the Lane Guidance™ system were analyzed. The results showed that the Lane Guidance™ system performed best when the driver was potentially at the least attentive, during the night and early morning hours with cruise control engaged at highway speeds, with dry conditions.

1.4 The Vehicle Systems Technology Center, a division of DaimlerChrysler Research and Technology North America

DaimlerChrysler Research and Technology North America, Inc. (DCRTNA) is a wholly-owned subsidiary of DaimlerChrysler. DaimlerChrysler is determined to be among the first to understand the shape of the automotive future, and to use technology to make our world safer, healthier, more convenient, and better informed. Through advanced research, forging project partnerships with local researchers and companies, hosting scientists from other DaimlerChrysler laboratories and fostering relevant research with world leading Universities and Institutions, DCRTNA is a successful symbol of research globalization within DaimlerChrysler.

DaimlerChrysler Research and Technology North America, Inc. is located along the West Coast of the United States in the form of two Research and Technology Centers and a Fuel Cell Partnership Office with each unit having a special strategic mission. The Vehicle Systems Technology Center (VSTC) in Portland is co-located at the Freightliner Headquarters with the charter to do research and develop technologies of direct value to DaimlerChrysler's trucking business. The Research and Technology Center (RTC) in Palo Alto is located in the heart of the Silicon Valley and is the largest part of DCRTNA. It has the mission to build upon the innovative scientific communities, technology and business environment of Silicon Valley. DCRTNA in West Sacramento is a founding member of the California Fuel Cell Partnership. It serves as a testing ground for advanced fuel cell technology in DaimlerChrysler vehicles in North America

The VSTC has a very strong partnership with Freightliner that is emphasized by its location within the Freightliner headquarters. It is a symbiotic relationship that assists to bridge the gap between long-term research goals and medium- to short-term product development. The VSTC is composed of four teams: Systems Development and Application, Simulation, Usability and Customer Acceptance, and Systems Interface Design.

The *System Development and Application Team* conducts research and develops systems to improve the safety and fuel efficiency of heavy-duty vehicles. Emphasis is placed on

using new in-vehicle technologies such as telematics, vision systems, and radar. Simulation environments are used to develop and test systems and algorithms, which are then tested and further developed in an experimental vehicle.

The *Simulation Team* conducts virtual testing and investigation of complex mechanical systems in simulation environments. This enables our engineers to predict the behavior of their designs as well as to analyze overall system performance prior to the existence of any hardware. This approach is advantageous in bringing products to market quickly and cost-effectively through reduced development cycle time, improved product quality and comfort, and reduced hardware costs for both prototypes and series production.

The *Usability and Customer Acceptance Team* aims to optimize usability, safety, and efficiency. In the context of a driving environment, this means identifying and accommodating the needs, capabilities, and preferences of the driving population. Our research and design process is iterative, alternating between the implementation of human factors design principles and user testing within the target population. This approach is also followed in developing automotive-related software applications, such as service and diagnostics tools for technicians.

The *Systems Interface Design Team* conducts research on vehicle systems development and simulation with an emphasis on heavy trucks. Special attention is paid to the unique requirements set forth by the heavy truck OEM. This includes managing high levels of truck customization and configuration options. We conduct system level simulation to analyze vehicle architecture and cross-functional, multi-technology domains to ensure that integration across modules is maintained. Results pertaining to overall issues such as vehicle performance and efficiency are also addressed.

2 Human Factors Aspects of the Roll Stability Advisor & Control (RA&C) System

This chapter summarizes the human factors aspects for the Roll Stability Advisor & Control (RA&C) system. It describes the driver messaging and tones for the Roll Stability Advisor (RSA), the Roll Stability Control (RSC) and the Hard Braking Event Detection (HBED) systems. Each portion of the RA&C system is defined and the methodology for developing the associated Message Center text is explained.

2.1 General RA&C System Description and Background

The Roll Stability Advisor and Control (RA&C) system is composed of three individual systems: a Roll Stability Advisor (RSA), a Roll Stability Control (RSC) and a Hard Braking Event Detection (HBED). The RSA and HBED systems operate by “sensing” when lateral acceleration or braking “risk” conditions occur and displaying this information to the driver at the end of the event. A succinct overview of the RA&C system can be found in “Freightliner/MeritorWABCO Roll Advisory and Control System,” (Ehlbeck et al., 2000).

The RSA and HBED messages are presented immediately after risky events to train drivers to modify their habits. As drivers experience these messages, they have the opportunity to learn to identify the conditions and maneuvers that led to a possible risky situation with the objective of increasing the probability of avoiding them in the future.



Figure 2-1: Centrally Located Message Center

Human Factors-related design practices played a large part in the design of the driver interface of the RA&C system. Advisory messages are provided to the driver via an alphanumeric driver message display immediately after a rollover-risk maneuver occurs. This message center, shown in Figure 2-1, consists of a vacuum fluorescent display capable of presenting 2 lines of 20 alphanumeric characters. It is centrally located in

front of the driver and placed high in the instrument panel to minimize the glance distance from the roadway and to maximize the drivers' message-detection probability.

In addition to presenting visual information, a buzzer working in concert with the message center has the capability of presenting a high-pitch tone, which can be clearly heard over ambient cabin noise by most drivers.

2.2 Roll Stability Advisor Characteristics

The RSA component of the RA&C system consists of a hierarchy of three messages that can be presented to the driver to indicate the seriousness of a rollover risk event. The level of seriousness of rollover-risk event is communicated to the driver using three methods: specific text, length of alerting tone, and overall length of presentation of the text message. Longer tone durations and overall longer presentation times indicate more serious risks. Short message duration with a brief tone indicates a less critical event.

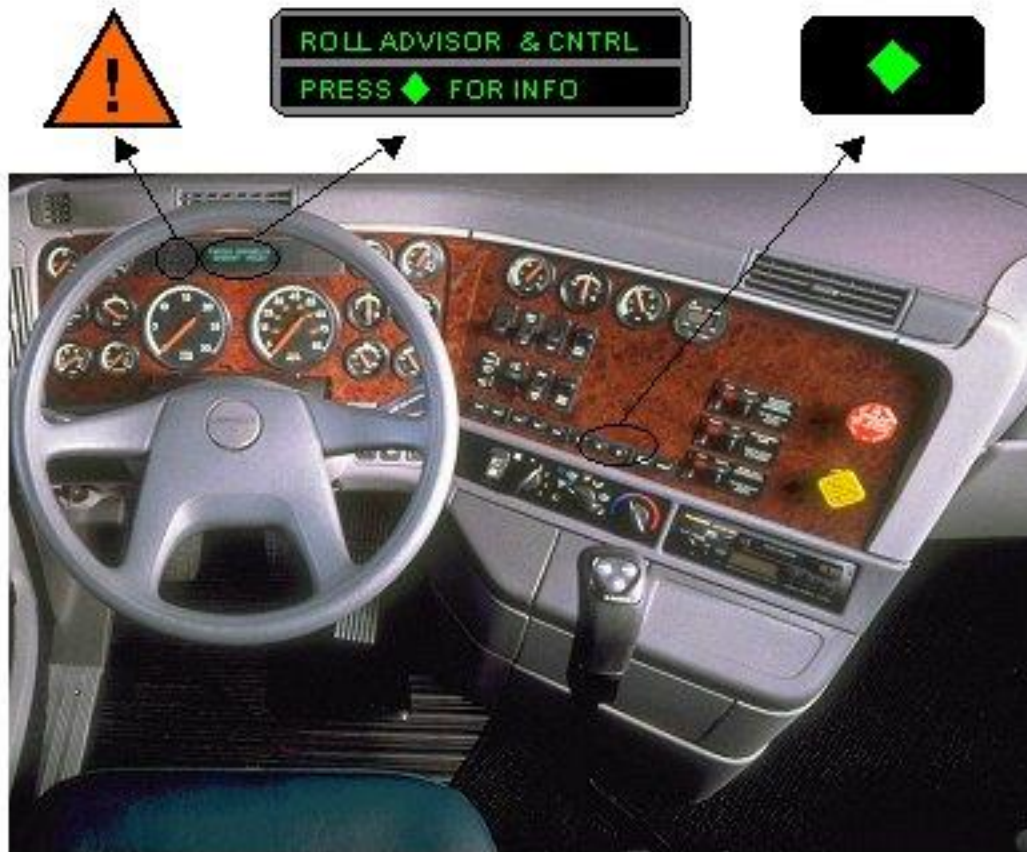
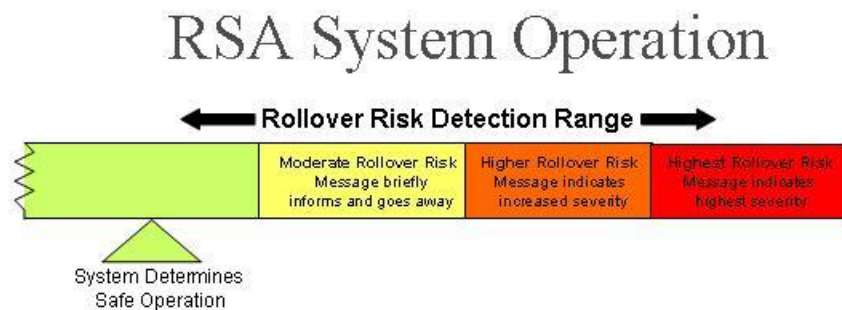


Figure 2-2: Message Center location, message center keys and the RSC indicator lamp location and telltale symbol

Higher levels of rollover risk are accompanied by a specific recommendation of speed reduction. Previous internal research at Freightliner has shown drivers prefer recommendation information consisting of specific real-time values as opposed to generic

messages. Thus, a speed reduction message is provided to the driver that states that the driver should slow down by a specific speed to improve his or her driving and avoid getting such a message in the future. Wording of messages and tone length were tested and altered through an iterative design process. Driver questionnaires were used to collect specific data to better understand and improve the final design (Volume III, Appendix-A). An at-a-glance overview of the displayed messages and their associated specifications is located in Volume III, Appendix-B. Additionally, Volume III, Appendix-C contains a copy of the driver's manual insert pages that were created for the RA&C system as an in-cab reference for the drivers.

Figure 2-3 through Figure 2-6 explain when the scenarios for each of the three levels of RSA messages would be triggered and how they would be displayed to the driver. Figure 2-3 highlights the “desired range” of driving. When the driver is within this range of driving performance, the system is “silent”.



- ◆ No Message is presented to the driver in this zone
- ◆ Value for rollover risk is below level 1 threshold
- ◆ Vehicle operation in this range is desired

Figure 2-3: RSA System Operation - Desired Driving Range

Figure 2-4 shows what the driver will experience after a “Level 1” rollover risk occurs. A message indicating that rollover risk has been detected and that the driver should reduce the vehicle speed by 3 MPH (for example) to avoid similar events in the future. The diamond indicates that the driver can press the diamond key (located on the B-panel) to extinguish the message. Notice that the tone is only ½ second and is primarily for the purpose of getting the driver’s attention. The text message is presented on the display for 8 seconds.

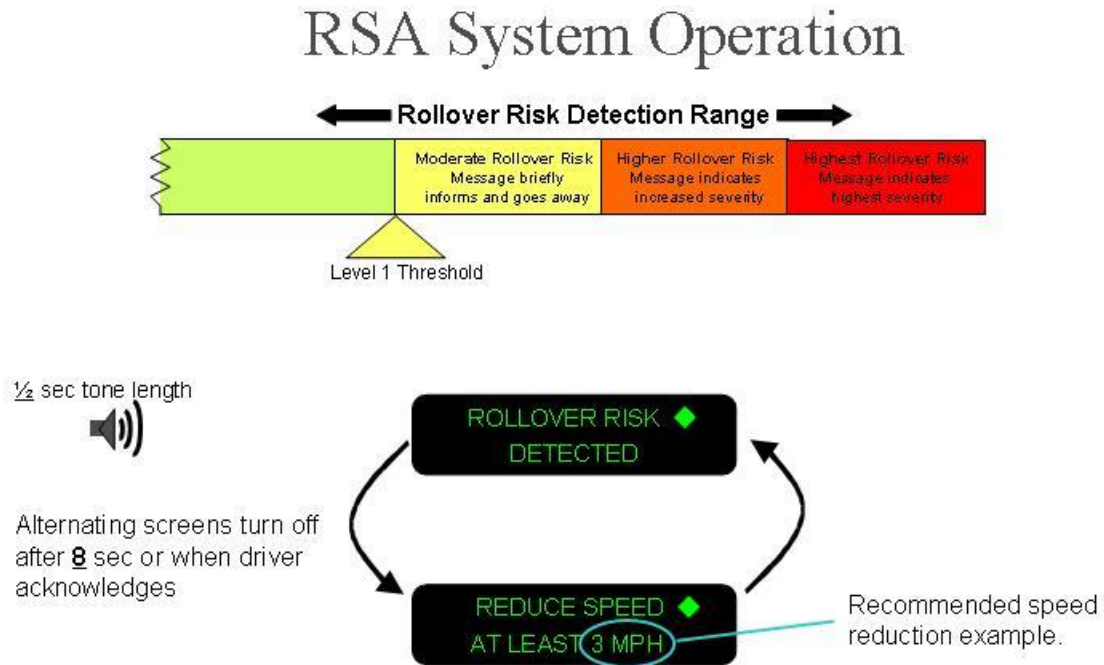


Figure 2-4: RSA System Operation - Level One Event

Figure 2-5 shows what the driver will experience after a “Level 2” rollover risk occurs. A message indicating that a high risk of rollover has been detected and that the driver should reduce the vehicle speed by 5 MPH (for example) to avoid similar events in the future. Notice that the tone is 5 seconds in length and the text message is presented on the display for 14 seconds. The lengthened tone is used to indicate to the driver the increased risk of the event (compared to the Level 1 event that employed a ½ second tone).

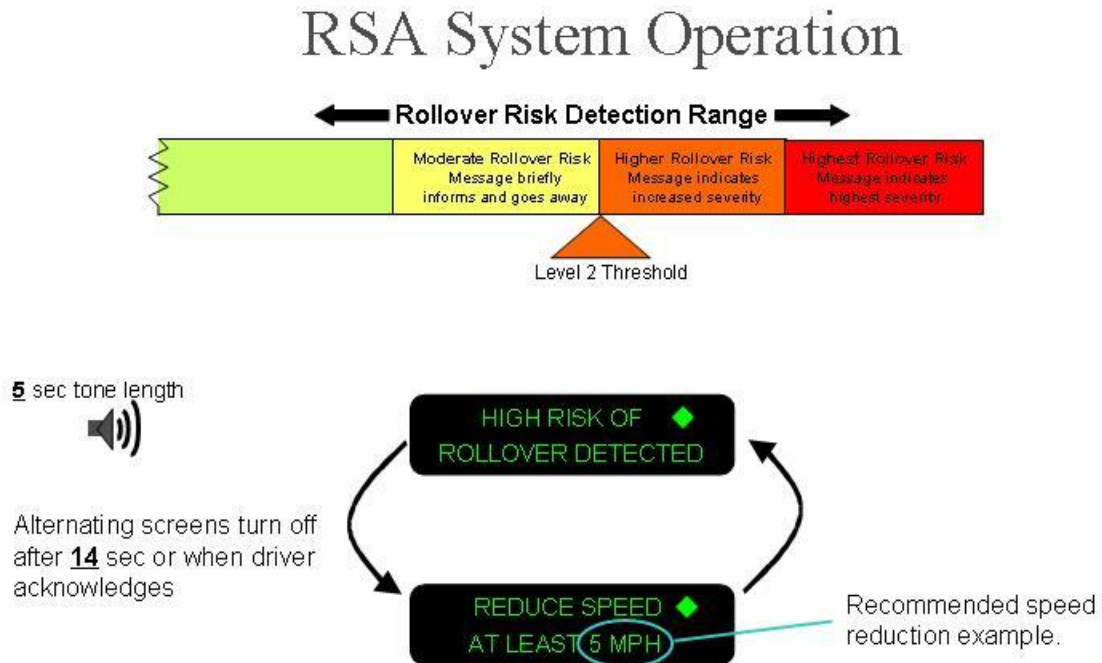


Figure 2-5: RSA System Operation - Level Two Event

Figure 2-6 shows what the driver will experience after a “Level 3” rollover risk occurs. A message indicating that a very high risk of rollover has been detected and that the driver should reduce the vehicle speed by 7 MPH (for example) to avoid similar events in the future. Notice that the tone is 10 seconds in length and the text message is presented on the display for 20 seconds. The lengthened tone is again used to indicate to the driver the increased risk of the event (compared to both the Level 1 and the Level 2 events).

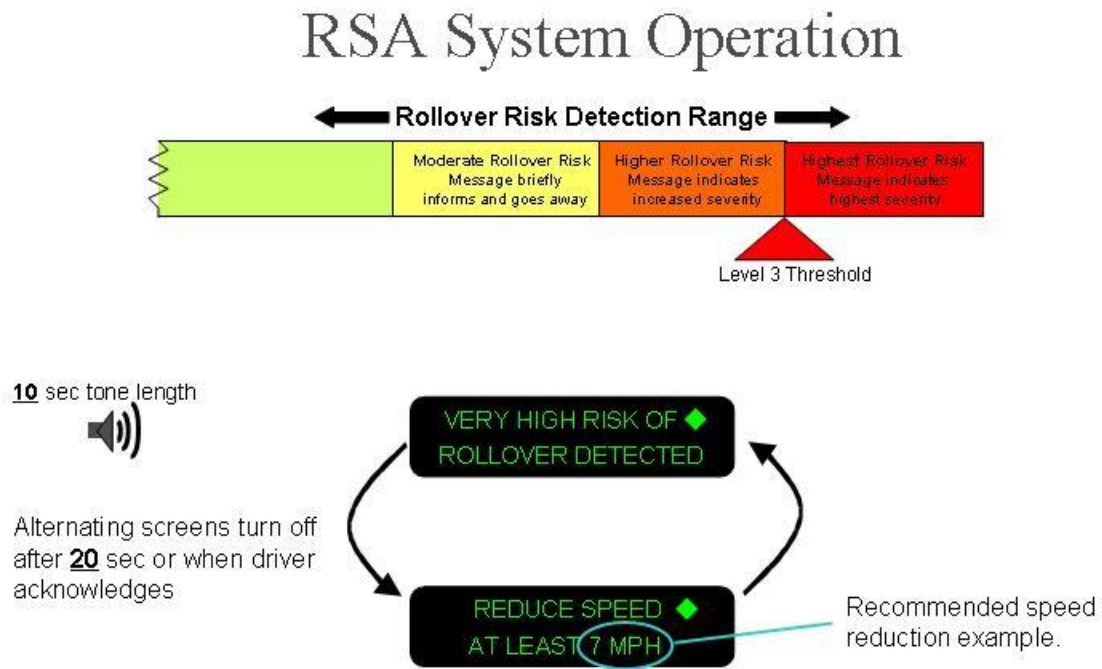


Figure 2-6: RSA System Operation - Level Three Event

2.3 Hard Braking Event Detection Characteristics

Similar to the RSA messages and tones seen above, the Hard Braking Event Detection (HBED) messages are also presented after an “event” has occurred. Figure 2-7 shows the three levels of HBED messages.

HBED System Operation

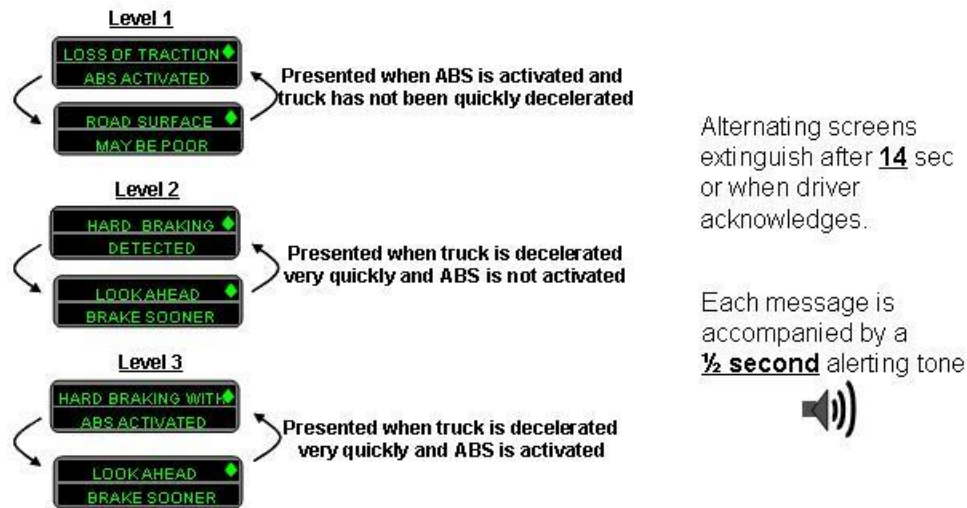


Figure 2-7: Hard Braking Event Detector (HBED) Messages and Tone

2.4 Roll Stability Control Characteristics

Roll Stability Control (RSC) is rather dissimilar to both RSA and HBED in that it is an active system. In other words, it actively controls the vehicle by reducing vehicle speed if an extremely high level of rollover risk is detected. The message that is presented occurs during the event as opposed to after the event as for RSA and HBED. Figure 2-8 shows the messaging as well as activation event explanation for both the RSC and the Automatic Traction Control (ATC) systems. The ATC information has been included to show similarity between the two similar functions. For both RSA and ATC, a dash mounted indicator lamp is illuminated during the event.

Roll Stability Control

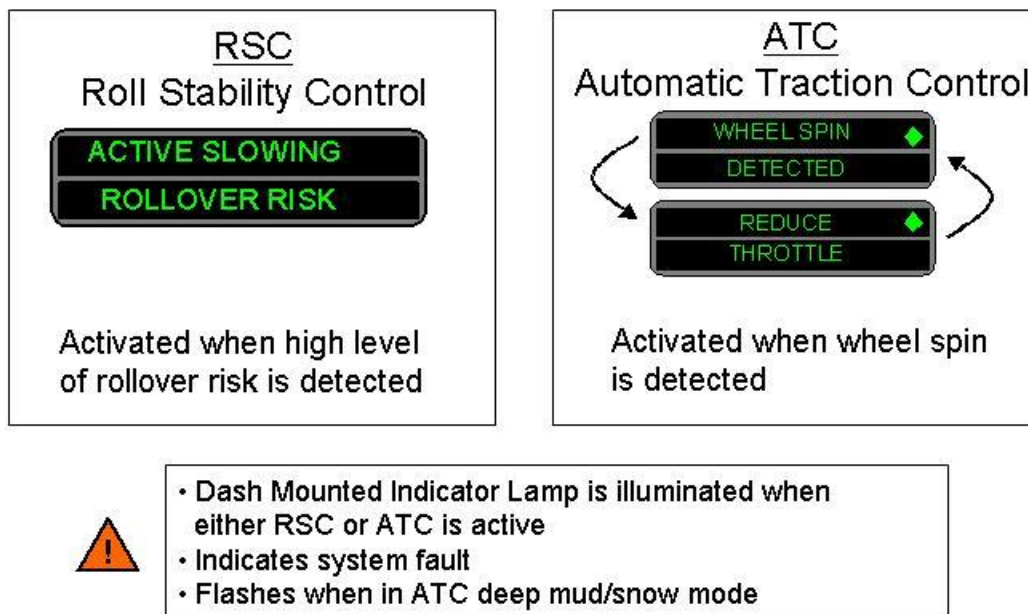


Figure 2-8: Roll Stability Control (RSC) and Automatic Traction Control (ATC) messaging and activation event explanation

2.5 Leg and Trip Related Information

Functionality has also been included in the system to allow the drivers to monitor their performance over a specific segment of travel (legs and trip). The driver can reset the trip and leg segments at any time, thereby following a self-management paradigm (and therefore, management interaction is not an element of this functionality). Research has shown this approach to be effective toward actively involving the participant in automotive environments. Figure 2-9 shows the leg and trip displays.

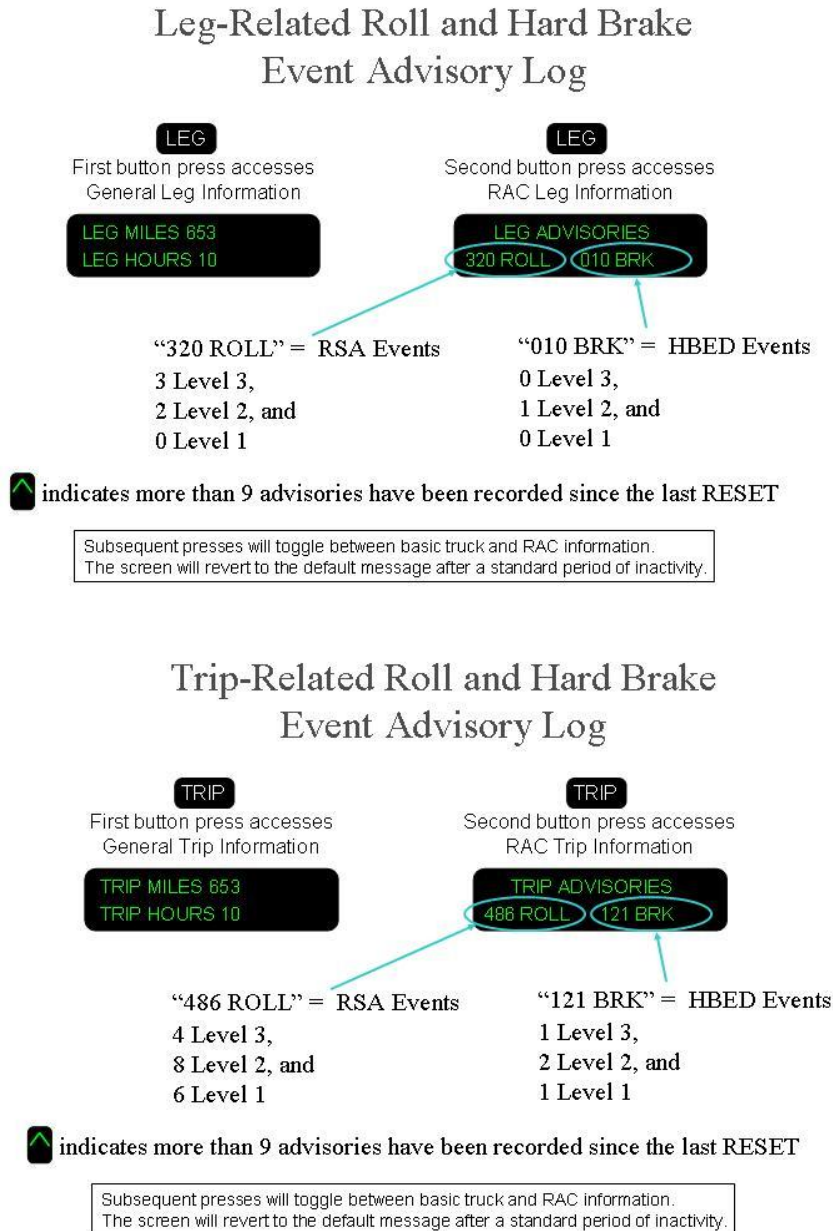


Figure 2-9: Leg and Trip Displays

2.6 System Startup and Fault Messaging

It is important that the driver knows that the RA&C system is onboard. Therefore, a message is displayed upon vehicle startup that identifies that the system is on board as well as gives the driver the option to learn more about the system. This message sequence is shown in Figure 2-10.

Introduction: System Start-up

Messages for:

- ❖ System identification
- ❖ Basic description
- ❖ Directions for more information

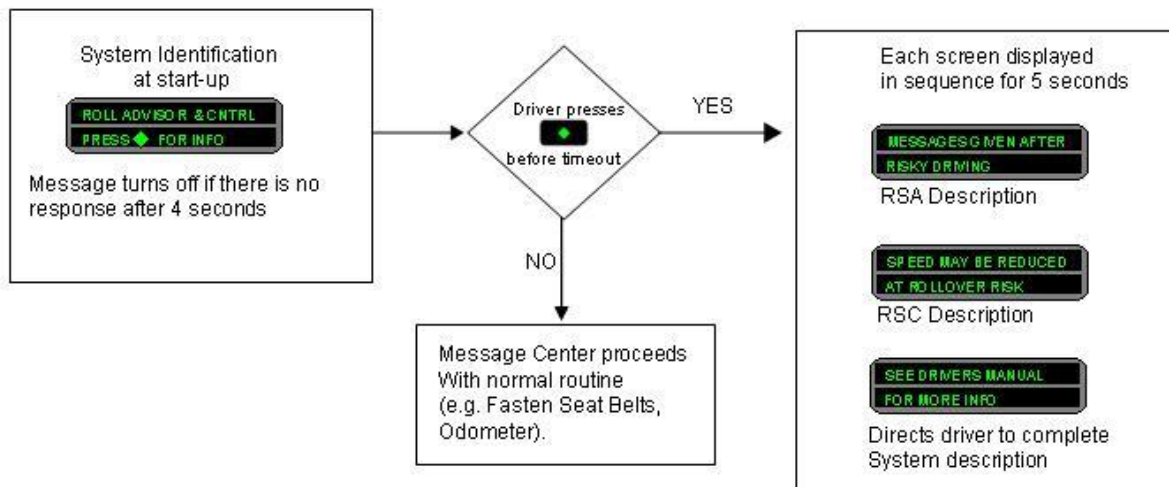


Figure 2-10: RA&C System Startup and System Description

As stated previously, it is important that the driver knows that the system is onboard. It is very important that the driver is informed if a system fault exists. The system fault message and its general characteristics are shown in Figure 2-11.

Introduction: System Fault Message



- ◆ Displayed immediately if failure is detected
- ◆ Displayed at each start-up until problem is remedied
- ◆ Alerting tone accompanies message

Figure 2-11: RA&C System Fault Message with Operating Characteristics

3 Theoretical Rollover Warning Effectiveness – Task 20

In this chapter, the concept of a predictive rollover warning system is introduced. First, a vehicle speed analysis is presented based on the FOT data for the two geographical locations that produced the most RSA advisories during Phase 2, referred to as Hotspots and originally identified by UMTRI. Next, a detailed dynamic analysis of these two hotspots is performed. This is achieved by applying multi-body dynamics simulations to the Praxair tractor-semitrailer combination to better understand the physical behavior of the combination vehicle as well as the driver input that produced each maneuver within the limits of the road geometry. The simulation results are then used to produce vehicle specific and maneuver specific dynamic rollover characteristics that accurately capture the essential elements of vehicle rollover. The intention of this study is to answer the question: What information is necessary to accurately predict combination vehicle rollover? Information gained through this analysis is used to better understand the requirements for a predictive system.

Next, the concept of extending the Rollover Stability Advisor to a proactive Rollover Warning System is described. It discusses results from a preliminary statistical analysis to understand the characteristics of rollover events as well as addresses the methodology and requirements of a Rollover Warning system. A demonstration of the predictive rollover-warning algorithm is performed for hotspots 1 and 2 as a proof of concept, based on data collected during the FOT. Finally the chapter closes with prospects for deployment of a Rollover Warning System.

3.1 A Predictive Rollover Warning System

The Roll Stability Advisor (RSA) element of the RA&C system is a training system that presents messages to drivers immediately following the occurrence of a maneuver in which there was a risk of rollover. As drivers experience these messages, they have the opportunity to learn to identify the conditions and maneuvers that lead to potentially risky situations with the objective of increasing the probability of avoiding them in the future. However, the system can only inform the driver once the dangerous situation has already taken place. A Rollover Warning system would change this scenario. It would predict if the vehicle would experience a risky maneuver based on the vehicle's current trajectory while taking into account the detailed road geometry directly in front of the vehicle. The intention of Task 20 is to demonstrate the potential capability of such a Predictive Rollover Warning system by analyzing the real world data that has been collected during the FOT and working with it within the confines of a laboratory environment. This will be achieved by analyzing the collected data, understanding the dynamic behavior of the specific Praxair tractor-semitrailer combination, developing a simulation approach that takes into account the detailed vehicle characteristics, the instantaneous vehicle trajectory, the three-dimensional roadmap data as well as driver performance to produce a prediction of vehicle rollover.

The concept of a predictive rollover warning system is not new. In fact, such a system that uses vehicle trajectory data in combination with upcoming road geometry has already been successfully investigated, albeit for an infrastructure-based system as opposed to an

in-vehicle system. The Federal Highway Administration (FHWA) mode of the United States Department of Transportation (U.S. DOT) conducted a study on the Evaluation of Prototype Automatic Truck Rollover Warning Systems (ATRWS), (FHWA-RD-97-124, 1998). The system essentially analyzed trucks, as they were about to enter exit-ramps with curvature. Three systems along the beltway of Washington DC were installed and tested (two in Virginia and one in Maryland). The system was able to identify trucks exiting the highway, assign a predetermined rollover threshold value for each individual vehicle, calculate the vehicle's speed and trajectory and then predict the risk of the vehicle rollover based on the geometry of the exit ramp curvature. If the system predicted that the vehicle would exceed the rollover threshold speed for the curve, or that the vehicle would exceed the posted maximum safe speed (MSS), it would display the warning, "TRUCKS REDUCE SPEED" on a dynamic messaging sign located adjacent to the roadway. The system was operated on and off over a three year period from 1994 to 1996. The results showed that the average speed reduction approaching the ramp entry was greater with the system activated compared to the system not activated. It also showed that all three installed systems caused truck drivers to reduce their speeds prior to entering the point of curvature of the ramp, based on their predicted speeds exceeding the maximum safe speed of the ramp. As it turned out, the MSS of the ramp was always lower than the rollover threshold speed so the MSS criterion caused the system to warn the drivers, not the rollover threshold speed. Nonetheless, the system effectively reduced the risk of truck rollover through reducing vehicle speeds. Additionally, zero rollovers occurred during the study. This is an interesting fact in that two rollovers had occurred at each of the Virginia sites between 1986 and 1989 and six rollovers had occurred at the Maryland site between 1985 and 1990. This study definitely illustrates that a predictive rollover warning system has potential to positively affect driver behavior.

3.2 Average Velocity Histories for Hotspots 1 and 2

The FHWA study reported on the average reduction (difference) in vehicle speed measured by successive stations located along the length of the tested off-ramps. However, it did not report the average vehicle speeds as measured at the entry point to nor within, the curvature of the off-ramps. These data would be beneficial in evaluating the hypothesis that over time, the feedback from a Rollover Warning System (such as the ATRWS) is able to reduce the risk of rollover by teaching drivers that specific geographical locations (such as the three exit ramps) are riskier than the drivers had originally thought. The measurement of such a phenomenon would appear as a reduction in vehicle speed as a function of passes through the risky location. This theory, of course, assumes that the same truck drivers pass through the same risky locations on numerous occasions in order to receive enough feedback to learn that their typical operating speeds are inappropriate. The RA&C FOT offers an excellent opportunity to investigate such a hypothesis in that the Praxair fleet tended to pass through the same curves on a routine basis.

An analysis has been performed on the FOT database for the two geographical locations that produced the most RSA advisories during Phase 2. These locations are referred to as RA&C Hotspots and were originally identified by the analysis of UMTRI. Hotspot 1 is a 270° on-ramp from US-31 North to I-80 West near South Bend, Indiana (curve number

751 according to UMTRI's naming convention). Vehicles passed through hotspot 1 a total of 126 times during phase 2 and produced 40 RSA advisories for an average of one RSA advisor for every 3.2 passes. Hotspot 2 is a combination of three contiguous curves (UMTRI curve numbers 76, 77 and 78) that initiates with a right-hand turn from Gary Avenue West to Cline Avenue North in Gary, Indiana. Vehicles passed through hotspot 2 a total of 156 times during phase 2 and produced 34 RSA advisories for an average of one RSA advisory for every 4.6 passes. It should be noted that these two hotspots are the main focus of much of the analysis contained throughout this chapter.

In the FHWA study, the change in driver behavior was measured through quantifying reductions in vehicle speed for the three specific exit ramps. A similar study has been performed for the two RA&C hotspots. These two hotspots represent the geographical locations where drivers were informed the most by the RSA system to reduce their speed because the particular maneuver had just caused a heightened risk of rollover. Based on the idea that the drivers would learn from receiving consistent and repeated feedback, it is assumed that vehicle speeds through the hotspots, or through specific sections of the hotspots would be reduced over time. A method to evaluate this assumption was to extract the vehicle speed history for all passes through each hotspot during the FOT and average the speed histories based on phase 1, on phase 2 as well as on both phases and then present the data as a function of position in the hotspot. This is done in Figure 3-1 through Figure 3-6.

Figure 3-1 shows the overall average vehicle speed for the entire FOT (phase 1 and phase 2) for hotspot 1 as a function of distance into the curve. It also contains the average vehicle speed separated in to phase 1 and phase 2, as well as the location where the RSA advisories were observed within the curve. It should be noted that the averaged data in Figure 3-1 is based on 242 total passes of which phase 1 contained 116 and phase 2 contained 126.

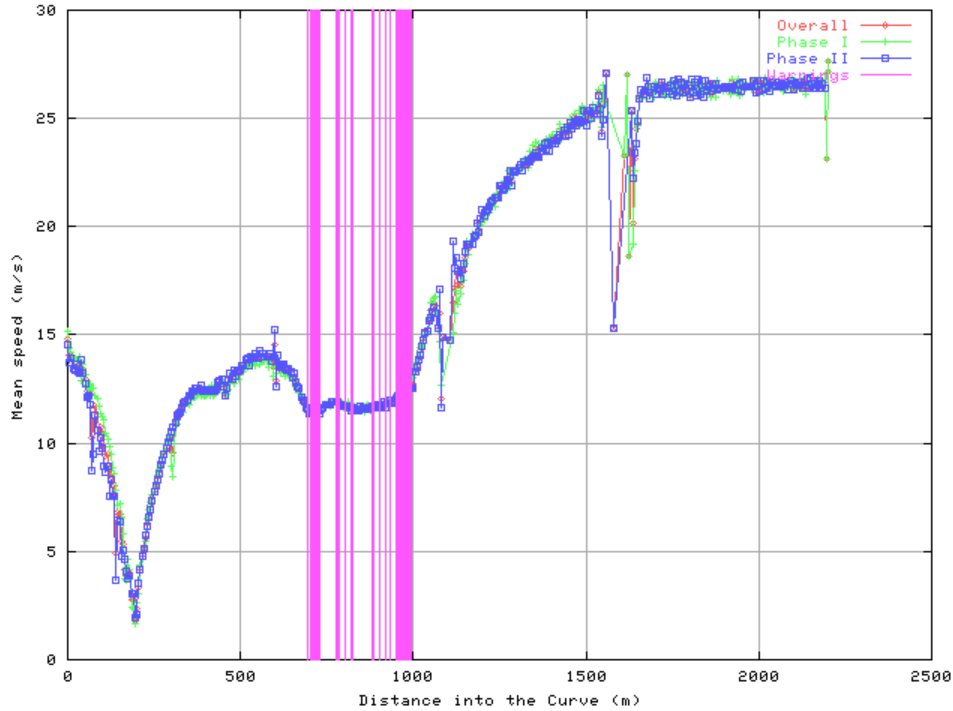


Figure 3-1: Average Vehicle Speed through Hotspot 1 for both Phases 1 and 2 with the location of the RSA Advisories (Warnings), entire length of the curve

In general, there appears to be little difference in the averaged velocities for hotspot 1. However, zooming in on the two regions with the highest concentration of RSA advisories illustrates that a difference in average velocity between phase 1 and phase 2 definitely exists. Figure 3-2 is a close up of the section between 690 meters and 730 meters. It shows that there was a slight trend toward slower average velocities for phase 2 compared to phase 1, albeit very minimal. Figure 3-3 is a close up of the section between 950 meters and 1000 meters where the highest concentration of RSA advisories was observed. It definitely shows a trend that the average vehicle velocities were reduced in phase 2 compared to phase 1. The maximum difference for this case was 4% (0.55 m/s = 1.25 mph). While this value may seem small in magnitude, the RSA system is focused on displaying incremental velocity reductions that range between 1 to 7 mph.

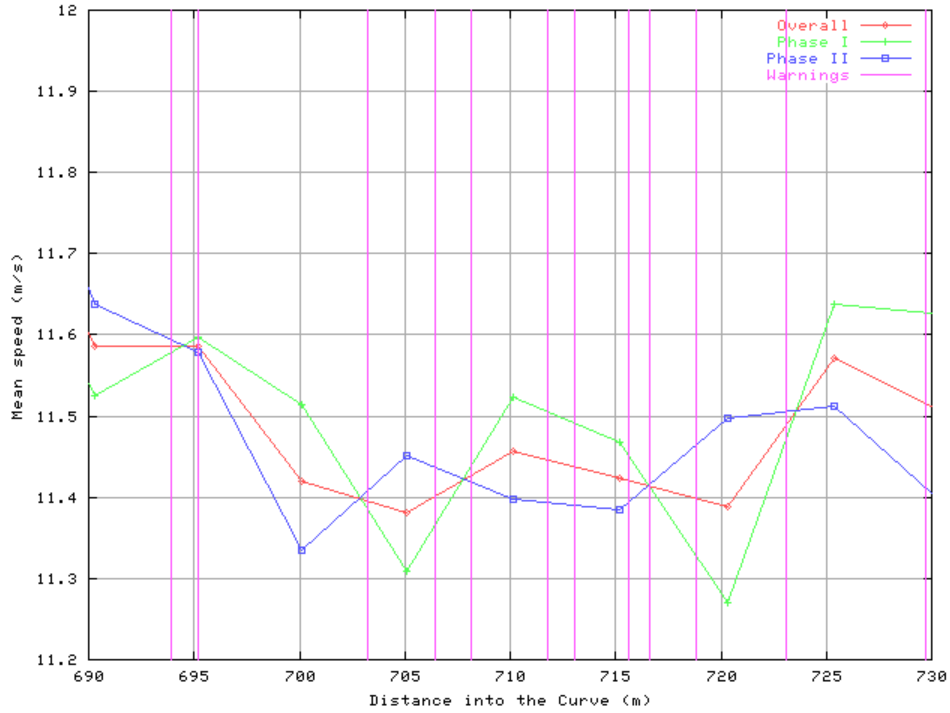


Figure 3-2: Average Vehicle Speed through Hotspot 1 for both Phases 1 and 2 with the location of the RSA Advisories (Warnings), curve between 690 & 730 meters

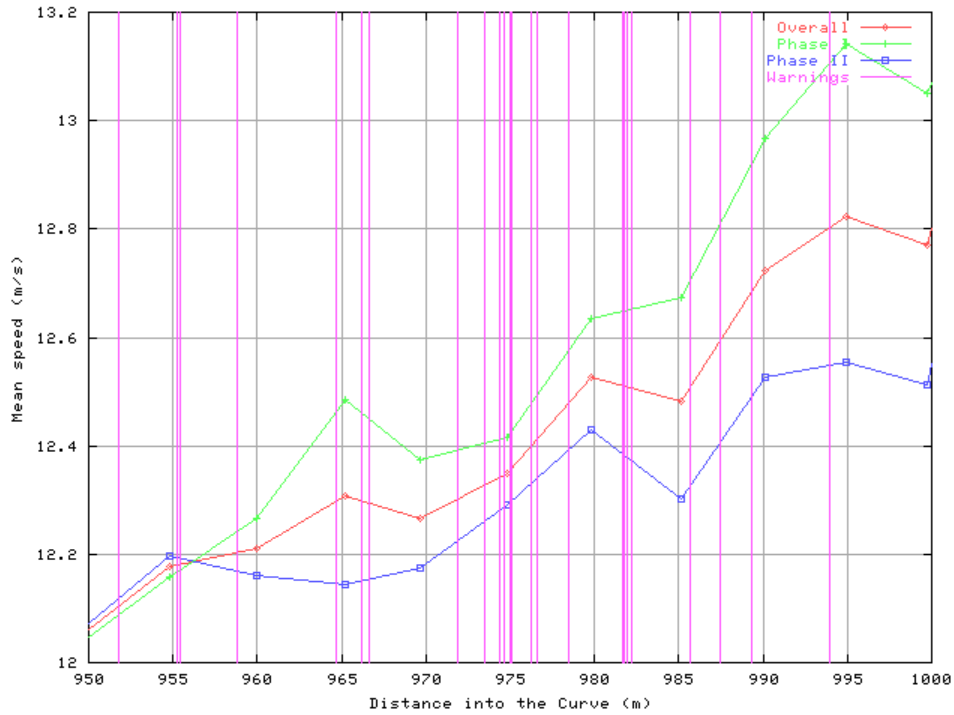


Figure 3-3: Average Vehicle Speed through Hotspot 1 for both Phases 1 and 2 with the location of the RSA Advisories (Warnings), curve between 950 & 1000 meters

Similar behavior is observed in hotspot 2 although the local trends for the average velocities in the RSA advisory concentrations are more consistent. Figure 3-4 shows the total average velocity history for the entire length of the curve for hotspot 2. Once again the macroscopic view of the hotspot shows very little noticeable differences in averaged velocities. These results are based on a total of 306 passes of which 150 occurred during phase 1 and 156 occurred during phase 2.

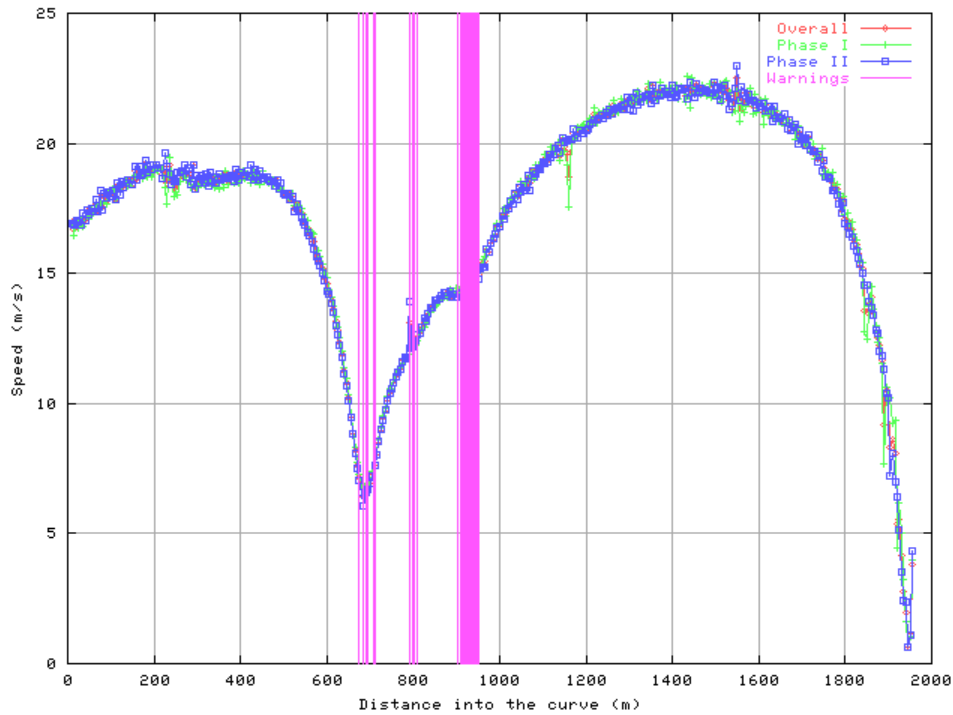


Figure 3-4: Average Vehicle Speed through Hotspot 2 for both Phases 1 and 2 with the location of the RSA Advisories (Warnings), entire length of the curve

A close up view of the region with the second highest concentration of RSA advisories is shown in Figure 3-5 and corresponds to the distance into the curve from 660 meters to 720 meters. The trend of reduced speed during phase 2 is very obvious and observed for all data points within the 60 meter section. The most dramatic difference corresponds to the slowest speed point located at approximately 685 meters, just before the cluster of the RSA advisories. The average velocity for phase 2 is over 10% less than for phase 1 with a magnitude of approximately 0.7 m/s (1.27 mph). Figure 3-6 shows the section of hotspot 2 that corresponds to the highest concentration of RSA advisories located between 900 meters and 960 meters. Once again, the general trend of lower speeds during phase 2 is consistently observed for the entire section with the maximum difference being approximately 3% with a value of nearly 0.44 m/s (1 mph).

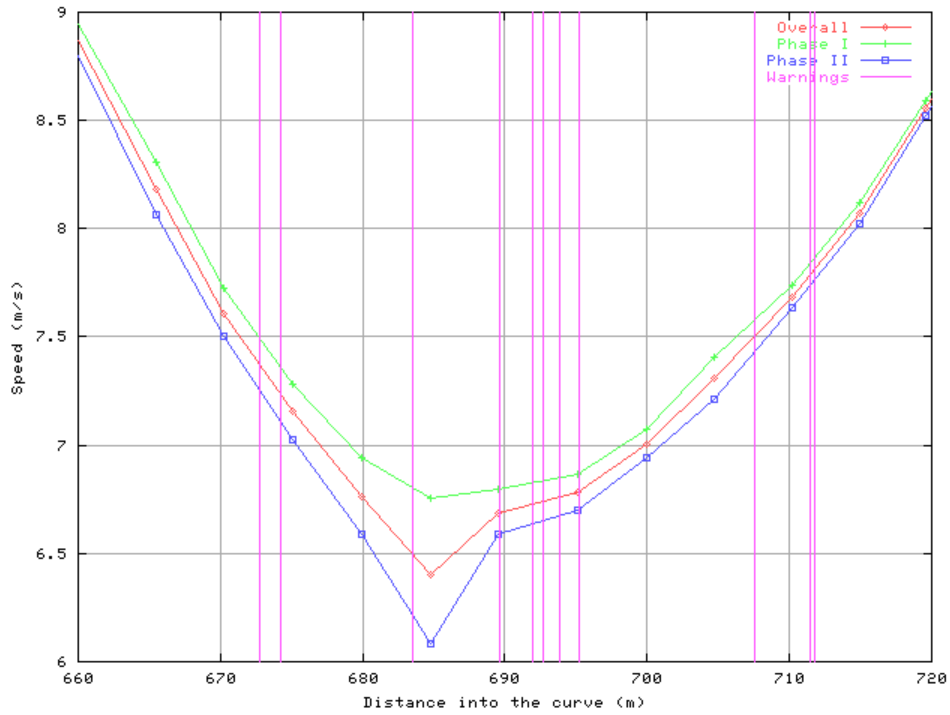


Figure 3-5: Average Vehicle Speed through Hotspot 2 for both Phases 1 and 2 with the location of the RSA Advisories (Warnings), curve between 660 & 720 meters

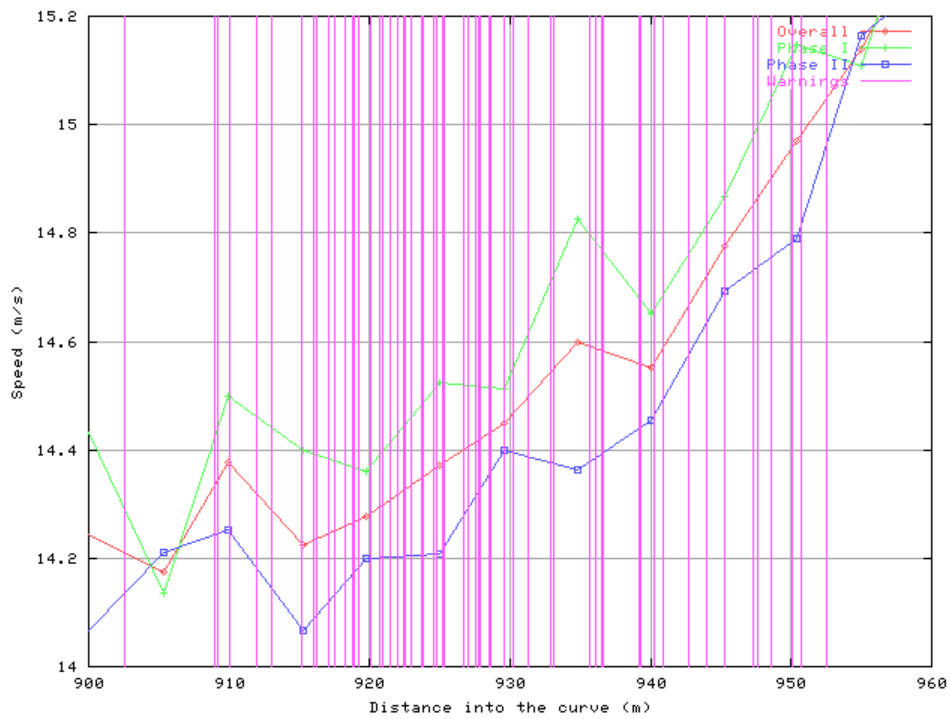


Figure 3-6: Average Vehicle Speed through Hotspot 2 for both Phases 1 and 2 with the location of the RSA Advisories (Warnings), curve between 900 & 960 meters

While there could many factors that contributed to these slight changes in average velocity magnitude (weather, construction, traffic jams, etc.), the trends are encouraging in that the analyses contained a significant amount of data points (hotspot 1, 240 passes and hotspot 2, 300 passes) collected over both phases (phase 1: November 2000 – May 2001, phase 2: June 2001 - November 2001), which together, tend to reduce the impact of singular events.

It should also be noted that this overall analysis was performed for only two hotspots and the focus was on the regions of highest RSA advisory concentrations. The analysis of other hotspots would have been beneficial as well as analysis of straight driving for comparison. If the hypothesis is true that drivers learn that specific geographical locations are risky based on receiving RSA advisories, and the measurement criterion is reduced vehicle speed, the difference in average speed would theoretically be greatest in the regions of highest RSA advisories and there should be nearly no difference in average speed in regions with zero RSA advisories. Additionally, a driver-by-driver analysis could also be beneficial in evaluating if this hypothesis is true.

Nonetheless, the results presented in Figure 3-1 through Figure 3-6 highlight that there is a general trend, albeit slight, toward reduced speed in the specific road sections where high counts of RSA advisories were recorded. While the magnitudes of the speed reductions between phases 1 and 2 were small, the general trend definitely exists. This trend gives some credence to the hypothesis that drivers could learn that specific geographical locations have a higher risk of rollover than they had originally thought, and consequently drive more slowly through the regions with their vehicles to reduce the risk of rollover. Additionally, this result should not be limited to just an in-vehicle advisory system. It is expected that a similar outcome would be produced by an in-vehicle predictive system, which would have the same effects of identifying risky events, and teaching drivers that particular geographical locations are risky. The remainder of this chapter will focus on the concept of a Rollover Warning System that would have the capability to predict rollover as opposed to simply advise of the risk after the fact.

3.3 Multi-body Dynamics Analysis of the FOT Vehicles

The Vehicle Systems Technology Center (VSTC) was tasked with simulating the Field Operational Test (FOT) vehicles. The purpose of the simulations was to replicate the FOT vehicles and their operating inputs in order to establish a “rollover margin” per Task 20 of the FOT. The sections that follow describe the simulation models and analysis using the simulation models. The former includes a description of the physical and simulation vehicles and how the simulations were implemented to recreate trips of interest from the FOT. The latter includes a validation of the simulation models and sensitivity studies of parameters that influence vehicle rollover.

3.3.1 Physical Vehicle

The vehicle simulation models are based upon the available data for the Freightliner Century Class S/T tractor and the LOX 8500 tanker semitrailer shown in Figure 3-7 and Figure 3-8 on the UMTRI tilt table rig. Additional information about the FOT vehicles is listed in Volume III, Appendix-D.



Figure 3-7: Oblique view of the UMTRI test vehicle



Figure 3-8: Side view of the UMTRI test vehicle

Salient geometric properties of the tractor and semitrailer are summarized in Table 3-1. This information was culled from Freightliner, Praxair, and UMTRI sources.

Table 3-1: Vehicle geometric properties

Property	Tractor	Semitrailer	Notes
	mm	mm	
Wheelbase	4367	10897	
Tandem spacing	1297.3	1245	
Track	1828	1816	
Fifth wheel height	1217.4	-	Tare tractor weight
Length	7327.1	12801.6	
Width	2438.4	2438.4	Outside tire to outside tire
Height	2837.9	3402	Tare (estimated)

3.3.2 *Simulation Models and Inputs*

3.3.2.1 *Simulation Environment/Software*

This section describes the two simulation software and vehicle models used for this project. Both simulation tools run in a MATLAB/Simulink environment known as VehicleSim. This environment provides a single interface to both tools because they share many common components (i.e. data pre- and post-processing, ABS brake model, maneuver library, etc.) necessary for simulation. The VehicleSim environment helps to ensure uniform treatment of input data by the two simulation tools and facilitates library sharing and model correlation.

The first software tool is a proprietary DaimlerChrysler program called STARCAT (Simulation of Trucks and ARticulated Combinations for Analysis and Testing). STARCAT is a nonlinear, three-dimensional rigid body vehicle dynamics simulation tool that is real-time capable. It is highly optimized (Rill, 1994) for heavy truck vehicle handling simulations (Sherman and Myers, 2000) and thus is used for sensitivity studies.

The second software package called DADS is developed by LMS International. It performs general mechanical multibody system simulation and is used to simulate more advanced topics that are beyond the capabilities of STARCAT. Such topics include three-dimensional roads, flexible chassis, and fluid sloshing.

3.3.2.2 *Simulation Vehicle Models*

The STARCAT and DADS simulation models are simplified representations of the Praxair vehicle. As such, it is expected that the models at least agree qualitatively with the FOT data and quantitatively with each other. Much more data is available for the tractor than the semitrailer. The tractor model is based upon data for FOT tractor 5 (see Volume III, Appendix-D) but all of the FOT tractors are essentially the same. The semitrailer model is based upon the L891 semitrailer (see Volume III, Appendix-D) and is also assumed to be representative of all the semitrailers involved in the FOT study.

An important principal assumption made about the tractor and semitrailer is that they are assumed to have rigid chassis. This is a reasonable assumption for the tanker semitrailer but less valid for the tractor. The effect of a flexible chassis on lowering rollover stability is not insignificant but is not accounted for in most of the simulations for the sake of

comparison of results between the STARCAT and DADS models. In the dynamic rollover simulations for the DADS model, the rigid tractor chassis assumption is relaxed.

Of primary concern for the simulation model parameterization is the inertial and the suspension properties. Most of the inertial data (center of gravity location and mass moments of inertia) are estimated based on available information from Freightliner and Praxair. Much inertial data for the tractor are available from Freightliner measurements. Semitrailer inertial information is estimated based on digital mockups of the available geometric data. Mass that is unaccounted for is assumed to be evenly distributed along the length of the tractor and semitrailer chassis and mass moments of inertia are scaled accordingly. The vehicle inertial data are summarized in Table 3-2.

Table 3-2: Vehicle inertial properties of the STARCAT and DADS models

Vehicle	STARCAT				DADS			
	Mass	CG ¹			Mass	CG ¹		
		x_{cg}	y_{cg}	z_{cg}		x_{cg}	y_{cg}	z_{cg}
	kg	m	m	m	kg	m	m	m
Tractor (tare)	6707	-2.01	-0.05	0.99	6707	-2.31	-0.01	0.91
Semitrailer (tare)	6760	-11.96	0.0	1.84	6914	-12.03	0.0	1.74
Semitrailer (full)	28351	-10.47	0.0	2.18	28505	-10.47	0.0	2.17
Tractor + semitrailer (tare)	13467	-7.00	-0.02	1.42	13621	-7.24	0.0	1.33
Tractor + semitrailer (full)	35058	-8.85	-0.01	1.95	35922	-8.92	0.0	1.93

¹ Reference coordinate system for the tractor and semitrailer is on the ground directly below the center of the front axle or kingpin, respectively. The x -axis is positive forward, the y -axis is positive towards the driver, and the z -axis is positive up.

Accurate and validated suspension and tire models are used for the tractor. The semitrailer uses a nominal trailer air spring suspension and tire models. The Praxair vehicles have Bridgestone tires but data is only available for Michelin tires for the tractor and semitrailer. The Bridgestone tires are equivalent in terms of basic geometric properties (i.e. diameter, width, tread depth, etc.) to the Michelin tires. It is assumed that the Michelin tire models will be representative of the dynamic performance of the Bridgestone tires.

There are several notable differences between the STARCAT and DADS vehicle models. The fifth wheel model for DADS is much simpler than that used by STARCAT, having three rotational degrees of freedom and a roll stiffness. For the purposes of this study, this difference is deemed acceptable. STARCAT uses a proprietary tire model and the DADS model uses the DADS complex tire model parameterized in the same manner as the STARCAT tires. The drivetrain model is more complex in STARCAT than in DADS which is shown in later model comparisons to be an appreciable difference.

3.3.2.3 Simulation Model Inputs

The issue of how to handle the driver inputs (steer, acceleration, and brake) required by the simulation models is important for two reasons. First, accurately represented inputs impact the ability to make a reasonable quantitative correlation with the vehicle FOT

data. Second, realistic driving data is useful in making meaningful conclusions about vehicle rollover stability.

Steering wheel inputs and brake pedal data are not available from the FOT vehicle measurements. (To be precise, brake pedal data is available but the data only indicate whether it is depressed or not). Accelerator pedal data is available. To provide steering wheel inputs, the roads for simulated trips are recreated using the FOT vehicle GPS data. The accelerator and brake pedal inputs are recreated by using the FOT vehicle speed as a control reference value.

3.3.2.3.1 FOT GPS data

It is possible to use a nominal or unique road description using the FOT vehicle GPS data. The nominal road is based on an average of all the trips in the same direction on the same road segment in a local geographical area. The unique road is based on the GPS data for a single trip along a road segment.

For this study, the unique GPS path for a trip is used to describe a road segment instead of the nominal path. This is because the unique path driven for a specific trip, in combination with the vehicle speed, is what is causing the high RSA scores. Using a nominal path along with a nominal speed profile is problematic. The main drawback to using the unique path is that problems with the GPS system exist, namely accuracy (based on a single trace) and loss of GPS.

The description of the unique path is based upon GPS longitude, latitude, and HAE (Height Above Ellipsoid) measurements. The GPS data for FOT trips of interest are filtered and turned into finite spline segments (usually on the order of three to ten meters in length) by DaimlerChrysler RTNA (RTC), where curvature and elevation are described as a function of spline length. The curvature of the starting point of a segment is taken to be constant over the length of that segment instead of linearly varying between the starting and ending points. This impacts accuracy especially when loss of GPS occurs for several consecutive data points.

The FOT vehicle GPS speed data were originally used as a model input. Figure 3-9 shows an example of the kind of problem that arises. The time interval from five to ten seconds shows that the accuracy can be poor when the GPS unit does not pick up enough satellite signals. The time interval from 50 seconds to 55 seconds illustrates that sometimes no satellites are visible to the GPS system. In this case, the GPS speed is totally unreliable. For these reasons, the velocity sensor data are used to represent the vehicle speed.

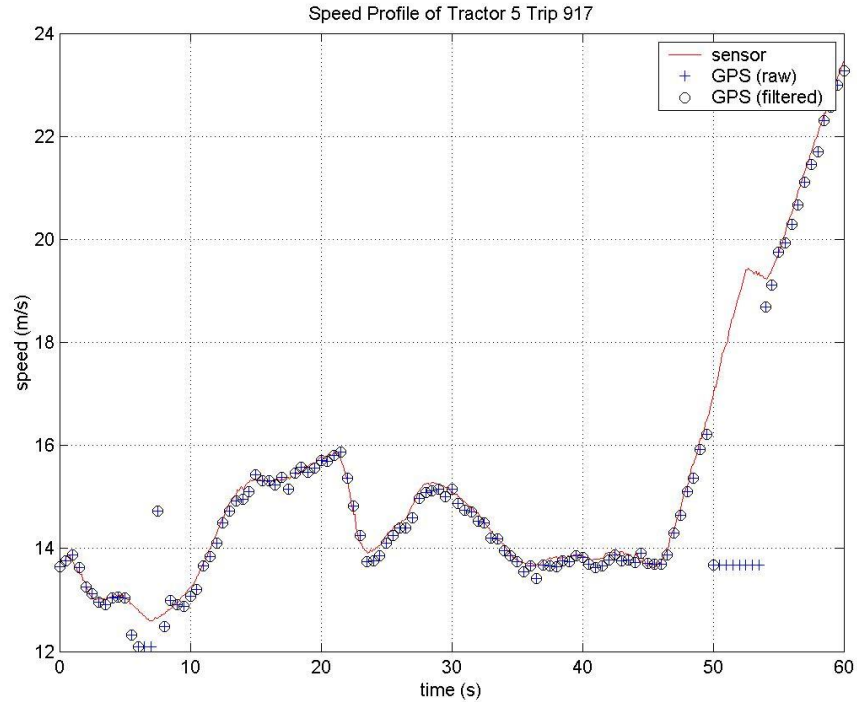


Figure 3-9: Example speed profile comparing the vehicle speed sensor data with GPS speed data

All GPS and GPS-derived data (e.g. curvature) are filtered based on whether or not the data at any given time step is different than the previous time step. This approach eliminates most of the spurious data resulting from loss of GPS that would be used for defining the mathematical representation of the road track.

3.3.2.3.2 Mathematical road description

STARCAT and DADS use different techniques for describing road inputs and also have certain limitations. STARCAT uses geometric primitives to build road models. Roads can consist of simply a flat track (xy plane) and/or a road profile (xz plane). STARCAT is optimized for using road profiles only on straight tracks. For most of this study, a flat track will be used to represent the roadway input for STARCAT and most of the DADS simulations.

3.3.2.3.3 Driver inputs

Digital PID controllers with saturation limits are applied to the steering wheel and accelerator and brake pedals to force the simulation models to follow the road input and speed profile of a given trip. The steering controller attempts to force the track deviation to zero. The accelerator and brake controllers are yoked together by a simple algorithm. It turns on the accelerator controller if the speed deviation (difference between actual speed and simulation speed) is greater than zero and turns on the brake controller if the speed deviation is less than zero. These controllers are implemented in the VehicleSim environment and thus STARCAT and DADS are receiving the same input signals.

3.3.2.3.4 Trip selection

Several trips have been selected for simulation from the FOT database based upon four criteria. The first is the trip must have an RSA score greater than 75 (which is directly related to the measured ABS ECU lateral acceleration), the second is based on specific GPS coordinates (hotspots), the third is the vehicle speed must be greater than 36 km/hr (at the time of the RSA event, to avoid RSA false positives), and lastly the ECU must be version 21300 (the latest version of the RSA algorithm).

The hotspots are geographic locations where the highest numbers of RSA events were recorded, irregardless of the number of trips through the geographic location. It is felt that focusing on a few problem areas provides insight into the rollover behavior of the FOT vehicles.

Two hotspots were selected for analysis because they represent two different types of classic maneuver cases. Hotspot 1 is a tight onramp/interchange whereas hotspot 2 is like an S-curve. The former is a quasi-static maneuver whereas the latter is more transient. Table 3-3 shows the trips selected from the database for hotspots 1 and 2 based on the aforementioned criteria.

Table 3-3: List of selected trips

Hotspot	Tractor	Trip	GPS Time	RSA Score
			ds	%
1	1	930	699655	75
	1	953	897865	79
	4	897	629535	85
	5	862	430875	76
	5	917	516740	94
2	1	878	680175	75
	1	939	349945	96
	5	862	469970	76
	5	939	956005	77
	5	982	521755	77

3.3.2.3.5 Hotspot 1 & 2 descriptions

Hotspot 1 is located at the interchange of Highway 31 (Hwy 31) and Interstate 80 (I-80) near Laporte, Indiana. The vehicles that received RSA alerts were traveling north on Hwy 31 and exiting to take the interchange to I-80 westbound (see Figure 3-10).

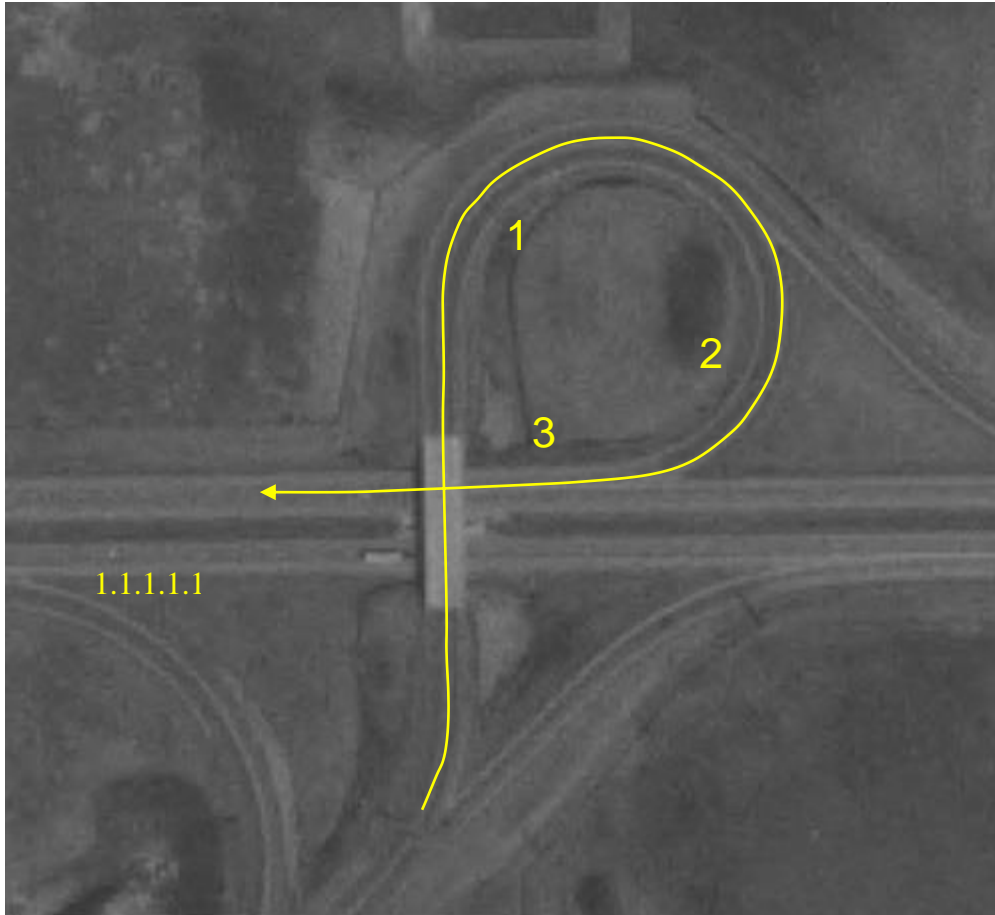


Figure 3-10: Aerial photograph of hotspot 1

Roadway information about hotspot 1 was obtained by conversations with the Indiana DOT (INDOT) (Wolfe, 2002). INDOT provided information from the road engineering drawings about this specific interchange. After the bridge overpass, the road has three curve segments. Curve 1 starts immediately after the bridge and continues to the point where the offramp from I-80 westbound joins it. Curve 2 begins at this point and continues to just before where the interchange joins I-80. The final curve continues from the end of curve 2 and continues to the point where it merges with I-80 West.

Table 3-4: Hotspot 1 road data (Wolfe, 2002)

Curve	Curvature 1/m	e cm/m	e_{max}^1 cm/m	Posted Speed km/hr
Hwy 31	n/a	n/a	n/a	88.5
1	-0.01329	1.5625	-	56.3
2	-0.01432	n/a	8.0	56.3
3	-0.00115	n/a	-	56.3
I-80	n/a	n/a	n/a	104.6

¹ Superelevation is positive when the road slopes downward towards the passenger side of the vehicle.

The data from INDOT shows that the second curve is tighter than the first curve and that the third curve is shallow as the interchange attempts to allow vehicles to speed up to merge onto I-80 West. The maximum superelevation of the interchange (4.6 degrees of road banking) is in curve 2. The INDOT road data are summarized in Table 3-4.

Figure 3-11 and Figure 3-12 show the information from the FOT database on hotspot 1 for tractor 5 trip 917. These data correspond quite well to the information in Figure 3-10 and Table 3-4, except for the GPS height. The plots show different features of the road: curvature, bank angle, and elevation as a function of curve distance.

The curvature (first) plot begins with the truck on the interchange and making the left turn towards the overpass (initial 150 meters). For approximately the next 125 meters, the truck is driving straight and the estimated road bank angle is nearly zero (second plot) and it is at the high point (third plot) in elevation of the interchange. At about 275 meters the truck proceeds to enter curve 1, road banking increases and the truck spirals clockwise downward towards I-80.

Some problems with the data are worth noting. Notice during the transient portions at the beginning of curve 1 and the end of curve 2 the bank angle oscillates and peaks at 6.5 degrees. This is clearly not correct and reflects the assumptions behind its estimation breaking down during a transient event. During the steady changes in curvature, the approximated bank angle agrees well with the data. The problems with GPS height data are seen at 180 meters and 330 meters of distance. The sharp drops and rises in elevation are not related to any true elevation changes. In fact, the height data actually reports that the vehicle is going uphill while following curves 1 and 2 (400 meters to 775 meters).

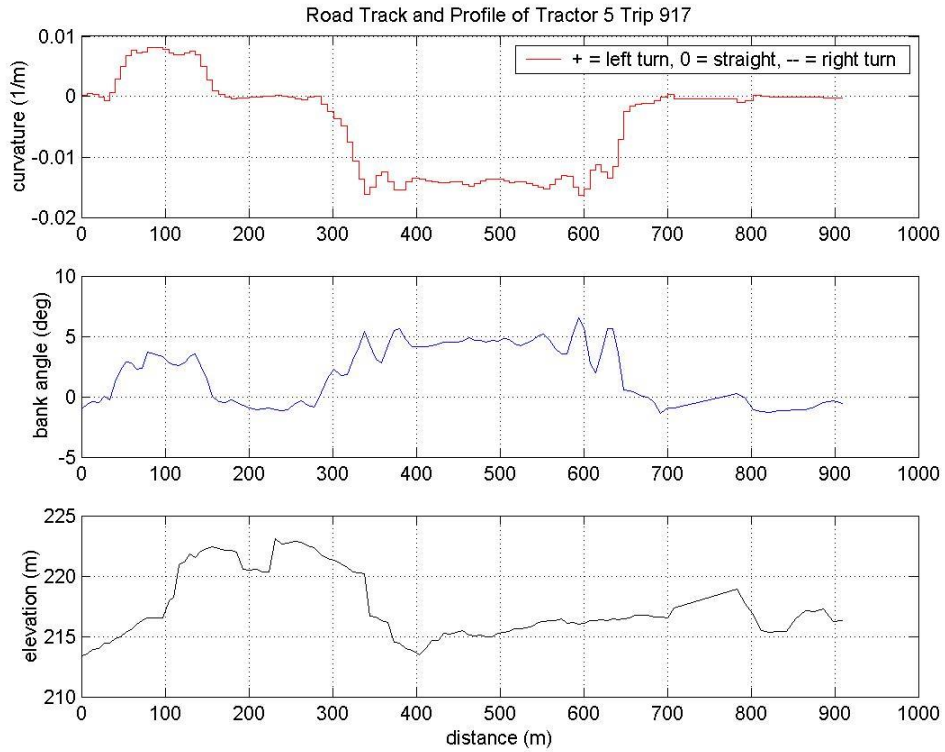


Figure 3-11: Hotspot 1 road data

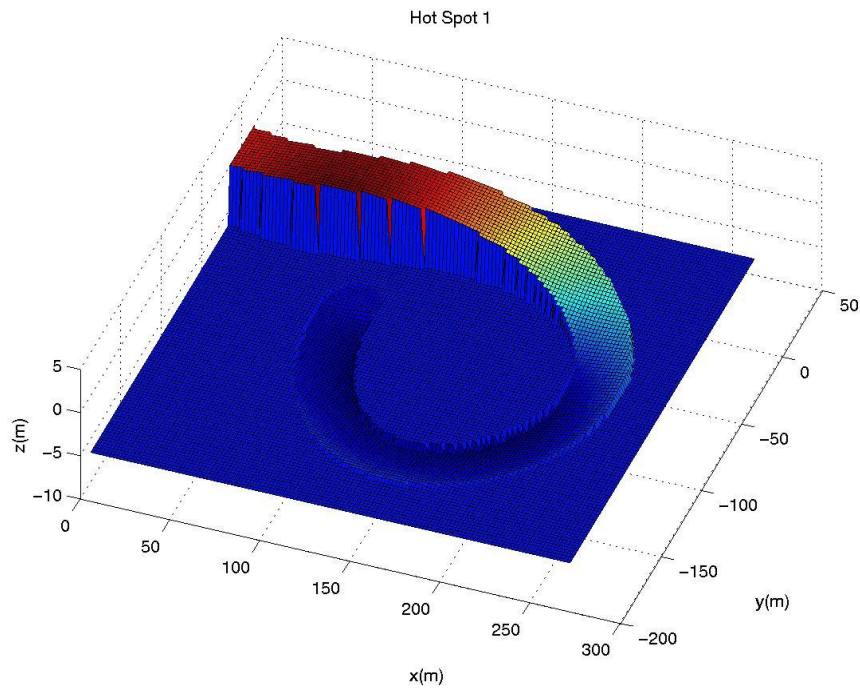


Figure 3-12: Three dimensional road reproduction of hotspot 1

An aerial photograph of hotspot 2 is shown in Figure 3-13. Like hotspot 1, this road segment is a complex curve with three curve segments. The difference between hotspot 1 and hotspot 2 is that the former has curvature segments with the same sign (spiral loop) whereas the latter has curvature segments that change sign (hard right followed by S-curve).

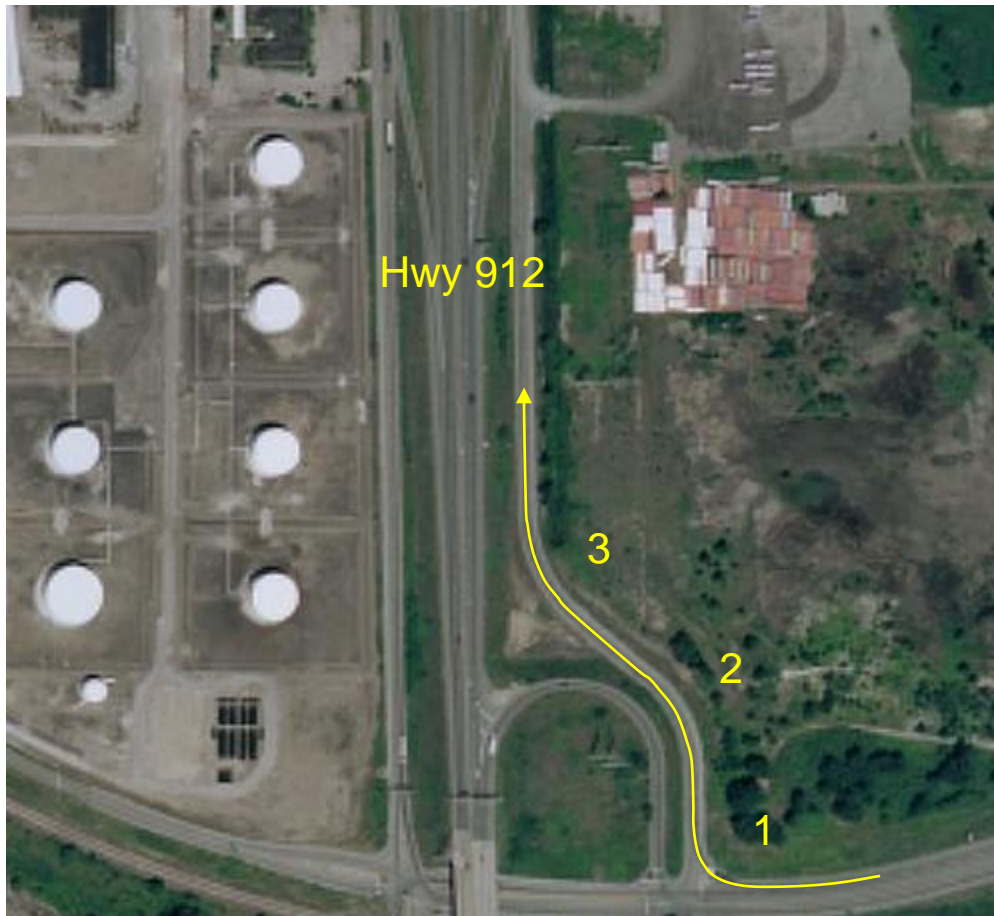


Figure 3-13: Aerial photograph of hotspot 2

Figure 3-14 shows the road data for tractor 1 trip 939 as it passes through hotspot 2. The S-curve (curves 2 and 3) is clearly seen in the curvature plot starting around 125 meters and continuing until 400 meters. When the curvature is changing constantly in curve 2 from 190 meters to 250 meters, the bank angle is again quite inaccurate. Figure 3-15 shows the three-dimensional road characteristics (bank angle and elevation change) for hotspot 2.

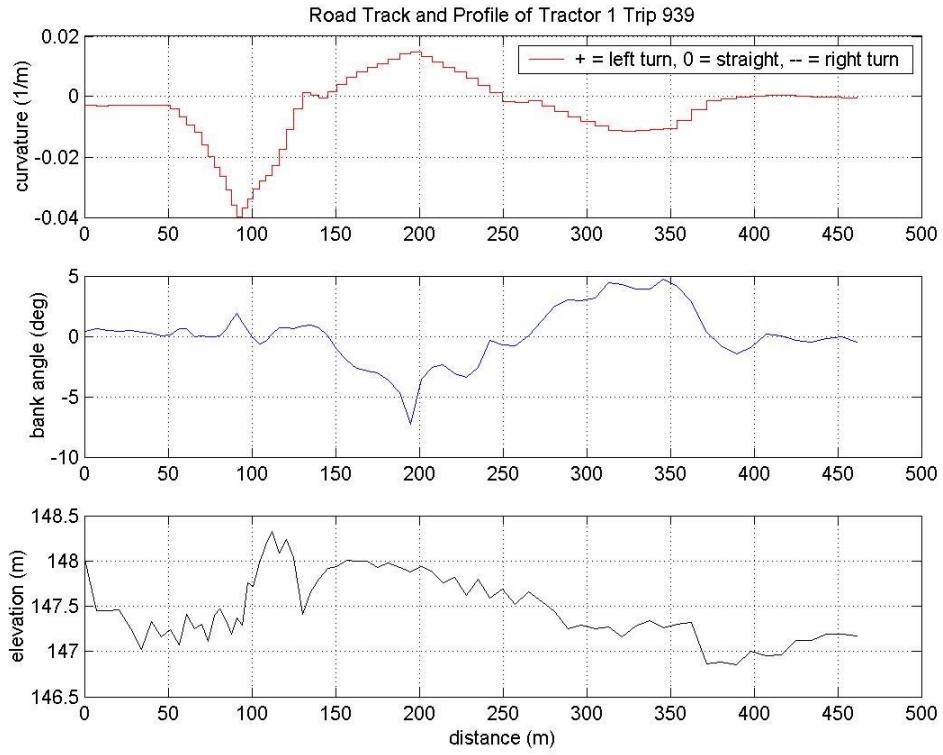


Figure 3-14: Hotspot 2 road data

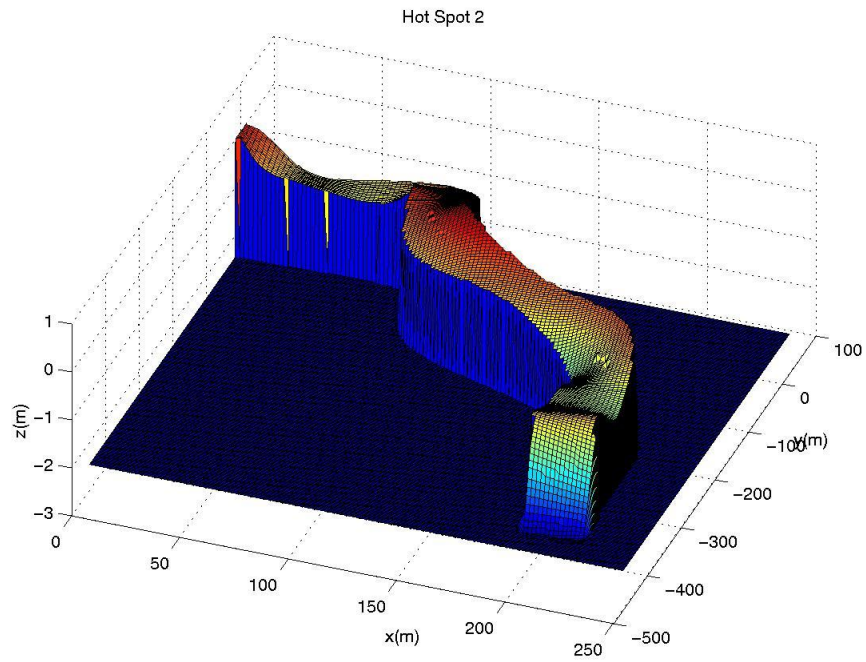


Figure 3-15: Three dimensional road reproduction of hotspot 2

3.3.3 *Simulation Model Correlation and Validation*

3.3.3.1 *Metrics*

The STARCAT and DADS models are correlated by input deviations (track and speed), lateral accelerations at the ABS ECU and steer axle locations, tractor yaw rate, and semitrailer axle wheel loads for two example FOT trips. The metrics for model and FOT validation are the same as the model correlation excepting the semitrailer axle wheel loads.

On the FOT tractors, the ABS ECU accelerometer is placed about three feet forward of the centerline of the rear tandem axle on the right frame rail. The steer axle accelerometers for the models are placed at the centers of gravity of the axle tube.

For the comparisons below, both models are set up in the same way such that both have a rigid tractor chassis and no load sloshing with a flat road as the input road track.

3.3.3.2 *Model Correlation*

The results for the STARCAT and DADS models are compared in Figure 3-16 through Figure 3-21 for the hotspot 1 (tractor 5 trip 917) and 2 (tractor 1 trip 939) example trips. To better see the correlation, these plots are deviations (difference between FOT reference value and model results) from the information derived from the FOT database for the respective trips.

For both trips, the track deviation correlates well both in a qualitative and quantitative sense. This is generally to be expected as both are using the same steering controllers and have very similar steering system models. However, the two models do not follow the desired speed in the same fashion. Both are using the same accelerator and brake controllers but have different drivetrain and brake system models.

The acceleration and yaw rate deviation results for the hotspot 1 example correlate well for the two models. In contrast, for the hotspot 2 example, these same plots do not correlate well because around fifteen seconds into the simulation the speed tracking begins to deteriorate, thus breaking the spatial relationship between the speed and the distance along the track at which it occurs.

With the final set of plots, the semitrailer axle wheel loads correlate well in light of the fact that the modeling approach is quite different for the suspension and tires. The two notable differences are slightly lower nominal axle loads for the DADS axles with respect to the STARCAT nominal. In addition, the time delay is seen again in the hotspot 2 plot later in the simulation, as noted previously.

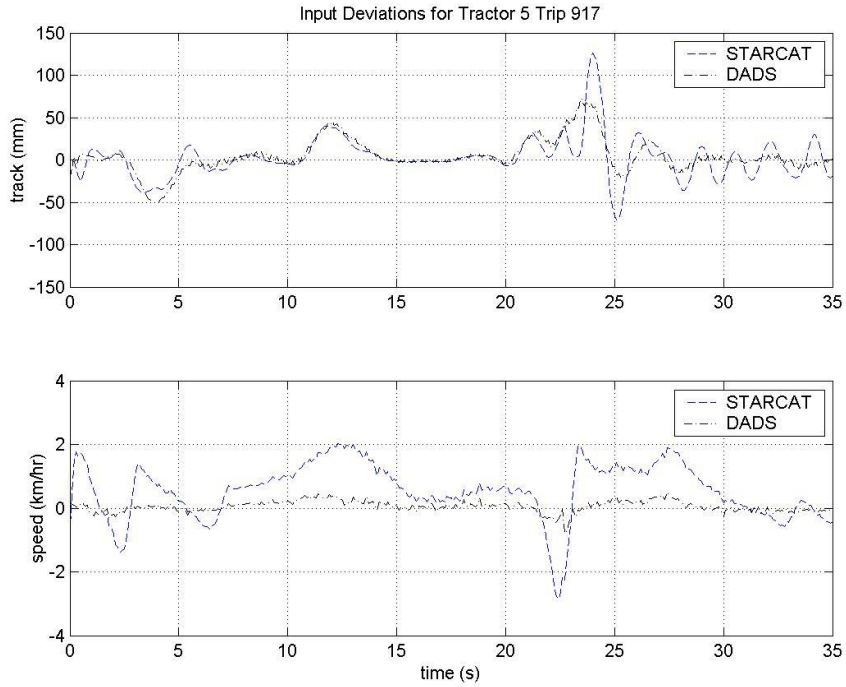


Figure 3-16: Input deviations of the simulation models for the hotspot 1 example trip

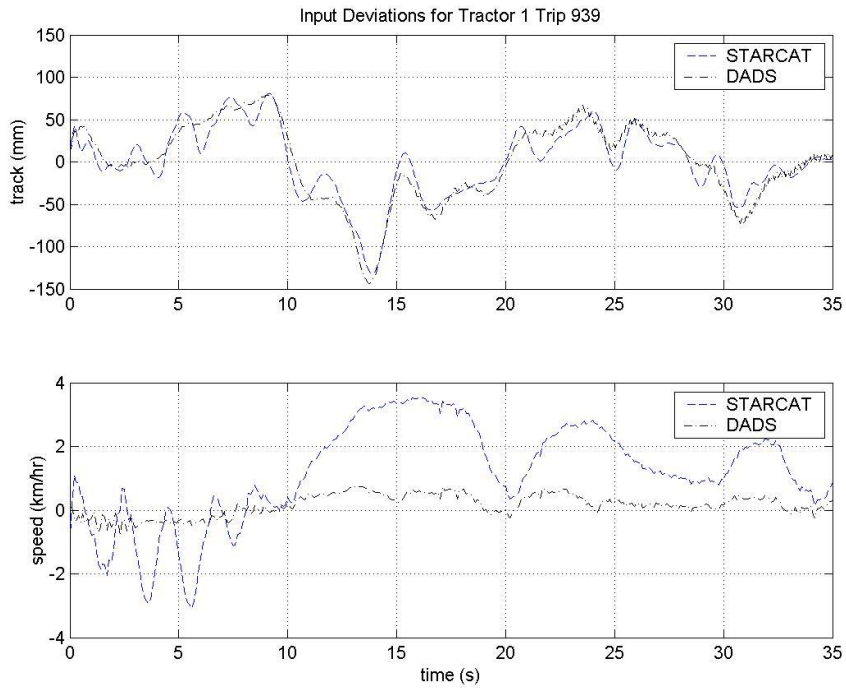


Figure 3-17: Input deviations of the simulation models for the hotspot 2 example trip

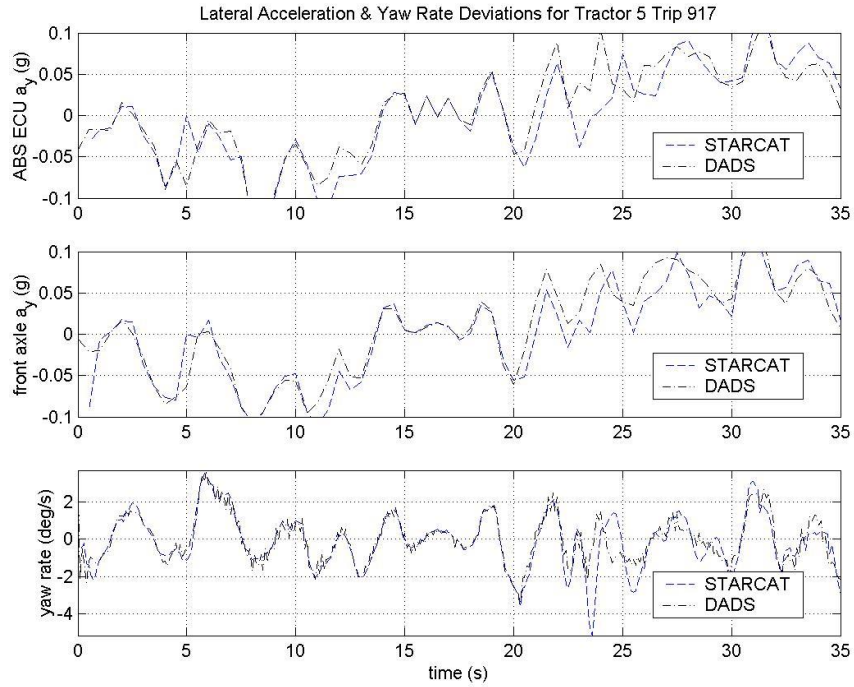


Figure 3-18: Sensor comparisons of the simulation models for the hotspot 1 example trip

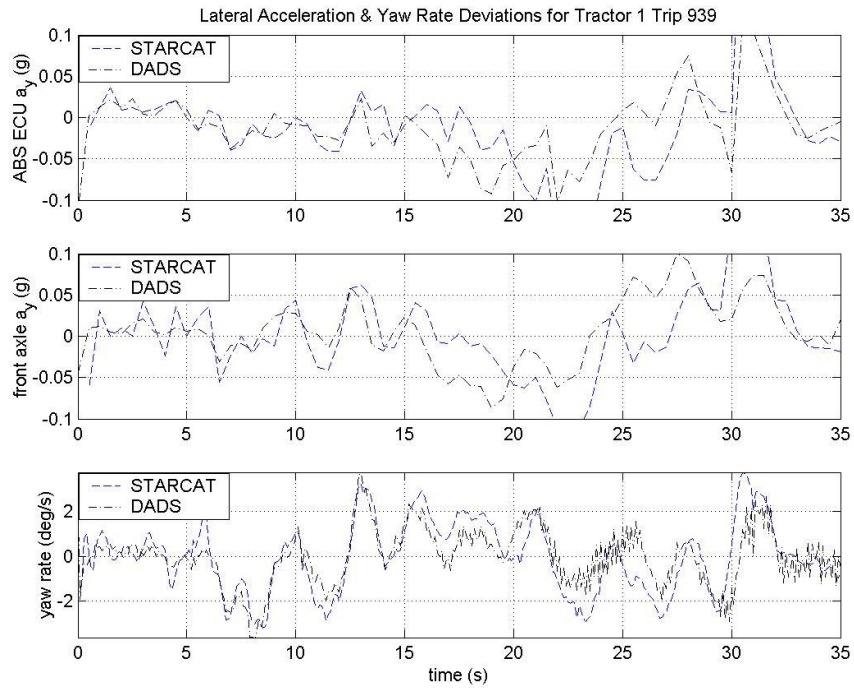


Figure 3-19: Sensor comparisons of the simulation models for the hotspot 2 example trip

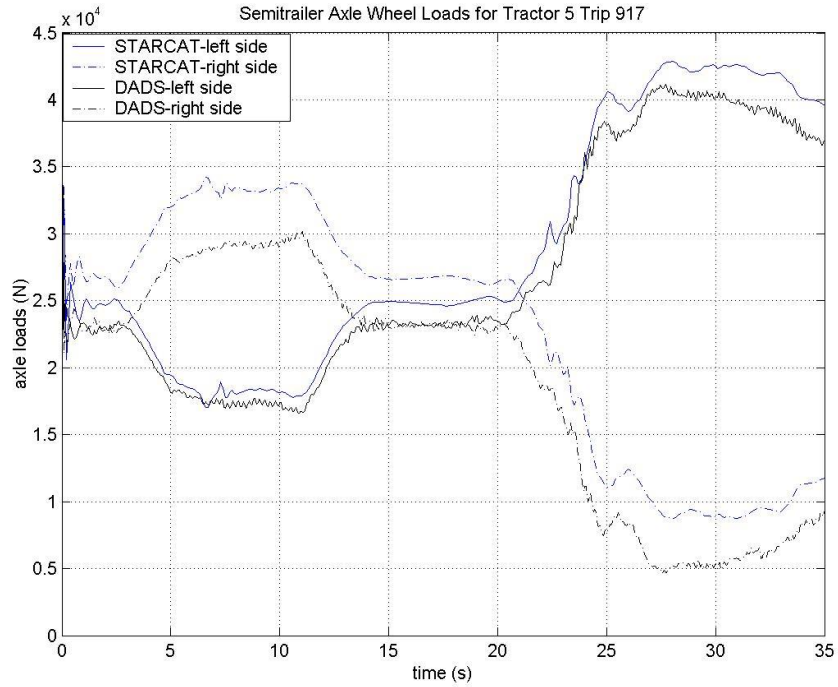


Figure 3-20: Axle wheel loads comparisons of the simulation models for the hotspot 1 example trip

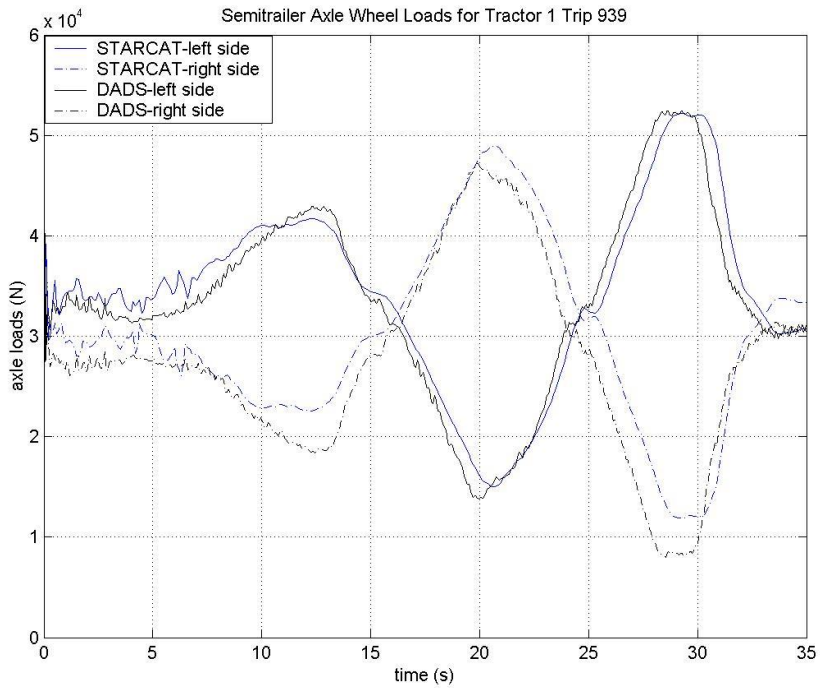


Figure 3-21: Axle wheel loads comparisons of the simulation models for the hotspot 2 example trip

3.3.3.3 FOT & Model Validation

The track deviation plots (Figure 3-16 and Figure 3-17) and the yaw rate deviation plots (Figure 3-18 and Figure 3-19) in conjunction with the path plots for (Figure 3-22 and Figure 3-23) show that the simulation models are tracking the mathematical description of the vehicle path relatively well. However, the yaw rate deviation can be significant with respect to the FOT tractor yaw rate. Thus, problems with GPS accuracy and the assumption of constant curvature over the length of a segment could be revisited to improve accuracy.

The lateral acceleration sensor measurement on a rigid, non-suspended vehicle (Tseng, 2001) can be written as Equation 3.8.

$$a_{y,m} = \dot{v} + ur - g \sin \varphi + n_a \quad \text{Equation 3.1}$$

where $a_{y,m}$ is the measured lateral acceleration (parallel to the road bank), \dot{v} is the vehicle lateral acceleration (parallel to the road bank), u is the vehicle longitudinal velocity, g is the acceleration of gravity, φ is the road bank angle (positive for left side up), and n_a is the accelerometer sensor noise.

Equation 3.8 infers that for the FOT and model validation, the lateral acceleration of the model, if perfectly accurate, would be off no more than the sine of the bank angle. For hotspot 1 and 2 this is approximately 0.080 g at the maximum superelevation. The flexibility of the chassis not represented in the model tempers this somewhat. Examination of the acceleration results shows that when the yaw rate is greatest, the acceleration deviations at the ABS ECU sensor and front axle are also highest, which corresponds to the peak road superelevation.

In summary, the flat road track coupled with the inaccuracies in the mathematical representation of the track and the rigid body assumptions make the quantitative validation less accurate. However, the qualitative trends results are certainly represented as seen in Figure 3-24 and Figure 3-25.

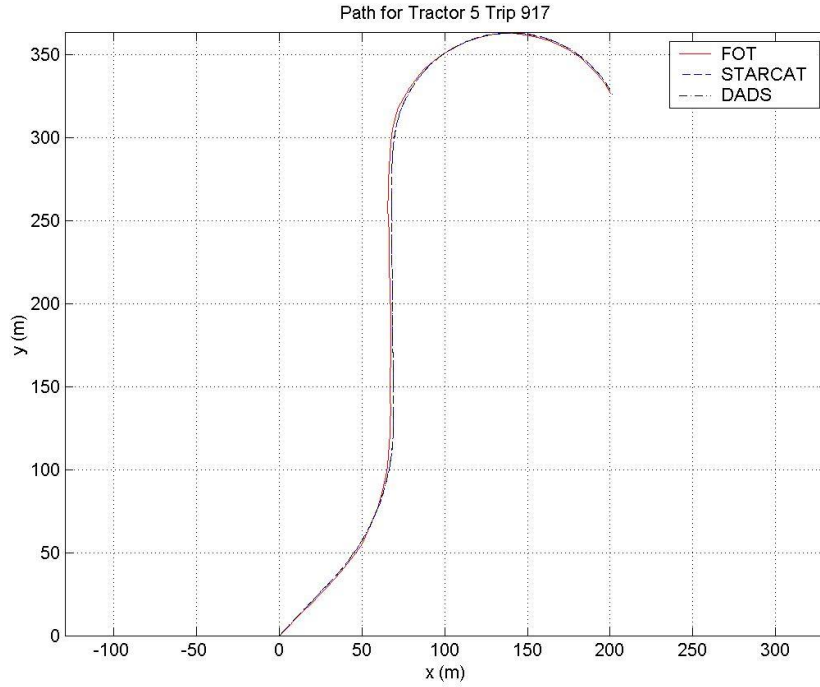


Figure 3-22: Path of the FOT vehicle and simulation models for the hotspot 1 example trip

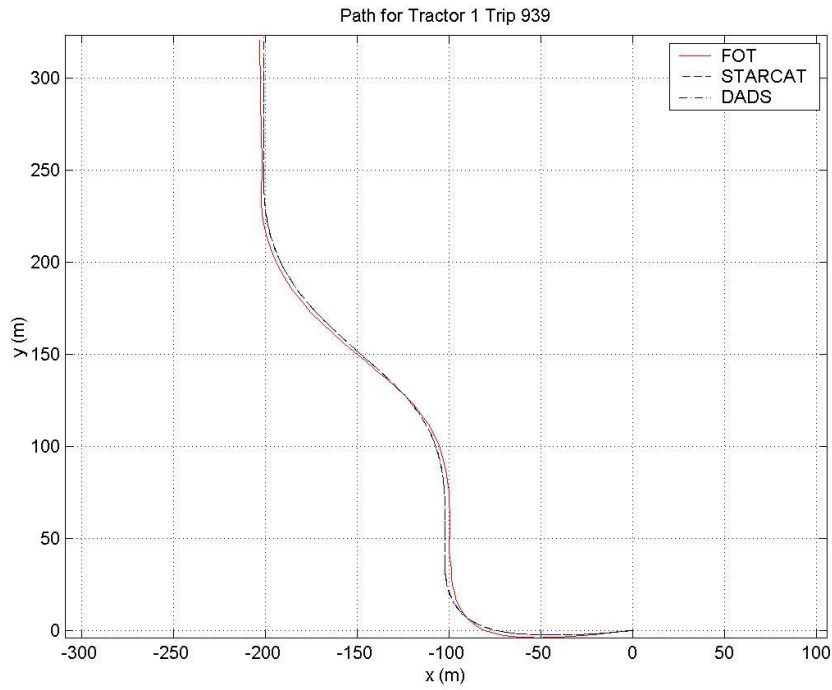


Figure 3-23: Truncated path of the FOT vehicle and simulation models for the hotspot 2 example trip

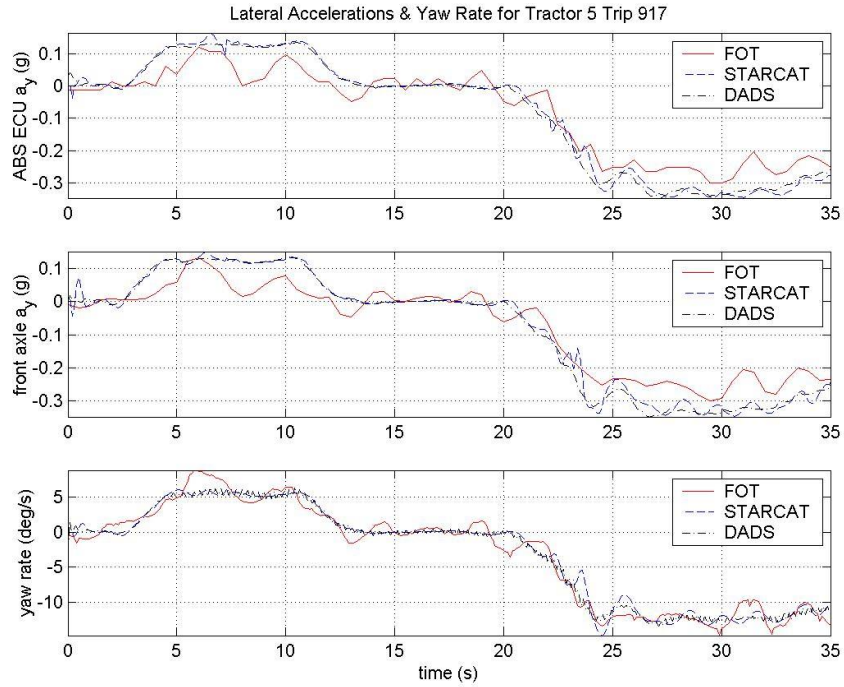


Figure 3-24: Sensor comparisons of the FOT vehicle and simulation models for the hotspot 1 example trip

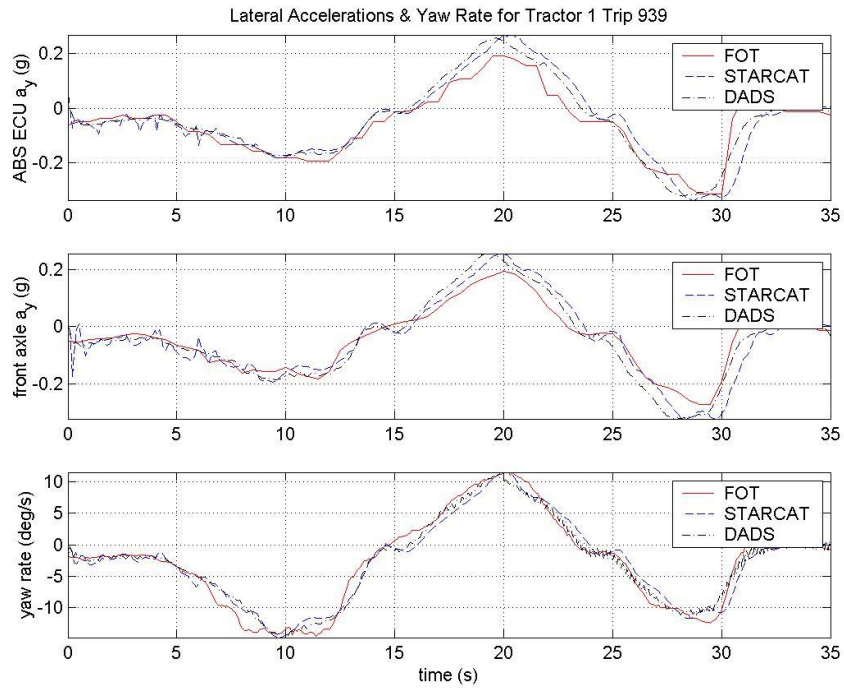


Figure 3-25: Sensor comparisons of the FOT vehicle and simulation models for the hotspot 2 example trip

3.3.4 Results and Analysis

3.3.4.1 Rollover Margin Definition

It is the convention to define the static rollover threshold of a vehicle as the liftoff of both axles on one side (Gillespie, 1992). For the purposes of this study, the static and dynamic rollover threshold is defined as the occurrence of tire liftoff of either semitrailer axle.

This more conservative rollover threshold is adopted for two reasons. First, for predictive purposes, it makes sense to have a more conservative measure of the threshold. Even when the threshold has been met, it is still possible to take corrective actions (e.g. active braking). Second, the semitrailer suspension may be designed such that the occurrence of rear axle liftoff is soon followed by liftoff of the front tandem axle.

Mathematically, this alternative rollover threshold can be expressed as Equation 3.2

$$\frac{a_{y,crit}}{g} = \frac{a_y|_{F_{N,tire} \rightarrow 0}}{g} \quad \text{Equation 3.2}$$

where $F_{N,tire}$ is the axle load on any semitrailer tire. This rollover threshold can be applied for static or dynamic conditions. Again, it is noted for the sake of clarity that this is the first occurrence of tire liftoff. Practically speaking, this will be the outside tire on the rearmost inside axle (with respect to the road curvature) of the vehicle.

A quasi-static model of a rigid, non-suspended vehicle (Gillespie, 1992) defines the rollover threshold as Equation 3.3.

$$\frac{a_{y,crit}}{g} = \frac{t}{2h_{cg}} + \varphi \quad \text{Equation 3.3}$$

where t is the vehicle track width and h_{cg} is the vehicle center of gravity height. This first-order approximation states the obvious about vehicle rollover: as far as the vehicle is concerned, the track and the center of gravity height have significant influence on the vehicle roll stability.

In general, the track width for heavy trucks is not going to vary as much as the center of gravity height. In the case of the FOT vehicles, the track width is fixed. Because all of the FOT tractors and semitrailers are essentially the same, the vehicle center of gravity height varies mostly due to changes in semitrailer payload. Since the FOT semitrailers always carry liquid nitrogen, the semitrailer pressure vessel and payload center of gravity height can be determined analytically.

The semitrailer pressure vessel is idealized as a cylinder that fills nonlinearly due to its circular cross-section. When the pressure vessel is combined with the rest of the semitrailer components, the overall semitrailer center of gravity height varies as shown in

Figure 3-26 for the STARCAT model. Note that the center of gravity height is the same at about 45% payload as at the empty payload condition.

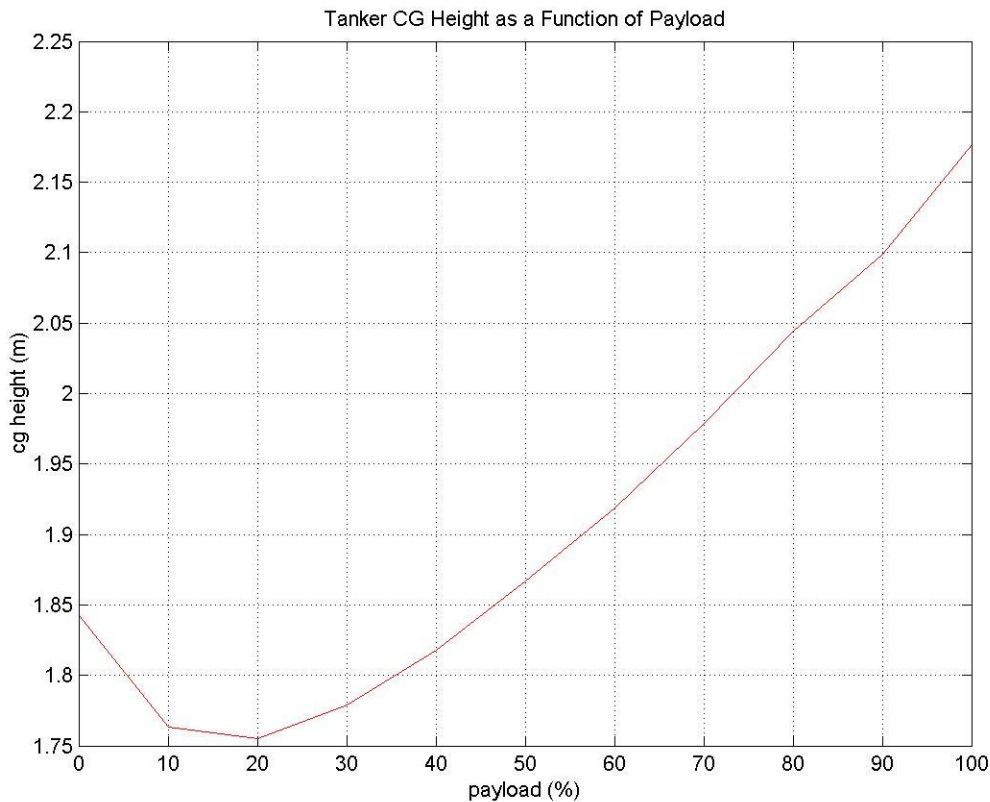


Figure 3-26: Nonlinear relationship between payload percentage and center of gravity height for the tanker semitrailer

In the static and dynamic analyses that follow, the results are expressed as a function of payload percentage, which is specific to the FOT vehicle. They can also be expressed as a function of the center of gravity height according to Figure 3-26. This makes the results more general and thus more useful.

3.3.4.2 Static Rollover

3.3.4.2.1 Test setup

To investigate the static rollover threshold, a tilt table test is simulated in the DADS environment. The DADS model described in the previous sections is placed on a rotating platform. The platform rises up to a maximum angle of 35 degrees during the simulation. Different payload conditions are simulated for the tare tractor and semitrailer up to full payload. Two different models are simulated, one with a fixed (solid) payload and a second version that accounts for the fluid sloshing in the inner vessel. Both have a rigid tractor chassis.

The semitrailer inner pressure vessel is divided into several compartments to minimize longitudinal sloshing during braking. For the fixed payload model, the payload is connected to the semitrailer with bracket joints. With the sloshing model, the payload masses are attached by spherical joints to the semitrailer in their respective compartments.

There are two boundary conditions used to define the static rollover threshold. For comparison with the dynamic rollover threshold (section 3.3.4.3), the boundary condition is Equation 3.2. To compare the model with the results of the FOT tilt table tests, it is assumed that the lateral acceleration at the time of first axle liftoff defines the static rollover threshold.

3.3.4.2.2 Tilt table tests

Figure 3-27 shows two plots of the tilt table test for the DADS model with a rigid frame. The upper plot shows the event with one tire liftoff as the rollover threshold criterion. Because of the lateral movement of the payload, the critical lateral acceleration for rollover is lower for the sloshing load than the fixed load. This effect is especially prominent in the mid-payload range. The lower plot shows the lateral acceleration, when axle liftoff occurs. The difference between tire liftoff and axle liftoff is that the rollover threshold increases on average 0.034 g and 0.036 g for the fixed and sloshing payloads, respectively.

The theoretical simulated static rollover threshold (SSRT) of a rigid (non-compliant) vehicle is defined as (Winkler, Blower, Ervin, 2000)

$$\frac{a_{y,crit}}{g} = \tan(\alpha) = \frac{t}{2h_{cg}} \quad \text{Equation 3.4}$$

where α is the tilt table angle. This critical acceleration is further reduced by vehicle compliances (tractor chassis, suspension, tire, and fifth wheel). The rigid SSRT shown in Figure 3-28 is calculated according to the Equation 3.4 by using the properties of the DADS vehicle model. The reduced slope of the rigid SSRT for near empty conditions is explainable by a lowered center of gravity height with increasing load (see Figure 3-26).

The results of the vehicle model with a fixed payload look very similar to the rigid SSRT, only shifted down an average of 0.11 g due to compliances in the model. The change in slope of the SSRT for the fixed payload model also has a reduced slope at near empty conditions like the rigid SSRT. The model results with the sloshing payload has the same tendency as the FOT vehicle test and (Winkler, Blower, Ervin, 2000), only shifted downward an average of 0.072 g relative to the FOT data.

As shown in Figure 3-28, the FOT SSRT slightly exceeds the rigid SSRT for an empty semitrailer. This is probably caused by differences in vehicle parameters used for the rigid SSRT calculation that are different from the FOT tilt table test setup. A summary of the tilt table results is given in Table 3-5.

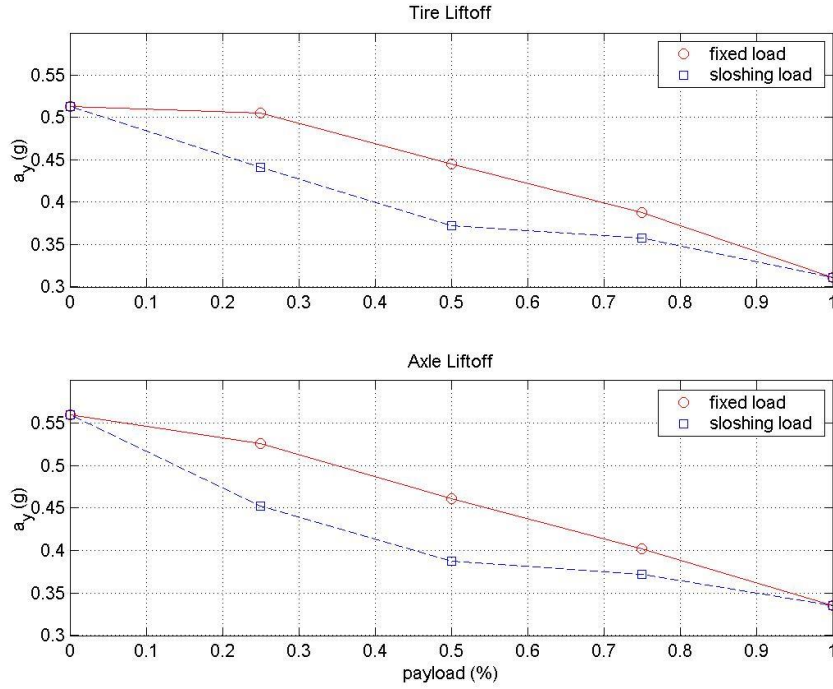


Figure 3-27: DADS tilt table tests of a vehicle with fixed and sloshing payloads and with different liftoff criteria

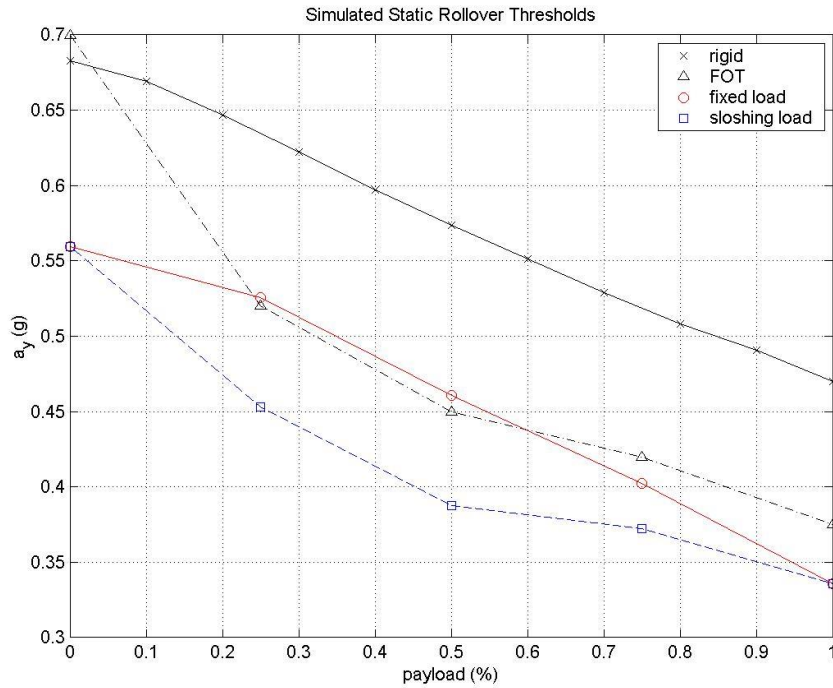


Figure 3-28: Comparison of tilt table test results for axle liftoff conditions

Table 3-5: Summary of tilt table tests

Payload	Vehicle Mass	SSRT ¹	FOT Vehicle	Fixed Payload		Sloshing Payload	
				Tire liftoff	Axle liftoff	Tire liftoff	Axle liftoff
%	kg	g	g	g	g	g	g
0	13,621	0.68	0.70	0.51	0.56	0.51	0.56
25	19,200	0.63	0.52	0.50	0.53	0.44	0.45
50	24,771	0.57	0.45	0.46	0.46	0.37	0.39
75	30,346	0.51	0.42	0.38	0.40	0.36	0.37
100	35,921	0.47	0.38	0.31	0.34	0.31	0.34

¹ Simulated Static Rollover Threshold.

3.3.4.3 Dynamic Rollover

3.3.4.3.1 Test setup

The data extracted from the database for the trips in Table 3-3 have been selected with the intent to look at more extreme cases according to the criteria specified in section 3.3.2.3.4. For the dynamic rollover tests, it is desirable to push the vehicle to the rollover threshold as defined in Equation 3.2. The road description remains the same for these tests but the question arises as to what realistic speed profile to provide the model. Here, the original speed profile for a given trip is scaled spatially.

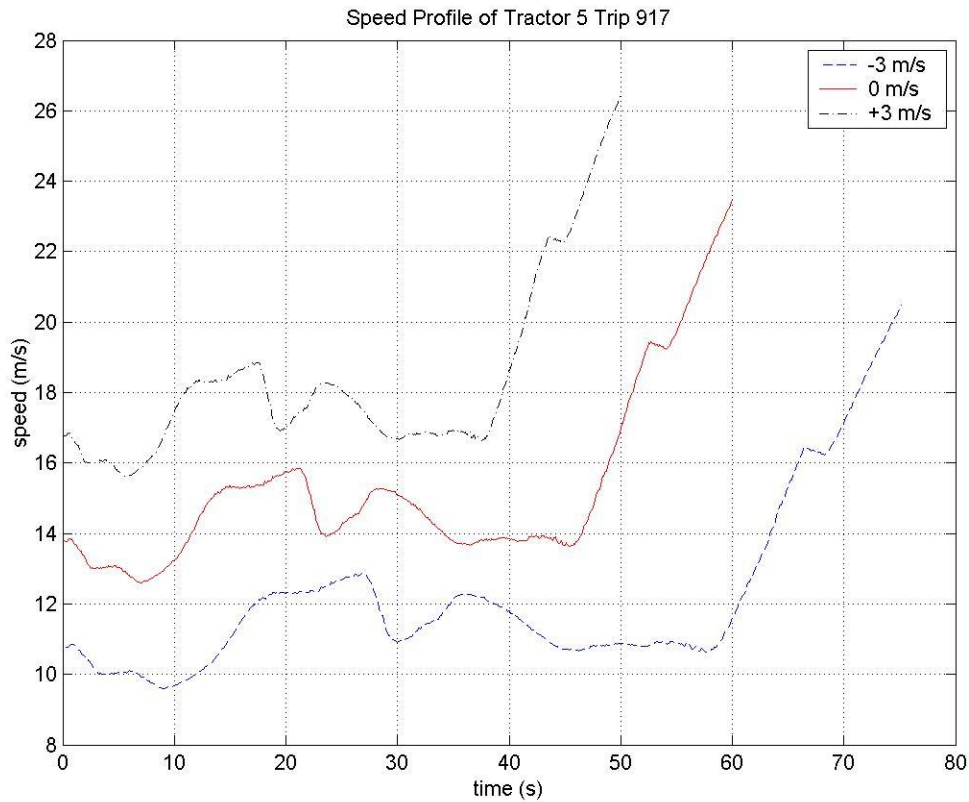


Figure 3-29: An example of speed scaling

This scaling is done by expressing the original speed profile as a function of distance traveled. In this way, a constant can be added to the velocity that preserves the spatial relationship of the velocity to the road (i.e. curvature). Then the velocity is transformed back to the time domain. Figure 3-29 shows the speed profile for the nominal case and where the speed has been spatially-scaled up and down by 3 m/s.

The results in Figure 3-29 are intuitive in that if a vehicle travels at an increased speed, then the time required to travel the same distance will decrease, and vice versa. The relationship between the curvature and vehicle speed is maintained.

Some final comments about the results should be made. All of the simulations are run on flat tracks and the effects of sloshing are not included, both of which lower the critical lateral acceleration. However, the tractor chassis is rigid, which increases the rollover stability. The lateral accelerations of the tractor and semitrailer are measured at their respective centers of gravity in order to eliminate the influence of tractor roll (as with the ABS ECU sensor).

The dynamic tests are conducted by simulating the trips in Table 3-3 and determining the critical vehicle lateral acceleration for varying semitrailer payload conditions (in 10% increments). The input conditions and lateral accelerations at the critical condition are examined for trends within the trips for each hotspot and against the trips for the two hotspots.

3.3.4.3.2 Example hotspot cases

The results for tractor 5 trip 917 and tractor 1 trip 939 are reviewed here concurrently as example results for hotspots 1 and 2, respectively. Figure 3-30 and Figure 3-31 show the paths followed by the vehicle for tractor 5 trip 917 and tractor 1 trip 939. The locations of tire liftoffs are clustered within segments of 13.0 and 19.5 meters in length, respectively. The former is nearly equivalent to the length of the semitrailer. This is typical of the other trips as well.

There are exceptions to this clustering as seen in Figure 3-31 for the empty payload case for the hotspot 2 example. The critical acceleration is almost achieved at the same location on curve 3 as the other payload cases. The scaled speed was incremented, which caused the vehicle to lose control on curve 1 instead of curve 3. These “outliers” occur in 18.2% of all the trips simulated, of which 95% were lightly loaded (30% payload or less). Due to the fact that hotspots 1 and 2 are complex curves, many of the outlier cases shifted to different curve segments or to the transition between curve segments.

The issue as to the cause of the outlier cases is worth pursuing in more detail. Because the center of gravity height is about the same with no payload as at 40% payload, it could be expected that an outlier case might occur at the 40% payload condition as well. However, as noted above, these outlier cases occur for 30% payload or less.

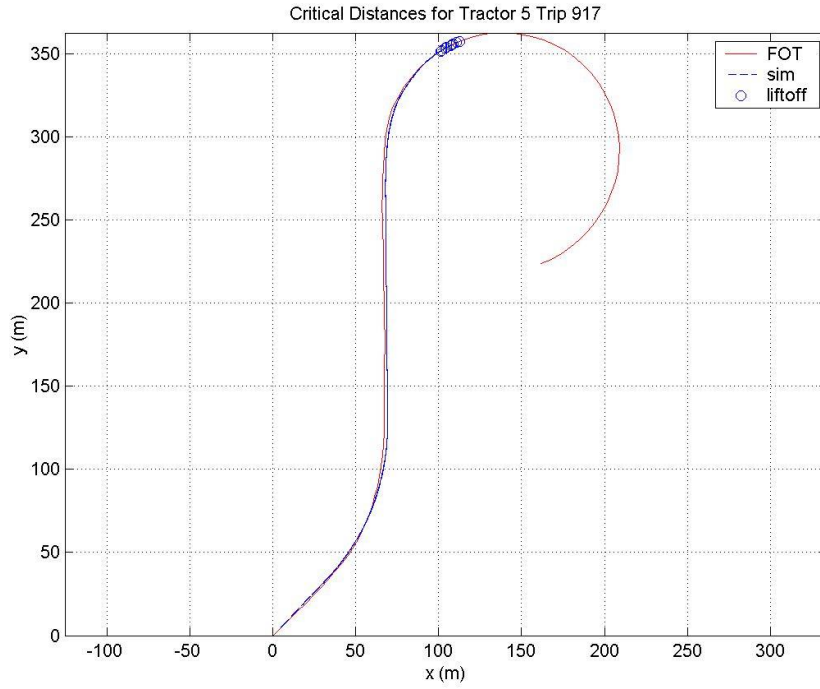


Figure 3-30: Locations of wheel liftoff for all payloads for hotspot 1 example

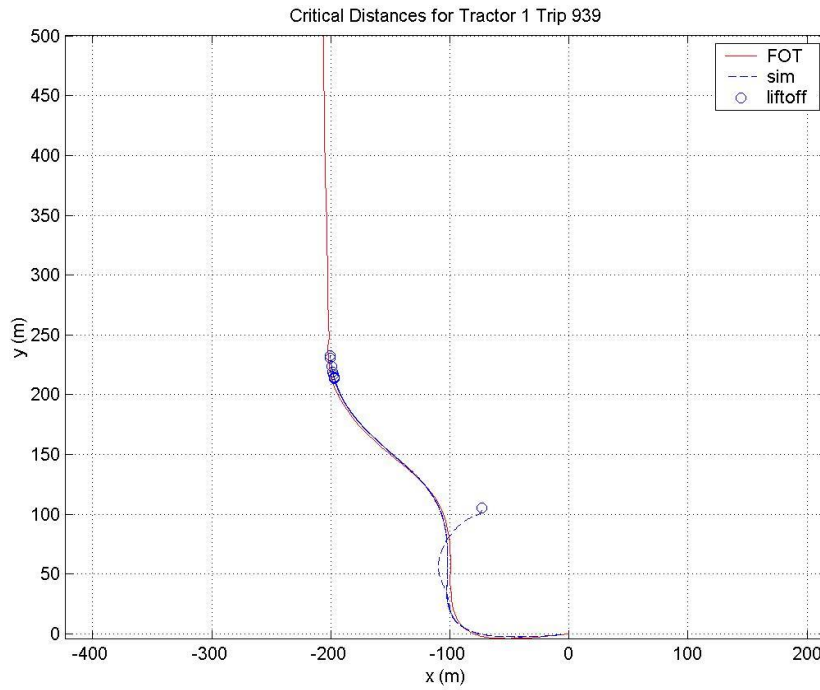


Figure 3-31: Locations of wheel liftoff for all payloads for hotspot 2 example

The simulations predict that the cause of the majority (about 75%) of the outlier cases is the vehicle is no longer able to develop the lateral forces sufficient to follow the required path at the required speed and either understeers (hotspot 1 and 2 trips) or slides out of control (some hotspot 2 trips). The vehicle slides out of control only for the hotspot 2 trips at a particularly transient point (see Figure 3-14) on the transition between curves 1 and 2. The tire models develops lower lateral forces at lower normal loads. This is consistent with the observation that these outlier cases occur at lightly loaded conditions. The outlier case for tractor 1 trip 939 is not included in the results plots because the model is not valid by the time tire liftoff occurs.

The inputs at the time that the critical acceleration occur are shown in Figure 3-32 and Figure 3-33. It is seen that the curvature is fairly constant for all payload cases due to the clustering effect seen in Figure 3-30 and Figure 3-31. The critical speed is seen to decrease in a nearly linear manner with respect to the payload cases. It is interesting to note that the difference between the critical speed at unloaded and loaded conditions for the two cases is approximately 3.2 m/s and 3.1 m/s, respectively. These results suggest the sensitivity of vehicle rollover to critical speed and that the speed need not be reduced significantly in order to prevent vehicle instability. The results for the other hotspot trips are summarized in Volume III, Appendix-E.

The critical lateral accelerations measured at the tractor and semitrailer centers of gravity and the ABS ECU location are shown in Figure 3-34 and Figure 3-35 for all payload cases. The absolute value of the critical accelerations are used for the sake of comparison. The acceleration data are curve-fitted by fourth-order polynomials.

The most important thing to note is how similar the range of critical lateral accelerations are between the two examples. The peak in the critical acceleration plots at 10 to 20% payload is due to the nonlinear relationship between the amount of payload and the semitrailer center of gravity height. Note that the sensor critical acceleration is offset due to chassis roll in both cases.

Expressing the critical accelerations as a function of payload condition (or mass) is specific to this FOT vehicle configuration. A more useful, general approach to looking at the data is to relate the same critical lateral accelerations to the center of gravity height as is done in Figure 3-36 and Figure 3-37.

The resulting transformed data now has a “hook” effect, again due to the nonlinear relationship shown in Figure 3-26. The empty and 10% payload conditions are neglected in the new curve fits. This is done to simplify the curve fits and is more conservative as these payload conditions have critical lateral accelerations higher than the resulting curve fit. With this simplification, the resulting data has a much simpler form and can be approximated with a second-order polynomial.

Volume III, Chapter 3
Theoretical Rollover Warning Effectiveness – Task 20

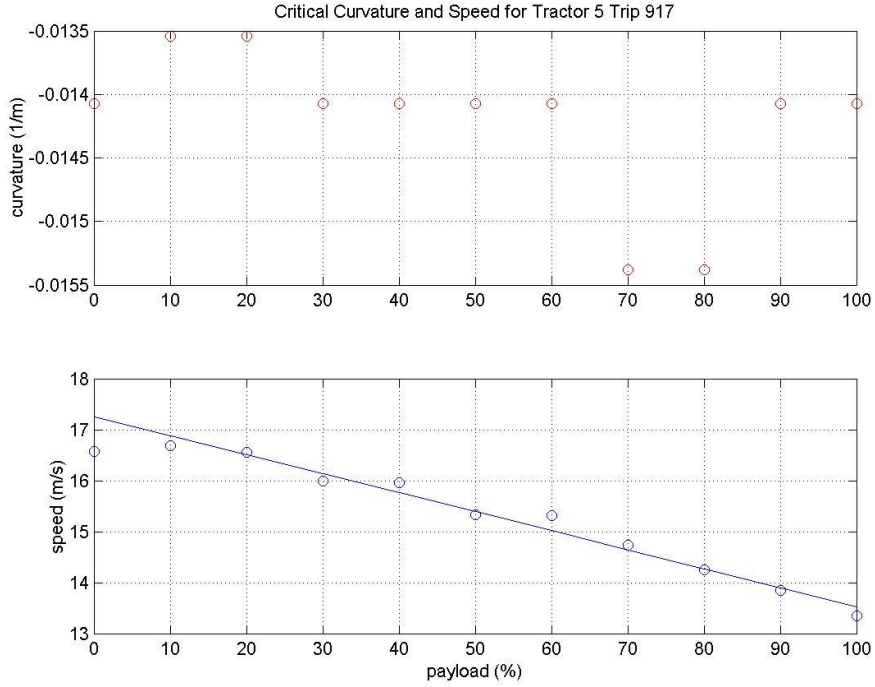


Figure 3-32: Critical curvature and speed as a function of payload for hotspot 1 example

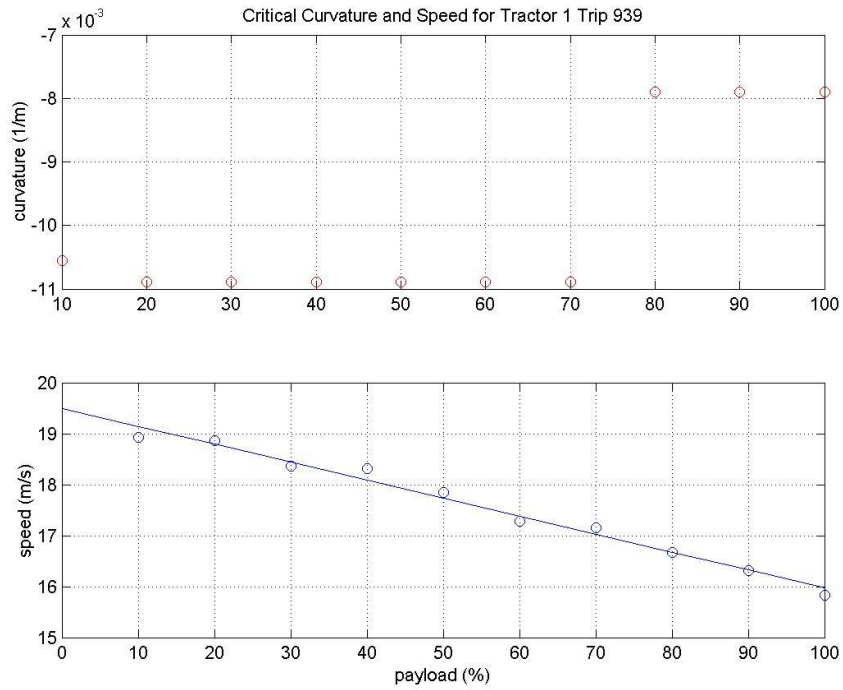


Figure 3-33: Critical curvature and speed as a function of payload for hotspot 2 example

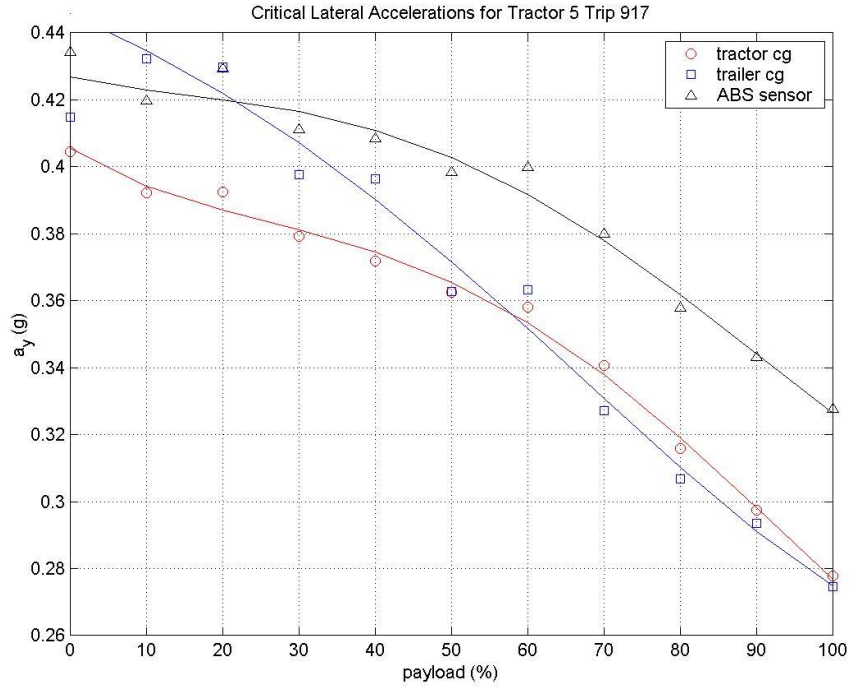


Figure 3-34: Critical accelerations as a function of payload for hotspot 1 example

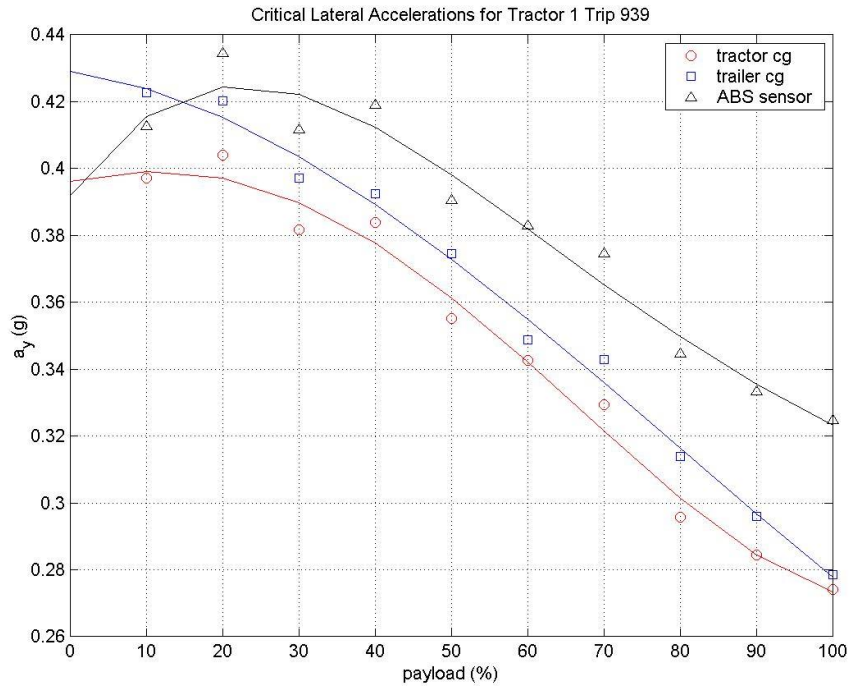


Figure 3-35: Critical accelerations as a function of payload for hotspot 2 example

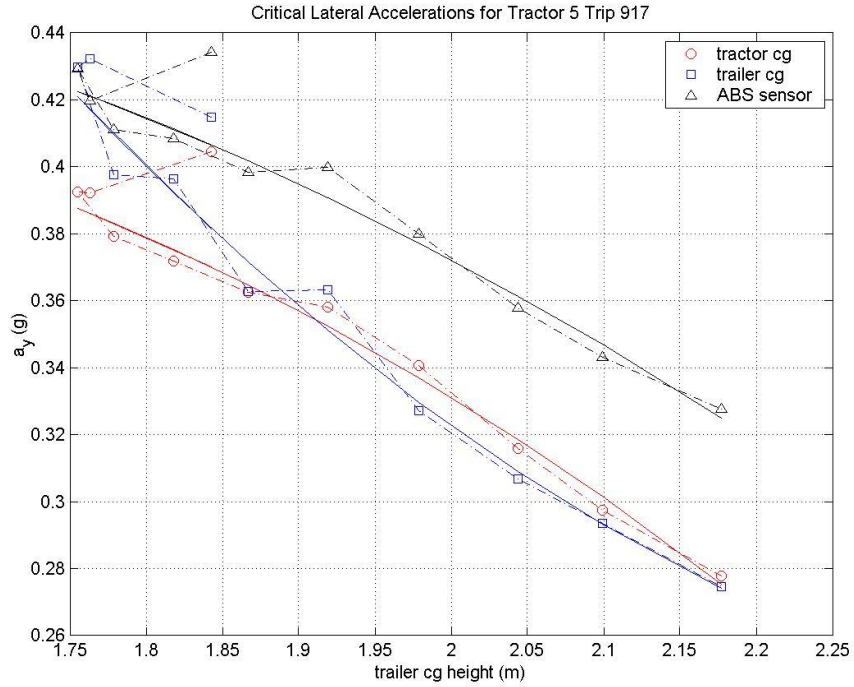


Figure 3-36: Critical accelerations as a function of center of gravity height for hotspot 1 example

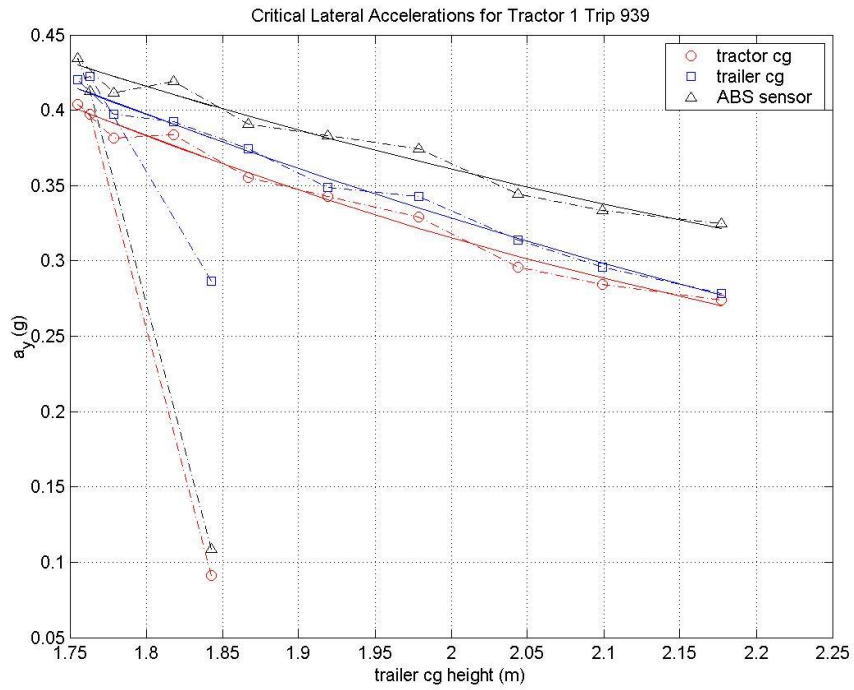


Figure 3-37: Critical accelerations as a function of center of gravity height for hotspot 2 example

3.3.4.3.3 Hotspots 1 & 2 comparison

Some trends appear when looking at all the trips simulated for hotspots 1 and 2. Figure 3-38 and Figure 3-39 show the critical acceleration plots with respect to semitrailer center of gravity height for hotspots 1 and 2, respectively. As before, the first two payload conditions (empty and 10%) are neglected in the second-order curve fit and are here not shown. The curve fit can be expressed as Equation 3.5.

$$f(z_{cg}) = c_2 z_{cg}^2 + c_1 z_{cg} + c_0 \quad \text{Equation 3.5}$$

and the curve fit coefficients are summarized in Table 3-6 for comparison.

While hotspot 1 and 2 are different, complex curves and each trip has unique path and speed inputs, qualitatively and quantitatively speaking the resulting critical lateral accelerations are quite correlated. Another trend that is apparent from Table 3-6 is most of the curve fits have a positive curvature, for both the tractor and semitrailer. Of those that have negative curvature, half are approximately linear.

Figure 3-40 shows that the critical speed trend observed in the earlier hotspot examples is typical of all the simulated trips. The average critical speed difference over the range of semitrailer center of gravity heights is on the order of 3 m/s.

Table 3-6: Relationship between critical lateral accelerations and semitrailer center of gravity height

Hotspot	Tractor	Trip	Tractor Curve Fit			Semitrailer Curve Fit		
			c ₂	c ₁	c ₀	c ₂	c ₁	c ₀
			g/m	g/m	g/m	g/m	g/m	g/m
1	1	930	-0.1812	0.3861	0.2855	0.2604	-1.3310	1.9362
	1	953	0.2932	-1.5145	2.2045	0.3215	-1.6080	2.2445
	4	897	0.0991	-0.6955	1.3332	0.1038	-0.6891	1.2884
	5	862	0.8348	-3.6402	4.2557	-0.0314	-0.1671	0.7845
	5	917	-0.1995	0.5187	0.0919	0.3022	-1.5362	2.1861
2	1	878	0.5129	-2.3176	2.8957	0.3129	-1.5735	2.2212
	1	939	0.2207	-1.1767	1.7862	0.1519	-0.9216	1.5641
	5	862	0.7973	-3.5374	4.2000	0.2801	-1.4354	2.0748
	5	939	-0.0249	-0.1853	0.7941	0.1560	-0.9483	1.6026
	5	982	0.2592	-1.3027	1.8918	0.0260	-0.4121	1.0534

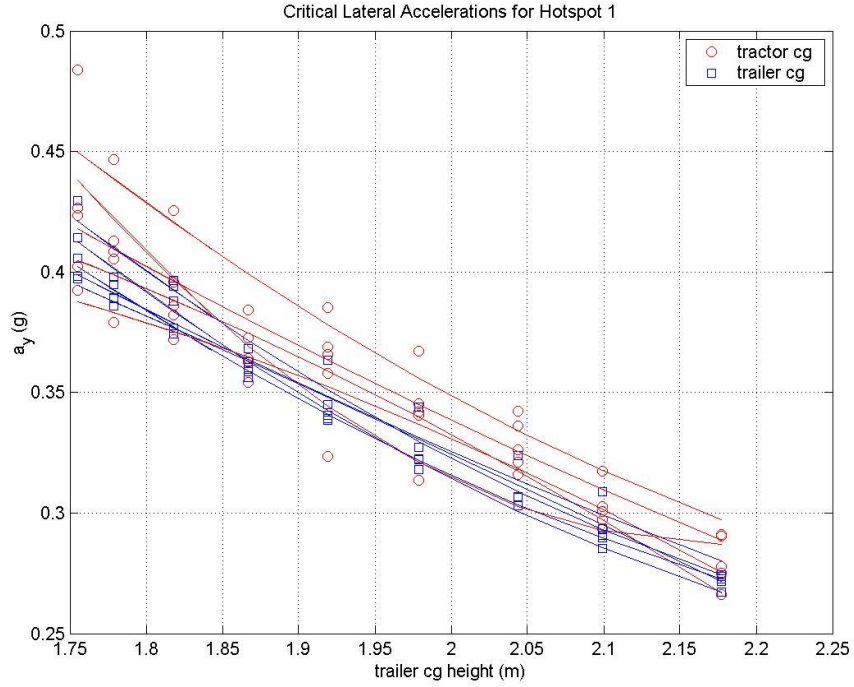


Figure 3-38: Critical accelerations as a function of center of gravity height for all hotspot 1 trips

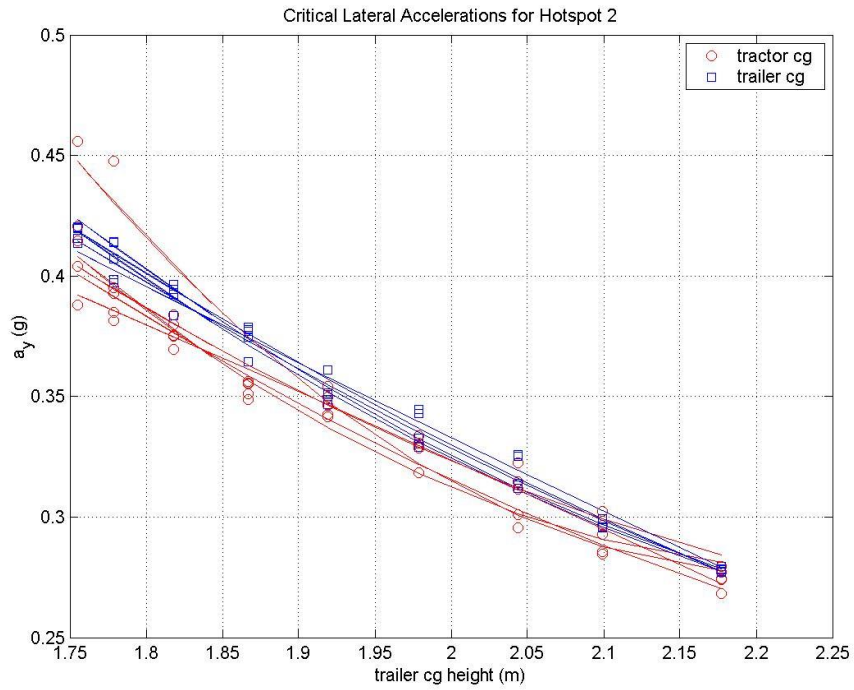


Figure 3-39: Critical accelerations as a function of center of gravity height for all hotspot 2 trips

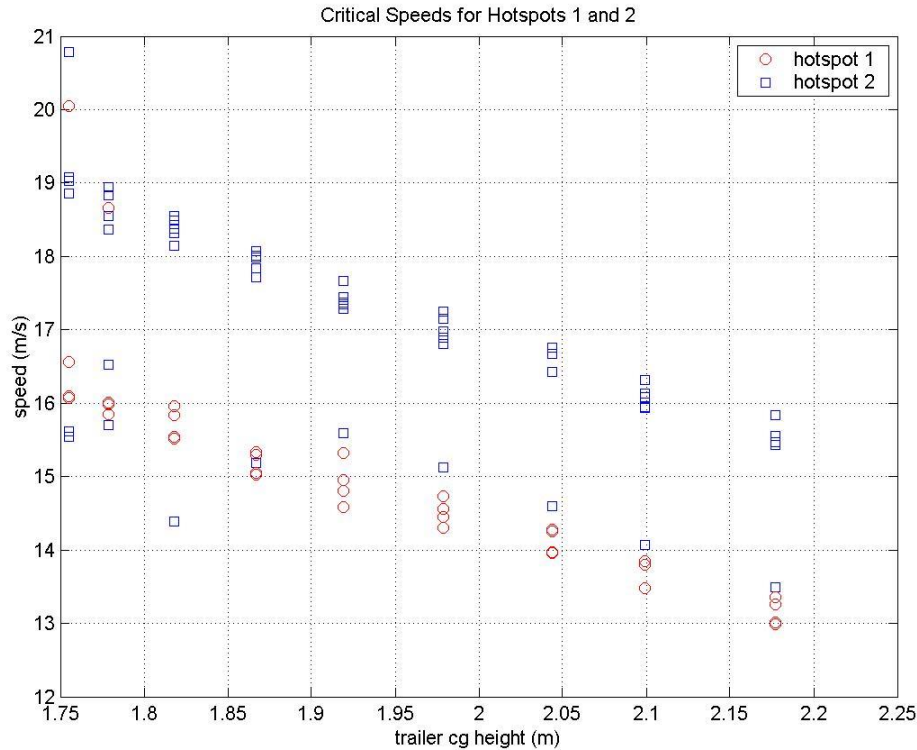


Figure 3-40: Critical vehicle speeds as a function of center of gravity height for all hotspot 1 and 2 trips

3.3.4.4 Static vs. Dynamic Rollover

At this point it is useful to compare the results of the static and dynamic rollover simulations from sections 3.3.4.2 and 3.3.4.3, respectively. The static results are the same as shown in the first plot of Figure 3-27. The dynamic results are the averaged critical lateral accelerations for all hotspot 1 and hotspot 2 trips. The STARCAT and DADS models, while not exactly the same, are well correlated as previously demonstrated.

It is clear from Figure 3-41 that the dynamic rollover threshold is lower than the static rollover threshold (for fixed payload). In an absolute sense, the difference between the thresholds narrows as the semitrailer center of gravity height increases. In a relative sense however, it is not possible to come to this conclusion without further simulations.

The results do suggest that for a nominal on-highway tractor and semitrailer combination the dynamic rollover threshold could be expected to be around 10 to 15% lower than the static rollover threshold. The results for the tilt table sloshing test indicate that the dynamic sloshing results could be lower by 10 to 15% as well, for the corresponding center of gravity height range.

These dynamic rollover threshold curves, which are the result of real-world driving conditions applied to reasonable dynamic models, are simple enough to be the basis for an algorithm that proactively attempts to mitigate heavy truck rollover.

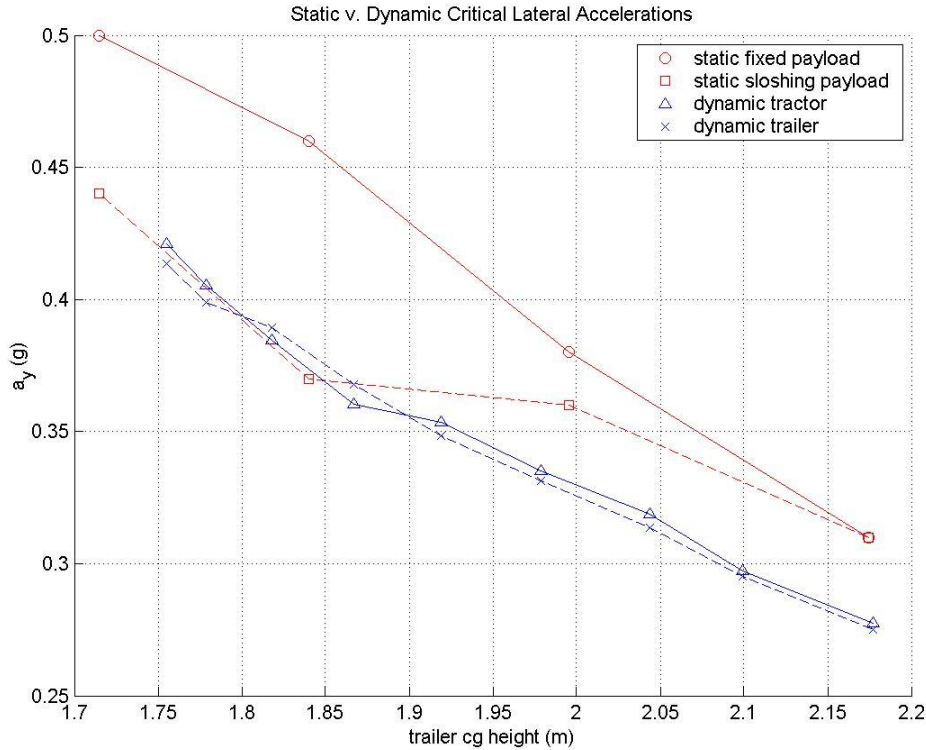


Figure 3-41: Critical accelerations as a function of center of gravity height for static and dynamic rollover simulation results

3.3.4.5 Advanced Topics

3.3.4.5.1 Fluid sloshing

To investigate the effect of fluid sloshing, the results of the simulations of two vehicles, one with a fixed load, and the other with a sloshing load, will be compared. Both cases are simulated on a flat road with the same conditions as the FOT reference trip of tractor 1 trip 939 (payload, speed, etc.).

Considering the rollover threshold as a balance of the moments about the rotating axis located along the outer tires, it will have an effect on the tire forces and the critical acceleration at which a tire liftoff occurs. This effect is caused statically by a lateral movement of the load and dynamically by the natural frequency of the load sloshing. In the simulation model, a first order approximation of this behavior is made as a pendulum rotating about the center of the tank.

Figure 3-42 shows the load transfer on the trailer axles during the maneuver for a fixed and sloshing load. The load transfer due to the maneuver characteristic of hotspot 2 is

visible, but in the case of the sloshing with a higher magnitude (approximately 10%). This expected effect decreases the critical acceleration for rollover even with a slightly loaded semitrailer. The maximum difference of axle loads, or 5000 N, occurs on curve 3 at the simulation time of about 28 seconds.

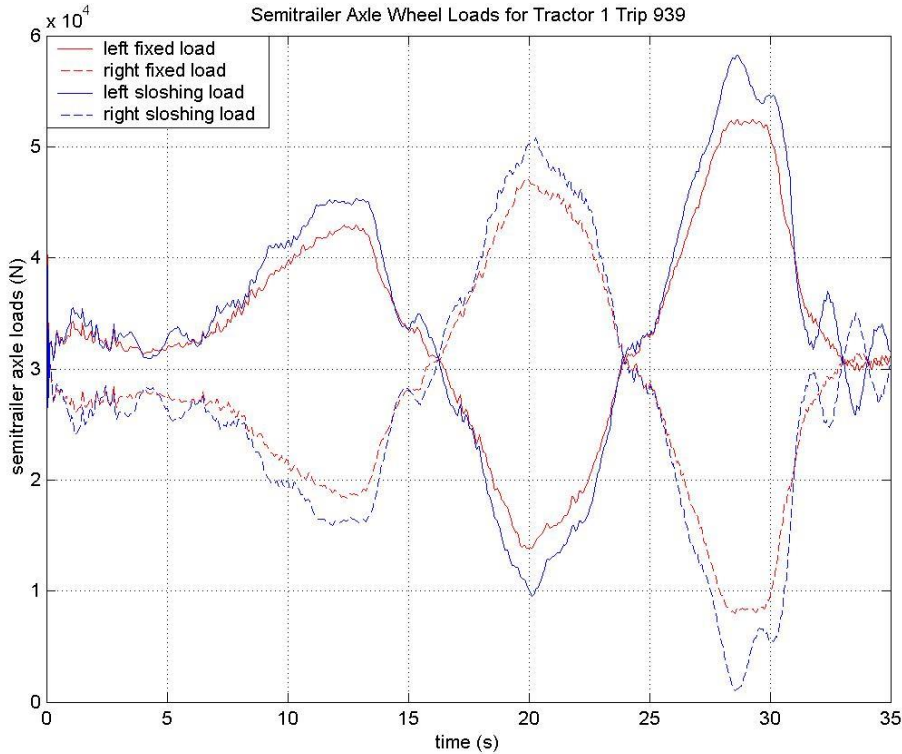


Figure 3-42. Axle wheel load transfer of trip 939 (hotspot 2) with fixed and sloshing loads.

In both simulations, a tire liftoff occurs at the rear semitrailer axle in curves one and two. The tire liftoff of the sloshing-loaded semitrailer lasts for a longer period of time than the model with the fixed load. Both lateral accelerations are about 0.25 g in the second curve and 0.35 g at the third curve.

In the third curve, the influence of sloshing is visible as well (Figure 3-42). There is an oscillating load on both axes with a frequency of 0.6 Hz, which is only observed for the sloshing load. The same phenomenon occurs at the beginning of the simulated trip. Figure 3-43 shows this movement of the loading by examination of the roll angle of the semitrailer center of gravity.

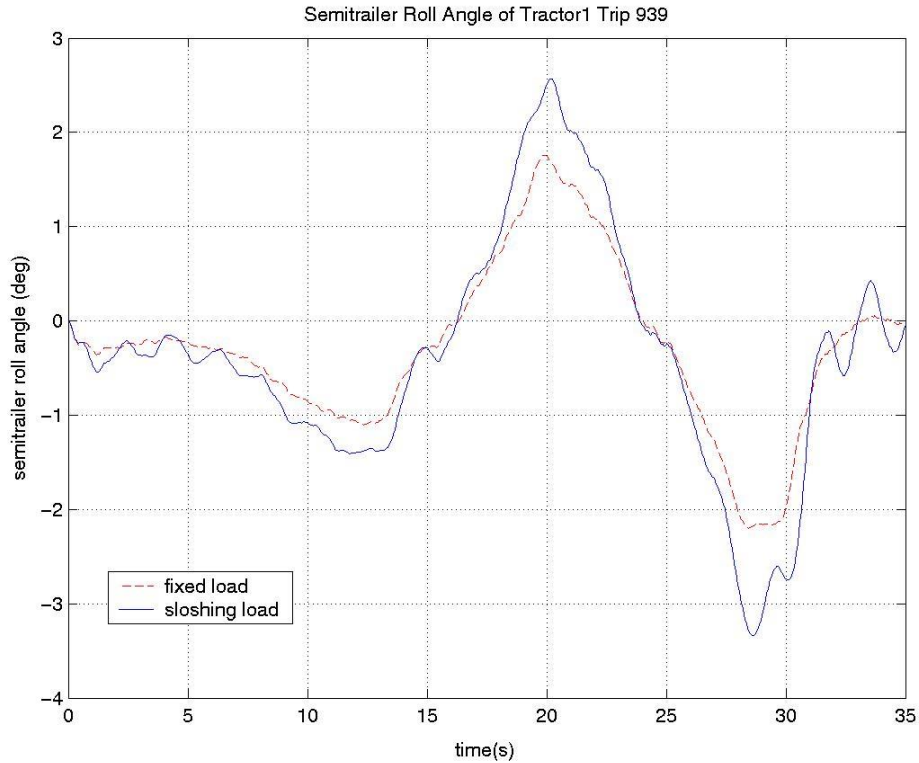


Figure 3-43. Semitrailer center of gravity roll angle with fixed and sloshing loads (hotspot 2).

3.3.4.5.2 Tractor frame torsion

The torsional frame is accomplished by dividing the tractor frame into a front frame and a rear frame. They are combined by a rotational degree of freedom about the longitudinal axis with a combined roll stiffness representing the torsional stiffness of the frame.

The simulation case is simulated on a flat road with the nominal inputs according to the FOT measurements of tractor 1 trip 939. This is compared to the flat road, fixed load vehicle model to isolate the influence of torsional stiffness. The effect of the torsional tractor frame is similar to the effect of sloshing. The semitrailer rolls more due to the decreased total roll stiffness of the vehicle which arises from the decoupling of the front and rear of the tractor frame.

3.3.4.5.3 Complex road

The complex road is a surface where the changes in elevation and the road bank angle are taken into account (see Figure 3-12 and Figure 3-15). The influence of elevation change for the risk of rollover is minor compared to the influence of banking. Elevation change affects the speed deviation of the model by approximately 0.1 to 0.2 km/hr compared to the reference simulation on a flat road.

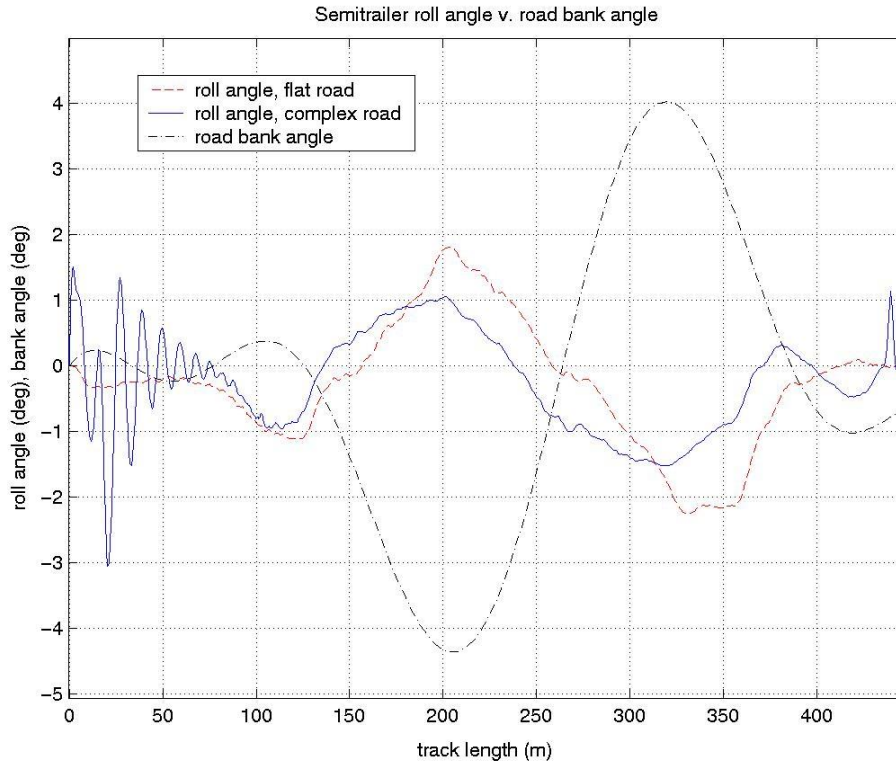


Figure 3-44. Semitrailer center of gravity roll angle for a fixed load, flat road case and a sloshing load, banked road case compared to the road bank angle.

Figure 3-44 shows the semitrailer center of gravity roll angle for a flat road surface and a road with elevation change and bank angle. The bank angle is a twelfth order approximation of the original GPS FOT data, which is used to generate the three-dimensional road. The peak bank angles occur in the second and third curve. At the start of the simulation, the bank angle has a very high oscillation, which forces the vehicle to roll. The semitrailer of the complex road model rolls less in the curves than the model on the flat road rolls. This is also confirmed by examination of the semitrailer axle loads.

The lateral acceleration is similar for both simulations. However, the load transfer is less for the rigid tractor frame model on a banked road with the same lateral acceleration. This indicates that the critical lateral acceleration on a banked road is higher than on a flat road.

3.3.4.5.4 Most realistic model

The most realistic model is the vehicle model with a torsional tractor frame, pulling a sloshing load, cruising down a three-dimensional road for tractor 1 trip 939. It combines all three partly antagonistic influences into one simulation to show give an idea how they interact.

It is shown in Figure 3-45, how the load is transferred through the maneuver. The stabilizing effect of the bank angle is significantly compromised. The sloshing influence

combined with the impact of the torsional frame is more dominant than the influence of banking. This type of maneuver, with a load transfer, increases the effect of sloshing.

The semitrailer roll angle is similar to Figure 3-44 with the additional effect from the sloshing load. It transfers the load to the outer tires about a mean value as well as applies an additional dynamic component, which makes the vehicle more unstable.

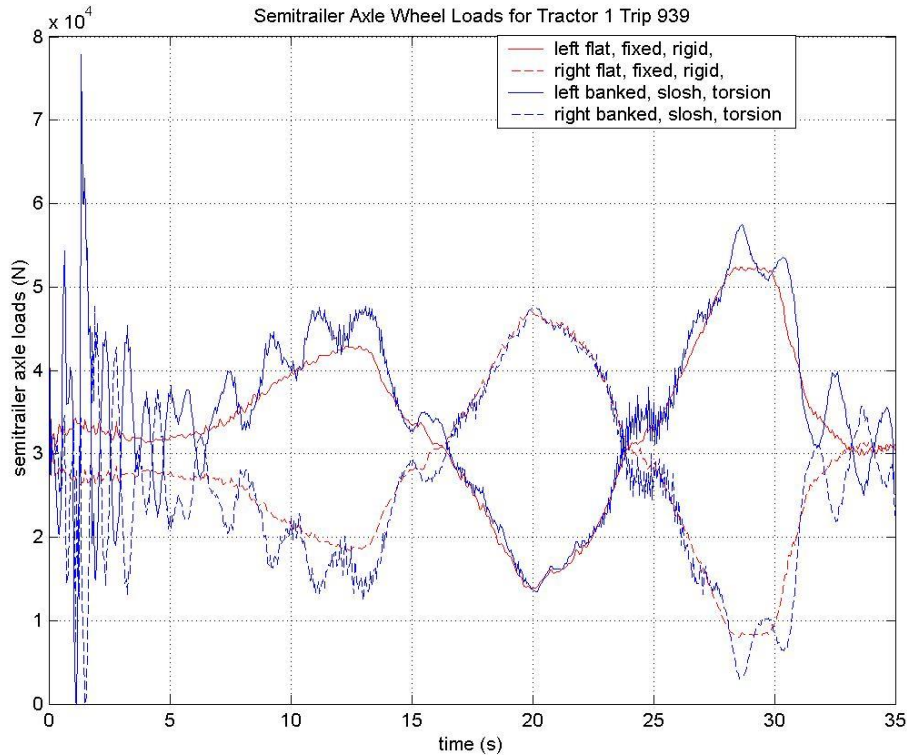


Figure 3-45. Semitrailer axle loads of the most realistic model and the flat road, bracket load model.

3.3.5 *Summary and Conclusions*

The results of this study have shown that vehicle GPS data can be successfully utilized to gain a better understanding of vehicle rollover dynamics. First, it was shown that the vehicle models used for the static and dynamic rollover simulations correlated well and can be reasonably validated by the FOT data. Simulated static tilt table tests were conducted and a static rollover threshold defined that compared well with theoretical and FOT static rollover thresholds.

Simulation models were applied to dynamic tests to determine in what cases vehicle rollover might have occurred and to establish a dynamic rollover threshold. The simulations showed that the resulting dynamic rollover thresholds for ten different sets of driving conditions between two different roads are highly similar. The nominal dynamic rollover threshold from the simulation tests was shown to be approximately 10 to 15% lower than the static rollover threshold of the same vehicle. In addition, it was shown

that the for the driving conditions simulated, the difference between the critical speed over the range of unloaded to loaded vehicle was on the order of 3 m/s.

The results were expressed in terms of semitrailer center of gravity height so that the critical lateral accelerations can be applied to other similar vehicles. It is concluded that the resulting nominal dynamic rollover threshold could be used proactively in a rollover prevention system for on-highway tractor trucks.

3.3.6 Further Work and Recommendations

Results of this project have brought about new ideas, as is usually the case, about how to extend the work done in this study. The most important simulation model change would be to account for tractor torsional flexibility either through lumped mass approximations or a finite element model. The road models for the simulation tools can also be improved through the use of higher order curvature approximations and also development of techniques to better approximate the road bank angle.

It is proposed that the dynamic rollover threshold be further validated by examining other hotspots. This experience gained could be used to develop more generic rollover algorithms that are not rigidly tied to a specific vehicle configuration. To fully apply this would also require that an algorithm be in place that can reliably estimate the semitrailer center of gravity height.

3.4 Evaluation of a Rollover Warning Capability

The RA&C project has used the Rollover Stability Advisor device as a test bed for rollover safety improvement. The basic technology seems effective, but system engineers have found that by the time the system recognizes that a truck is in a dangerous state, it is too late to take action. The system instead has an educational function, informing the driver after the fact and aiming to encourage the driver to drive safer in the future. Within the bounds of Task 20, it was undertaken to develop a theoretical system that uses any additional information available (detailed road geometry, specific vehicle characteristics, etc.) to detect imminent rollover situations while there would still be time to take action. However, as in all warning systems, false warnings that annoy the driver and reduce effectiveness must be avoided.

Next, the concept of extending the Rollover Stability Advisor to a proactive Rollover Warning System is described. It discusses results from a preliminary statistical analysis to understand the characteristics of rollover events as well as addresses the methodology and requirements of a Rollover Warning system. A demonstration of the predictive rollover-warning algorithm is performed for hotspots 1 and 2 as a proof of concept, based on data collected during the FOT. Finally, the chapter closes with prospects for deployment of a Rollover Warning System.

3.4.1 Statistical Analysis

A preliminary analysis was carried out on concentrations of high RSA scores and characteristic driving that led to high RSA scores. Across the data set, the distribution of high RSA scores versus road class is shown in Figure 3-46. These results show that

many dangerous situations occur on ramps, where there is often high curvature for 270 degree turns. Fortunately, all vehicles move in a predictable way on ramps so it may be possible to anticipate dangerous situations. On the other hand, some dangerous situations occur on highways, where curvature is generally low. These cases may be due to quick lane changes or other unpredictable maneuvers. Unfortunately, a lane change maneuver is difficult to predict until it starts, and by then it is too late for a warning. Finally, some high RSA scores occur on arterials and local roads. These may be due to turns. If the driver has a known or predicted route, it is again possible to anticipate problems, but this is beyond the scope of this report. Based on these results, the focus of this investigation will be on preventing rollovers on onramps and other roads with high curvature.

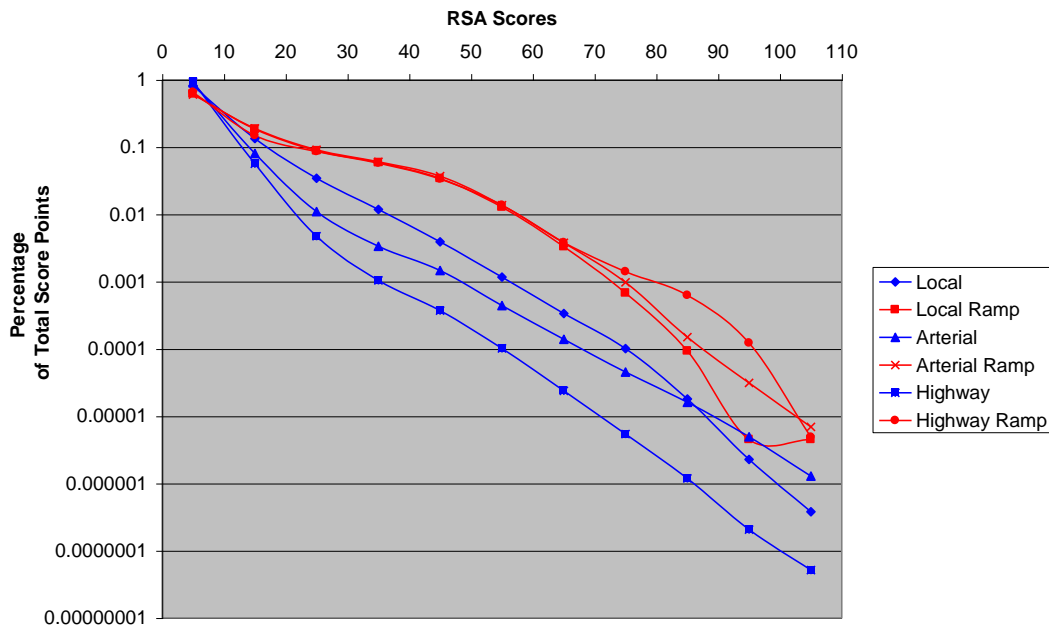


Figure 3-46: RSA frequency by road class. High RSA scores are much more common for ramps.

On these onramps and similar segments, most traversals go smoothly without excessive RSA scores, but some result in warnings. As an example, “Hotspot 1” is considered. Please note that “Hotspot 1” has already been described earlier in this chapter as well as in the report for Task 18, Road Geometry. To reduce data volume, only tractor 1 is considered in this analysis. Of the 44 passes over this hotspot by tractor 1, 4 result in warnings. In general, these traces result in warnings because their peak RSA score is over 75. Figure 3-47 shows the RSA score for every point on hotspot 1 against its distance into the segment. The plot shows that the RSA score accelerates quickly when the sharp curve begins, for example trace 953 goes from an RSA score of 0 to 78 in 3.5 seconds as the driver only decelerates by 8 m/s. It is interesting to note that behavior in the straight portion is indistinguishable from the nominal traces, but scores in the earlier curve (0 – 100 m) are on the high side.

Looking at the speed plot in Figure 3-48, the difference is more evident- all warning traces are on the high side of the distribution, even in the straight section. But there are several other high-speed traces that do not receive a warning. To understand why that is, it is necessary to examine the other factors in RSA warnings, such as vehicle parameters, simplified to mass in these tests. Figure 3-49 shows the mass for the warning traces versus the overall mass distribution. All the traces are near the high end of the distribution. This implies that trucks traveling at a fairly high speed with fairly high loads are susceptible to rollover warnings. As the load is constant, the main problem is predicting the speed. Since the data show that traces generally stay at the same point in their speed distribution for some time, it may be possible to build a model of future speeds and predict warnings some time in advance, giving drivers time to slow down before the warning.

As a final observation, RSA scores are still high by the end of the segment, so the curve is not yet finished. At this point, the segment merges with another onramp, but this one is basically straight. This may prove problematic for labeling dangerous segments in the map, because some trucks on this segment (those entering from hotspot 1), will still be experiencing high RSA scores, whereas others (those entering from the straight onramp) will not. It would be better to move the joining node forward so that all trucks completely finish their turn in a single segment.

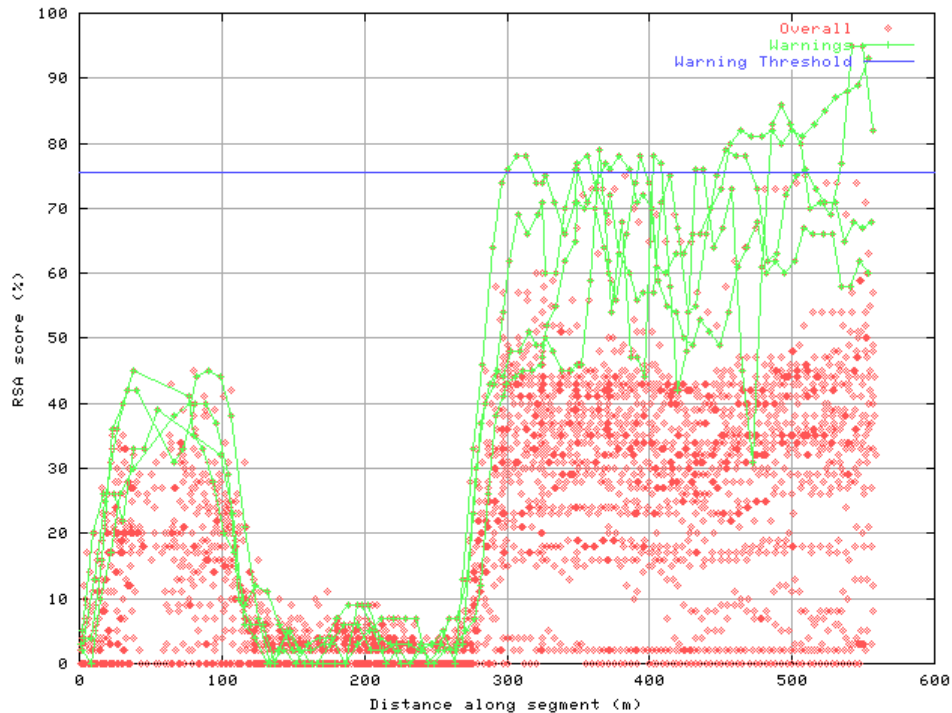


Figure 3-47: RSA score for Hotspot 1. 100% means a likely rollover; 75% leads to an RSA warning.

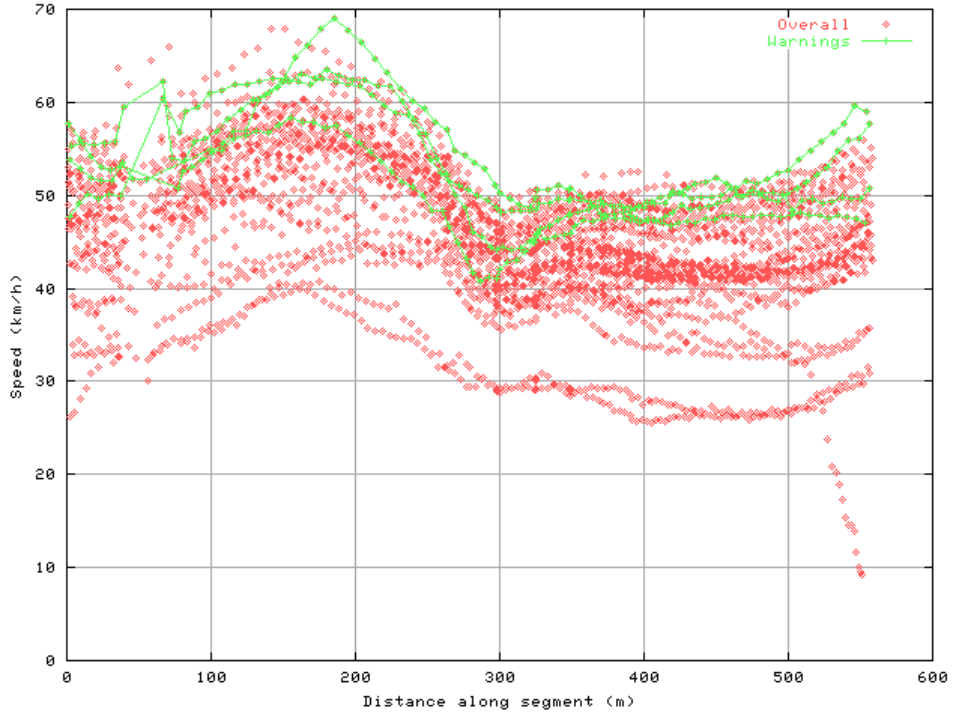


Figure 3-48: Speed for Hotspot 1. The traces that got a warning are towards the top of the distribution all the way through the segment

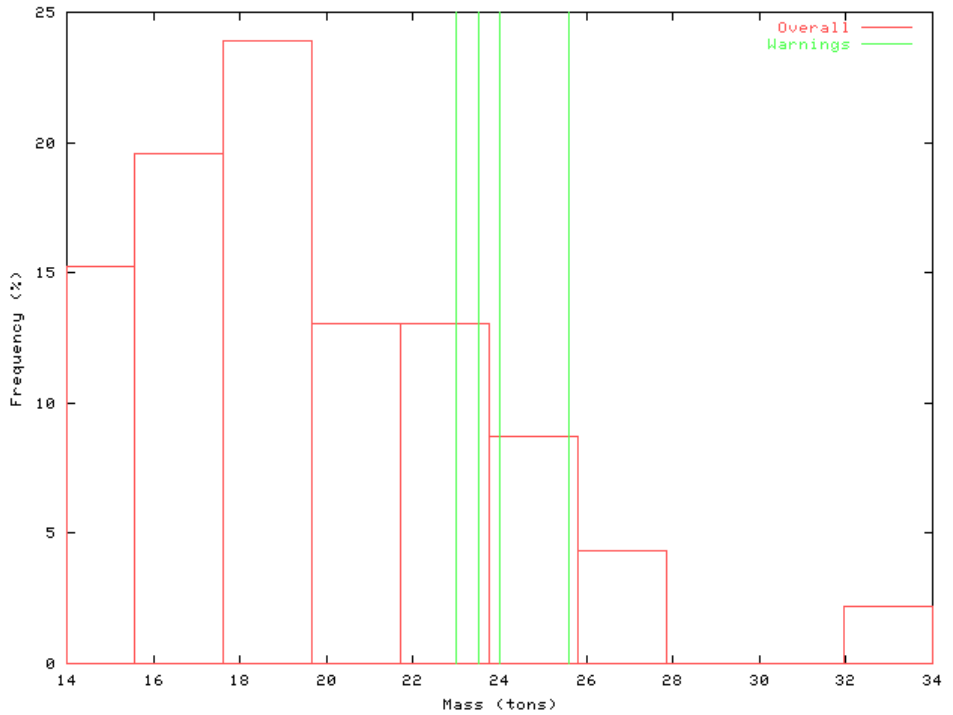


Figure 3-49: Mass distribution. The traces that got a warning are towards the top of the mass distribution as well.

3.4.2 *Rollover Warning Components*

Rollover warning, as formulated herein, is based on longitudinal speed monitoring and projection. This is based on the observation that rollovers are caused by a combination of factors, including road geometry, vehicle physical parameters, and driver behavior. Since drivers generally have no control over the road or their trucks, they must adapt their behavior to the conditions. Assuming the vehicle's forward path is fixed to the center of its current lane (violations of this assumption include lane changing), the only way to avoid dangerous lateral accelerations is to control the longitudinal speed of the vehicle. The objective of the rollover warning system is to determine the maximum safe speed given the conditions, and warn the driver when he/she is in danger of exceeding it. Breaking this objective down results in three major system components: determining safe speed, projecting the current state to predict future speed, and determining when to give a warning if the predicted speed is unsafe.

3.4.2.1 *Safe Speed*

In terms of rollover, risk has been formulated as the fraction of the current lateral acceleration over the maximum safe lateral acceleration. The current lateral acceleration, in turn, is a function of the vehicle speed, the curvature of the road, and the banking of the road. The maximum safe lateral acceleration is a function of the physical characteristics of the vehicle and its load. In the case of a liquid load, distribution is not an issue and the vehicle mass is sufficient. Given a known maximum safe lateral acceleration, the curvature and banking of the road at a point x , we can calculate the maximum safe speed of the vehicle at x to be the speed at which lateral acceleration is less than some factor of the maximum, 80% for example. This is the instantaneous speed at each point x . Note that when the curvature at x is 0, speed is infinite.

Continuous driving at the maximum safe speed requires unrealistic longitudinal accelerations, so a continuous safe speed curve is needed that never exceeds the instantaneous speed limit, yet is physically achievable by the vehicle. This is referred to as the “red-line” curve. If a vehicle exceeds this curve, it will not necessarily immediately undergo excessive lateral acceleration, however, eventually it will due to its inability to decelerate enough before the curve. In practice, this curve needs to be computed dynamically for the upcoming road geometry and current vehicle parameters, such as mass, center of gravity height, etc.

3.4.2.2 *Instantaneous Safe Speed*

There are several possible approaches for determining this “red-line” curve. The simplest way is to directly calculate the velocity at each point that will give the maximum safe lateral acceleration. This velocity can be determined from the relation:

$$v^2 \cdot \kappa - g \cdot \theta = a_{lateral} \quad \text{Equation 3.6}$$

where:

v is the velocity of the vehicle

κ is the curvature of the road

$a_{lateral}$ is the lateral acceleration

g is the acceleration due to gravity
 θ is the bank angle of the road in radians

By setting the lateral acceleration to the maximum allowed lateral acceleration a_{max} , one can solve for the maximum velocity.

$$v_{max} = \sqrt{\frac{a_{max} + g \cdot \theta}{\kappa}} \quad \text{Equation 3.7}$$

One will notice that by this equation alone, v_{max} becomes infinite as the curvature approaches 0. Therefore, one would have to introduce a maximum value for v_{max} . However, even with taking precautions to prevent v_{max} from becoming infinite, this approach does not lead to very useful results. The problem is that the resulting velocity curve will have unobtainable accelerations as it will have the same frequency content as the curvature of the road. Figure 3-50 shows an example of a safe velocity curve calculated using Equation 3.7 for hotspot 1. The top plot shows the calculated safe velocity in red along with the recorded velocity from the RSA database for tractor #5, trip #917. This particular recording registered high RSA scores, therefore it is included in the figure as a comparison. The safe velocity is calculated with the settings of $a_{max}=2.75$ m/s*s and the maximum value of v_{max} set to 20 m/s. The second plot shows the curvature along the road segment and the final plot shows the RSA score in the above-mentioned recording.

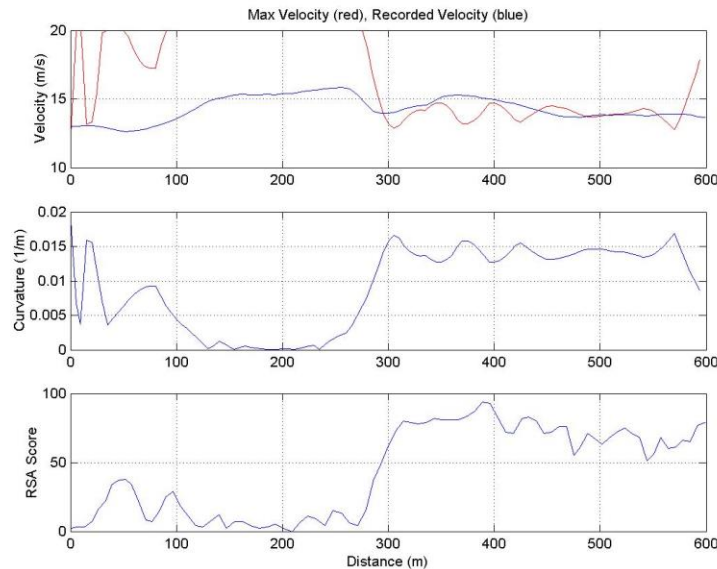


Figure 3-50: Safe Velocity curve Calculation using only current road information based on the instantaneous safe speed approach

One can see that the algorithm correctly identified that the vehicle speed should have been lower in the 300-400 meter region, which corresponds to the region of the highest

RSA scores. However, the safe velocity curve decelerates from 20 m/s to about 13 m/s over a distance of about 25 m (from 275 to 300 m). This is an unreasonable rate of deceleration for a heavy-duty vehicle. Therefore, a useful algorithm must somehow include a look-ahead or prediction element. This is, of course, what normal drivers do everyday when they see upcoming curves and slow down appropriately before entering them.

3.4.2.3 Predictive Safe Speed

As shown in section 3.4.2.2, it is not adequate to determine the safe speed based only on the curvature at the current position. In order for a vehicle to achieve the proper safe speed, it must know the upcoming curvature so that it can decelerate in a realistic and comfortable manner. The approach taken in this study of determining this safe speed in a predictive manner is based on the ideas of optimal control. A cost function is defined which penalizes certain conditions of the vehicle, such as high lateral accelerations. Then a series of control inputs, in this case the requested engine torque, are determined which minimize the cost function.

The first step in developing this control algorithm is to define the appropriate system equation. In this case, the vehicle state of interest is the velocity. The state equation for the velocity is:

$$\frac{d}{dt}v = f(\varphi(t), v(t), T_{eng}(t)) \quad \text{Equation 3.8}$$

where:

$\varphi(t)$ is the grade of the road at time t

$v(t)$ is the velocity at time t

$T_{eng}(t)$ is the engine torque at time t

It is convenient to define the state equation in terms of a position on a particular road rather than in terms of time. Therefore, the following substitution is made:

$$dt = \frac{1}{v} ds \quad \text{Equation 3.9}$$

into Equation 3.8. In addition, an approximation for the derivate is made to create a discrete equation. The resulting state equation is:

$$v(k+1) = f(\varphi(k), v(k), T_{eng}(k)) \quad \text{Equation 3.10}$$

Equation 3.10 indicates that the velocity at position $k+1$ is a function of the grade, velocity and engine torque at position k . One may notice that the brakes are not included in this equation. For simplicity, only one control input is considered in the system. Instead, the engine torque is allowed to become negative and up to a certain extent, this is achievable through the use of the engine brakes.

The next step in the control algorithm is to define a cost function to be minimized. The cost function for this system was defined as:

$$J = \sum_{k=0}^n J_{lateral_accel} + J_{velocity} + J_{fuel} \quad \text{Equation 3.11}$$

where the individual cost terms are defined as:

$$J_{lateral_accel} = \frac{1}{2} K_{accel} (v_k^2 \cdot c_k - g \cdot \theta - a_{max})^2 \cdot \sigma \quad \text{Equation 3.12}$$

$$J_{velocity} = \frac{1}{2} K_{vel} (v_k - v_{des})^2 \quad \text{Equation 3.13}$$

$$J_{fuel} = \frac{1}{2} K_{fuel} \cdot T_{eng}^2 \quad \text{Equation 3.14}$$

Equation 3.12 contains the variable sigma (σ), which is defined to be equal to 1 whenever the lateral acceleration is greater than a_{max} and 0 at all other times. Therefore, the entire lateral acceleration cost function will only be non-zero if the lateral acceleration should exceed the maximum limit. The other two terms in the cost function (Equation 3.13 and Equation 3.14) take into account velocity errors and fuel usage.

The individual gain terms in Equation 3.12 through Equation 3.14 are used to adjust the weighting on the different terms in the cost function. The sum of the individual cost functions at each point, k , are summed along the entire prediction horizon as shown by Equation 3.11. The prediction horizon is the distance ahead of the vehicle for which the algorithm is trying to minimize the cost. It is represented by n on top of the summation symbol in Equation 3.11. The reason for the summation is that the goal is not to have a minimal cost at any specific point, rather to have a minimal cost during the entire maneuver.

The objective now is to find the series of states (velocity) and control inputs (engine torque) that minimize Equation 3.11 while maintaining the system constraint of Equation 3.10. This is done in an iterative fashion that will be described generally. First, a desired speed must be chosen for each point along the prediction horizon. This desired speed will be the default maximum speed when the lateral acceleration is not exceeding limitations, for example on straight roads. A reasonable choice might be a function of the speed limit. It is reasonable to assume that a navigation system will know the speed limit at various positions on the road. Whether the desired speed should be actually equal to the speed limit or set a little higher is unknown and not the point of the current study.

The algorithm will first calculate the cost if the vehicle drives through the prediction horizon with the desired speed. If there is a curve in the upcoming prediction horizon which should be navigated at a slower speed, then the $J_{lateral_accel}$ term will have a large positive value whenever the predicted lateral acceleration is higher than the limit. This will cause the overall cost function value to increase. Normally the gain for the lateral acceleration term, K_{accel} , is set quite high to emphasize this value. On the next iteration, the algorithm adjusts the speed profile in order to reduce the overall cost. It continues this process several times in order to reduce the cost to a minimum. Notice that the inclusion of J_{fuel} in Equation 3.11 forces the algorithm also to consider the fuel consumption in performing the maneuver. The results of this fuel consumption influence will be shown later in the results section.

The following series of figures should help explain the algorithm. Figure 3-51 shows the road information for hotspot 1. The top plot shows the overhead view of the road and the bottom plot shows the road curvature with respect to the distance along the road. The zero distance point is the bottom point (approximately $-86.337, 41.726$).

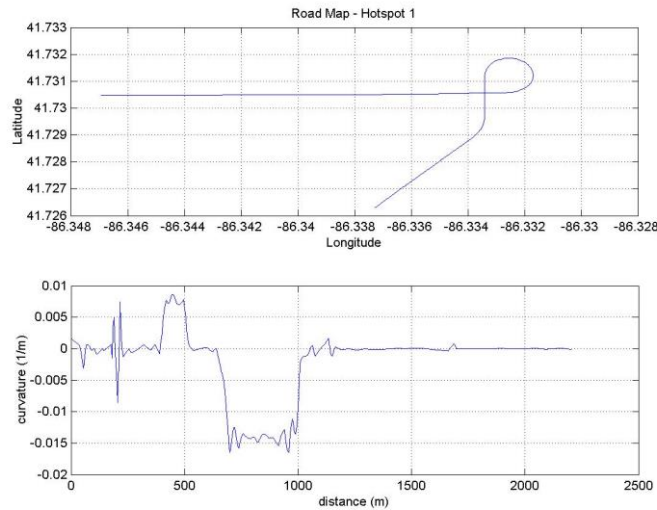


Figure 3-51: Hotspot 1 road information. Top plot shows overhead view and bottom plot shows curvature.

Figure 3-52 and Figure 3-53 show the progression of the desired velocity and individual cost function terms during the 15 iterations. The first iteration is shown as red. The desired velocity during the first iteration is just the initially set desired velocity of 20 m/s. While the cost function term from the fuel and speed error is very small (or even zero), the cost due to the lateral acceleration is very high. In this case, a_{max} was set to 2.0 m/(s*s). As the iterations progress, one can see that the velocity is reduced along with the cost due to the lateral acceleration. The cost due to the fuel usage and the speed error increases, but at a much smaller scale compared to the reduction in the lateral acceleration term. This is due to the choice of a very large K_{accel} compared to K_{fuel} and K_{vel} . It is clearly better for the overall minimization to reduce the lateral acceleration even at the cost of higher speed error and more controller effort.

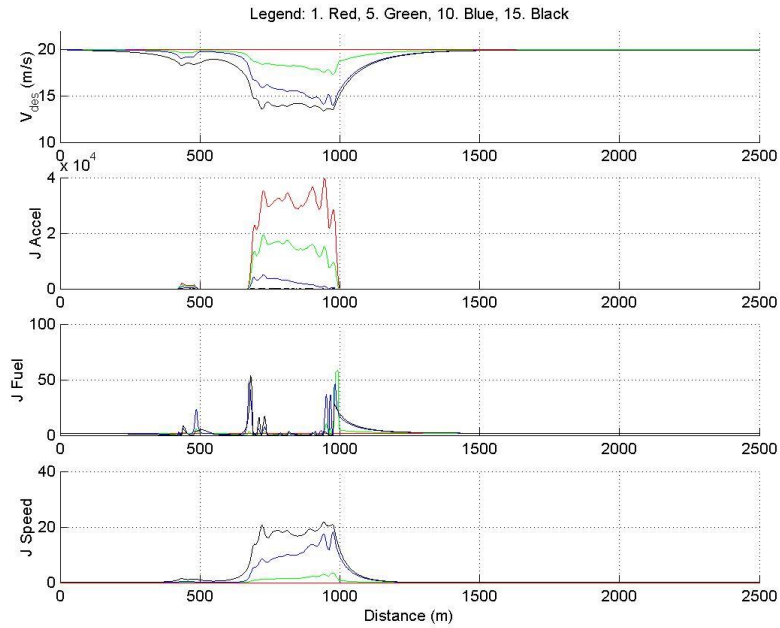


Figure 3-52: The desired velocity and individual cost function terms for each point during the maneuver. Four sets of data are shown from the 15 performed iterations. The legend indicates the color of each iteration.

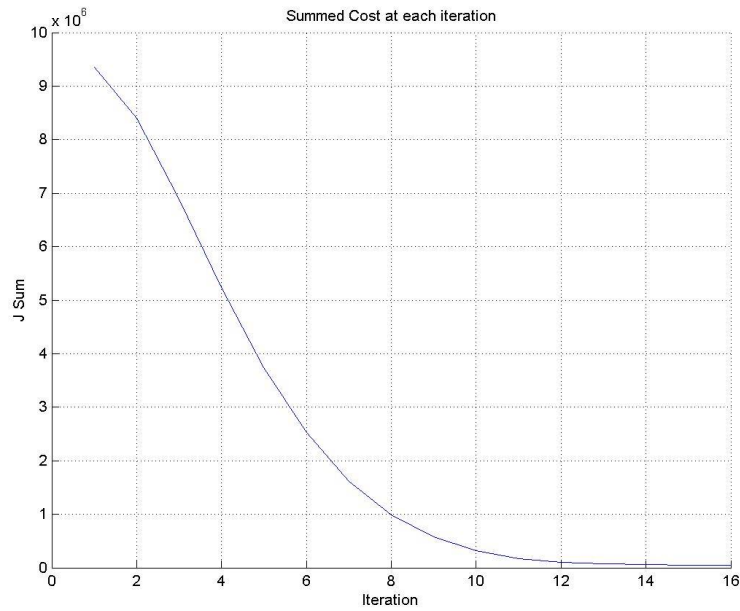


Figure 3-53: Total cost for the maneuver through hotspot 1 at each iteration.

Figure 3-53 shows the summed cost at each of the 15 iterations. Clearly, the cost is reduced with each iteration and it appears to have reached a minimum by the final iteration.

3.4.3 *Vehicle Velocity Prediction*

When the vehicle is above the red line, it is too late to take action. However, before the vehicle crosses the line, there is by definition a chance that the driver will not push the truck past the line. In fact, the purpose of a warning system is to change the behavior of the driver so that what might have been a dangerous situation without a warning is corrected. In this case, the warning system must *predict* that the vehicle will cross the red line in a few seconds. This gives the driver enough time to slow down safely, but not so much time that the driver will probably correct the situation himself. Concretely, the warning system needs a means to project the vehicle's velocity from a starting point into the future, stopping if and when the vehicle's velocity crosses the red line. The following list defines several models of increasing complexity for velocity prediction.

- **Constant Speed.** In the simplest model, when a projection is needed, the model assumes that the truck's speed remains constant. This model performs well in the middle of curves and straightaways, but fails to predict early enough that the truck will slow down when it is entering a curve, or stop accelerating when it is exiting a curve
- **Constant Acceleration.** In the next simplest model, when a projection is needed, the model assumes that the truck's acceleration remains constant. This model performs well in constant speed areas, as well as the beginning and end of curves where the driver is changing speed. However, it cannot predict when the driver will stop changing speed, so only short-term predictions are likely to be accurate.
- **Global Median.** In this model, the predicted speed is the median speed for that point on the road. We initialize the model from the speed profiles of all previous trucks passing over the road. This model ensures that the predicted speed will follow the general profile of previous vehicles, but it does not take into account information on the current speed: it predicts that the speed at the next map point will be the median, no matter what the current speed or acceleration is.
- **Constant Percentile.** The most complex model is inspired by the observation that drivers who are driving relatively fast in the straight sections often also drive relatively fast on the curves, incurring rollover warnings. If the drivers keep the same relative position in the speed distribution (percentile) for each point of the road, this model will perfectly predict upcoming speed from current speed, and the speed distributions for each map point from previous passes. In actuality, drivers will certainly change percentiles, but hopefully not as often as they change speed or acceleration. This model reduces to the Global Median model if the driver's speed is currently in the middle of the distribution.

3.4.4 *Intervention timing*

Finally, once the system predicts a crossing of the red line at time t , it must decide the moment at which to warn the driver. The driver response model studied assumes that the driver takes some time to respond, then hits the brakes with constant force to decelerate

to some speed below the red line. Parameters for this driver model include the driver reaction time, the vehicle's maximum deceleration, the minimum time necessary to reach this deceleration, and a speed "cushion" to keep away from the red line. Given these parameters, the warning moment is the time such that, after the reaction time, the maximum deceleration regime will bring the vehicle to the given cushion below the red line by the time t . This time must be updated dynamically to account for unexpected changes in acceleration.

The velocity prediction function must be at least accurate enough to predict crossing the red line so that the driver can intervene in time. An additional safety function could automatically slow the vehicle when it predicts danger. Since a control system is more predictable and faster reacting, this function could wait longer before activating, easing requirements on velocity prediction and permitting fewer false positives.

3.4.5 Rollover Warning Theoretical Results

The mass of data collected during the Field Operational Test offers ample opportunity to calibrate models and compare predicted outcomes with actual outcomes.

3.4.5.1 Methodology

The objective of these experiments is to measure the warning effectiveness and the sensitivity of the effectiveness to different experimental conditions. In these circumstances, the most appropriate evaluation of the entire warning system is the prediction of how long until the vehicle will exceed the maximum lateral acceleration versus whether the vehicle actually exceeds the limit. This enables an estimation of the accuracy of the warning system as a function of how much advance warning is available.

It is also possible to evaluate the individual pre-intervention components separately. In the case of the maximum safe speed, it is feasible to evaluate the correlation between actually crossing the red line and receiving a warning. The experimental conditions include the quality of the curvature map used to derive the red line. Up to four maps will be tested: a spline fit to the geometry in a commercial digital map, a spline fit to a single trace, a spline fit to ten traces, and a spline fit to all available data. In the case of velocity prediction, it makes sense to compare the predicted velocity with the actual velocity. The experimental conditions include the choice of model.

These evaluations take place on selected "hot spots" in the data set where high RSA scores are common.

3.4.5.2 Maximum Speed Curve Evaluation

The predictive safe speed algorithm described in section 3.4.2.3 has been simulated using the road data from hotspot 1, which was shown in Figure 3-51. The starting point on this road is in the lower left hand corner of the figure, so this is the distance = 0 point. The simulated data has been compared to the recorded data from tractor #5, trip #917, which recorded high RSA score values.

Volume III, Chapter 3
 Theoretical Rollover Warning Effectiveness – Task 20

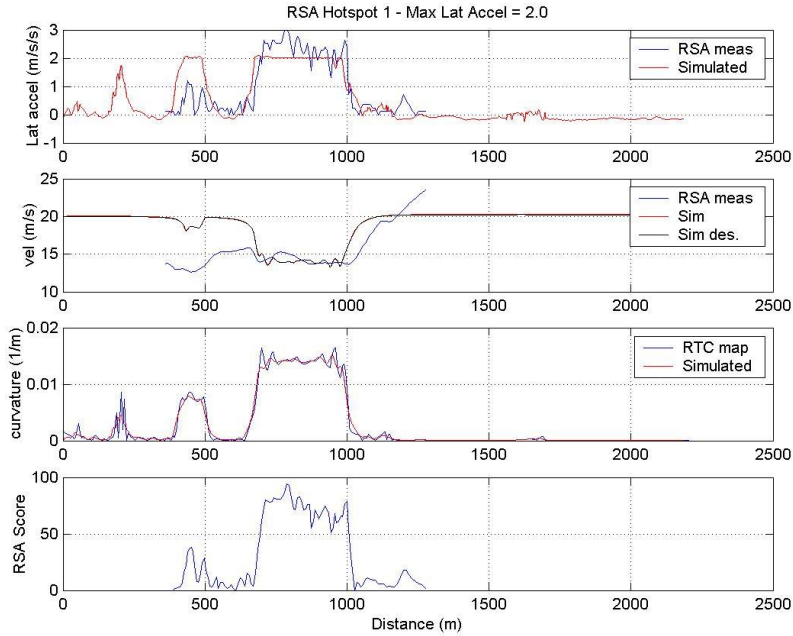


Figure 3-54: Predictive Safe Speed simulation results for hotspot 1. $a_{max} = 2.0$ m/(s*s), $v_{des} = 20$ m/s, low K_{fuel} value.

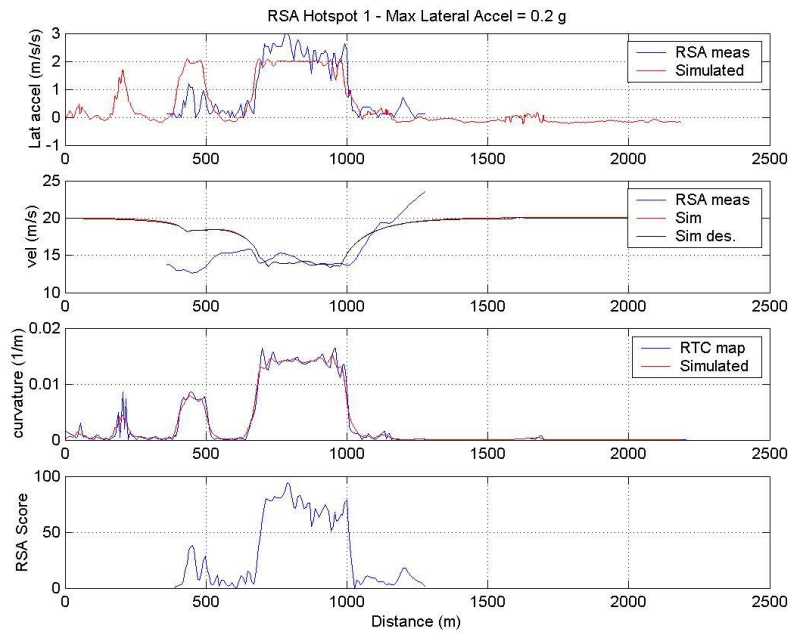


Figure 3-55: Predictive Safe Speed simulation results for hotspot 1 $a_{max}=2.0$ m/(s*s), $v_{des}=20$ m/s, high K_{fuel} value.

Figure 3-54 and Figure 3-55 show the simulation results when computing the safe speed for hotspot 1. The top plot shows the simulated lateral acceleration in red and the

recorded lateral acceleration in blue. The second plot shows the simulated safe speed in black and the recorded vehicle speed in blue. The third plot shows the calculated curvature in red and the curvature taken from the RSA database in blue. The final plot shows the actual recorded RSA score.

The calculated curvature in the third plot is calculated in the RSA algorithm. The reason a value is calculated rather than just directly using the value from the database is that the map information is stored in the RSA algorithm as a series of polynomials which represent the road in all three-dimensions. The curvature is then calculated from these polynomials. The third plot just shows how this calculated curvature compares to the curvature created by the statistical analysis of the RSA data.

Both Figure 3-54 and Figure 3-55 show that the algorithm produced a safe speed trajectory which reduced the lateral acceleration to the desired level of 2.0 m/(s*s) in the region of 300-600 meters, which had the highest RSA scores according to the last plot. One may notice the safe speed leads to higher lateral acceleration values in the first 100 meters. This is because the initial desired speed was set to a high value of 20 m/s. The algorithm does not change the desired speed at the very first point. Therefore, it would require an extremely high effort (and in fact may be impossible) to reduce the speed sufficiently before the first point of high curvature at about 20 meters. An actual algorithm which was running continuously would not have this problem, as it would see the high curvature far enough ahead to respond properly.

It is interesting to notice the differences in the two figures. The only difference in the algorithm between the two different simulations was the value of the gain on the fuel term in the cost function, K_{fuel} . In Figure 3-54, K_{fuel} was set 10 times lower than in Figure 3-55, such that the algorithm placed more emphasis on the lateral acceleration and the speed error. The result is that the safe speed trajectory rises back up close to 20 m/s in the region 500 - 700 meters where the road curvature is very low. In Figure 3-55, the safe speed continues to decrease during this region even though this is introducing a larger speed error. However, it is more fuel efficient to continue to gradually decrease the speed rather than to increase it and have to decrease it again as the vehicle approaches the curvature at 700 meters as is done in Figure 3-54. The difference can also be seen in the region 500 – 800 meters. In Figure 3-54, the velocity changes slightly and the lateral acceleration is rather smooth and stays right at the limit of a_{max} . The changing velocity is in response to the slight changes in the grade and bank angle of the road. This is because it is more cost effective to use the additional control effort and reduce the speed error as much as possible. In Figure 3-55, the velocity remains smoother and the lateral acceleration value is noisier in response to the road changes. This is due to the controller's desire to minimize control effort.

In both figures, one may notice that the lateral acceleration makes a sudden jump at approximately 560 meters. This is attributed to reaching the end of the data for the road bank. Therefore, this value is set to 0 which translates into increased lateral accelerations as described in Equation 3.6.

The choice of $a_{max} = 2.0 \text{ m/(s*s)}$ is probably low as this result leads to a desired velocity significantly lower than the recorded velocity. However, this value was chosen in order to clearly demonstrate the possible effect of the algorithm. Simulations have also been made at other maximum lateral acceleration values with the expected results of the speed increasing so that the lateral acceleration reaches the desired level. Figure 3-56 shows a simulation with $a_{max} = 2.25 \text{ m/(s*s)}$. This value was chosen because it is slightly greater than the lateral acceleration threshold of 0.21 g that normally triggers Level 1 RSA warnings in the experimental vehicles. As expected, the simulated safe speed trajectory is less than the measured velocity of the vehicle. The resulting simulated lateral acceleration stays below a_{max} in the region of 700 - 1000 meters, where the high RSA scores occurred.

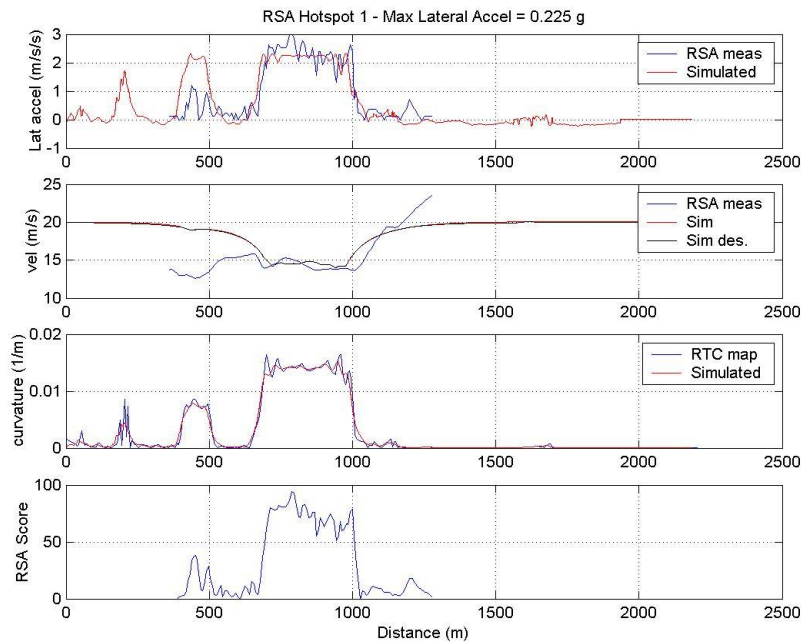


Figure 3-56: Predictive Safe Speed simulation results for hotspot 1. $a_{max}=2.25 \text{ m/(s*s)}$, $v_{des}= 20 \text{ m/s}$, high K_{fuel} value.

The safe speed prediction algorithm was also tested on hotspot 2. The overhead view of hotspot 2 is shown in Figure 3-57 in which travel originates on the bottom right side of the curve and progresses to the left and then upward. Figure 3-58 shows the results of the simulation compared to the actual results taken from tractor 1, trip 939. The velocity plot shows that the calculated safe speed is less than the measured vehicle speed. This results in the lateral acceleration staying below the a_{max} value of 2.0 m/(s*s) , whereas the measured lateral acceleration for this particular case reached about 3.0 m/(s*s) in this region. Once again, artifacts of the algorithm initialization are obvious as can be seen by the heightened values in the lateral acceleration values within the first few meters of the prediction horizon.

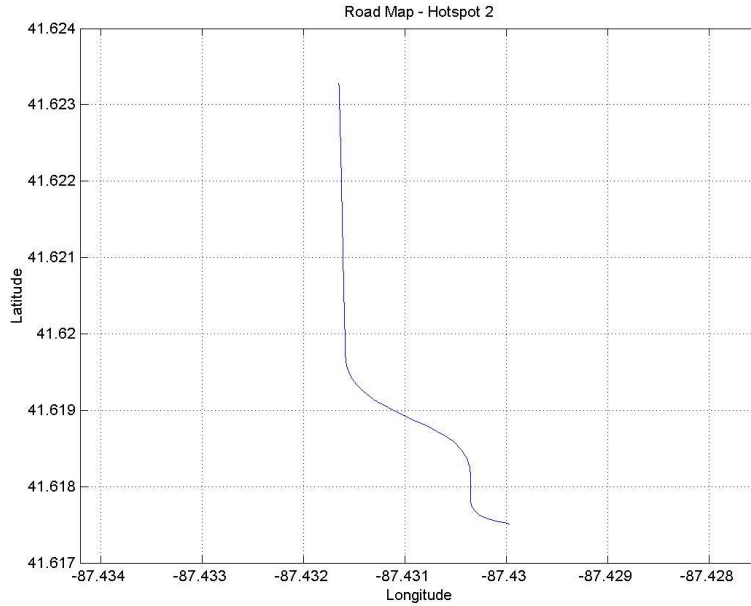


Figure 3-57: Overhead view of hotspot 2.

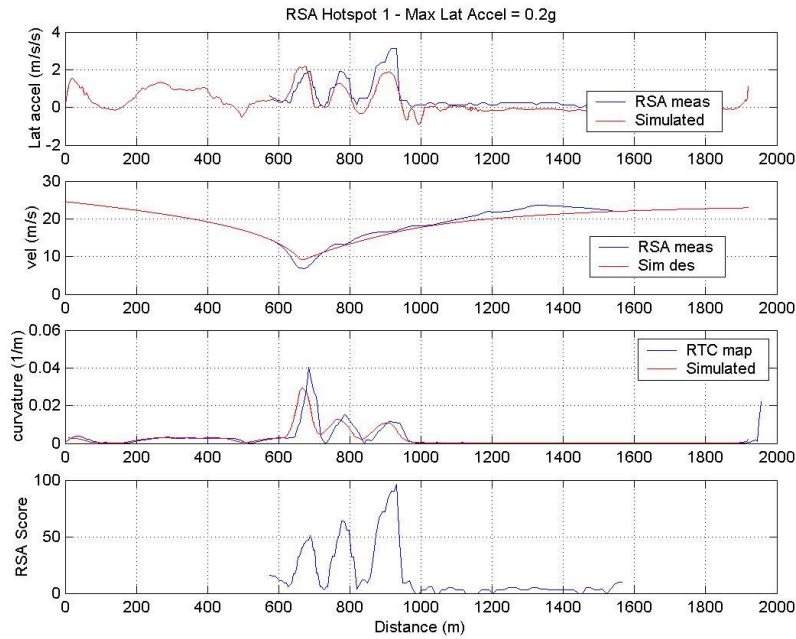


Figure 3-58: Predictive Safe Speed simulation results for hotspot 2. $a_{max} = 2.0$ m/(s*s), $v_{des} = 20$ m/s, high K_{fuel} value.

3.4.6 Vehicle Velocity Prediction Evaluation

The four speed prediction models were run for hotspots 1 and 2 as described earlier in this chapter as well as in the report for Task 18. First, for those models that needed a

speed distribution, the Field Operational Test dataset was used to build distributions for each map point on each hot spot. Second, for every pass over the hotspot, that pass's data was removed from the distribution (this is a technique called leave-one-out cross validation), and for each point on the pass the speed was projected forward using the four models. At each map point, the models made a speed prediction, and the actual speed was measured.

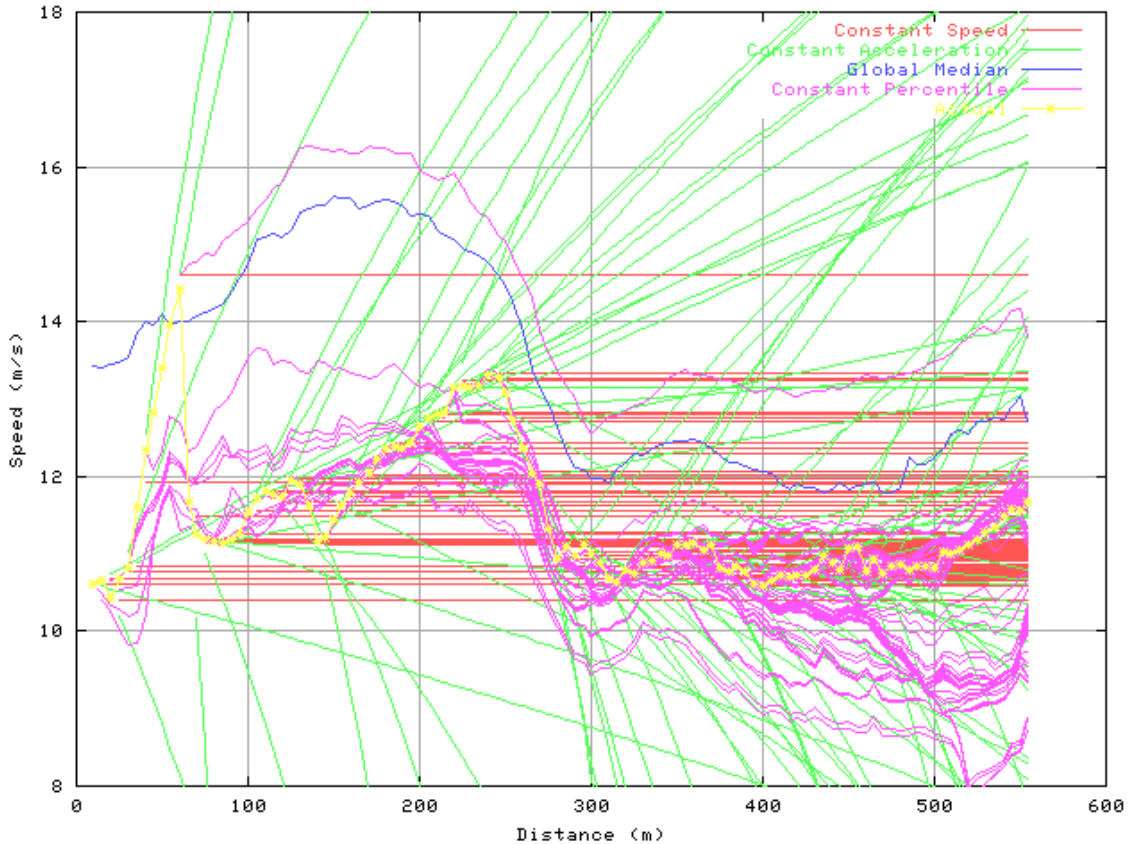


Figure 3-59: Speed predictions from all 4 models on a pass over hot spot 1.

Figure 3-59 shows the performance of each model on a pass over hot spot 1 from tractor 1, trip 1761. At each point in the trace (the asterisks), each model begins making its own predictions on the future speed profile. The constant speed model (red) does best in the second half of the hot spot, where the driver keeps a constant speed according to the actual speeds (yellow). The constant acceleration model (green) does even worse as the distance from the start point grows large, but it does remarkably well predicting the deceleration in the middle of the hot spot. The global median model (blue) makes the same predictions for each point. In this case, it performs poorly because this pass is quite slow- the mean percentile is 14.6. The constant percentile model (purple) predicts the deceleration and the constant speed portions pretty well, for a very good result- for predictions 10 seconds in advance or less, mean absolute speed error is only 0.35 m/s.

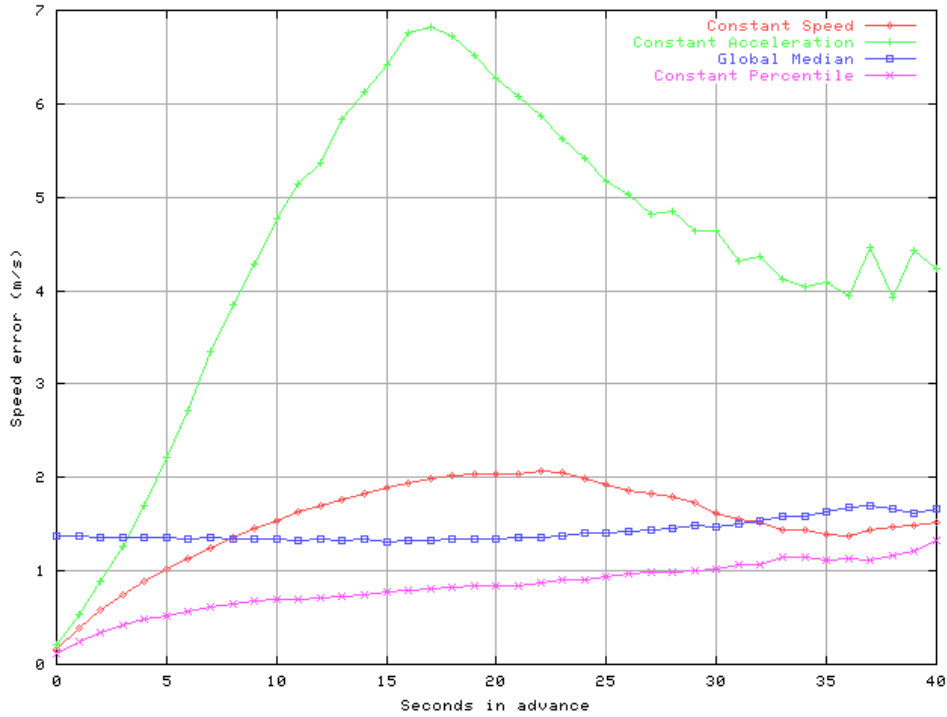


Figure 3-60: Performance on hot spot 1.

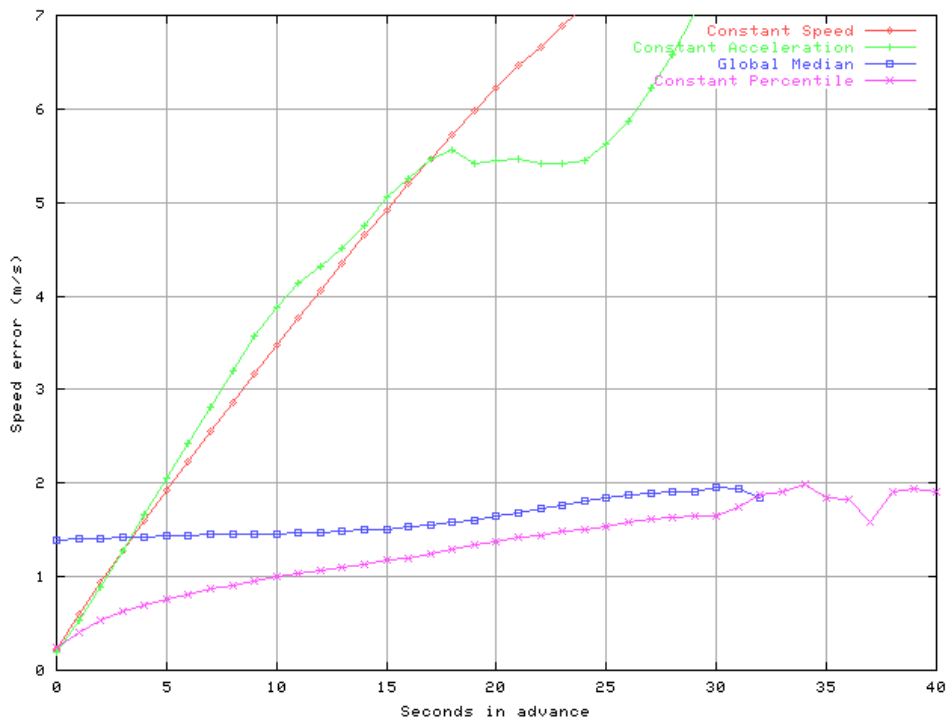


Figure 3-61: Performance on hot spot 2

Figure 3-60 and Figure 3-61 show the overall results for hot spots 1 and 2. Results for hot spot 2 are slightly worse, but the constant percentile model is clearly the best for both

areas. There is a strange hump in the results for hotspot 1 that is probably an artifact of the shape of the curve. Overall, the constant percentile model seems promising, with mean accuracy of less than 1 m/s after 10 seconds.

3.4.7 Complete System Evaluation

The warning system can use the vehicle velocity predictions, coupled with the known curvature and bank on the upcoming road, to predict the lateral acceleration of the vehicle as it moves around the curve. This acceleration may be used in a physical simulation to predict if the vehicle will roll over. If the system predicts a rollover, it can intervene by warning the driver or slowing down the vehicle. Instead of a complex simulation, the current RSA device uses a table lookup indexed on the mass of the truck to find the precomputed maximum lateral acceleration for a truck of that mass. If the truck's acceleration is more than 75% of that limit, the device activates a warning. A predictive warning system can extend this method to predict how close the truck will be to the limit, and react accordingly.

Such a simple warning system has been evaluated based on the FOT data, using the percentile model for speed prediction. For each speed prediction sequence, predicted lateral accelerations were computed and compared with the actual lateral accelerations. If the actual acceleration crossed the limit (set to $0.229 g = 2.25 \text{ m/(s}^2\text{)}$ the same value used in the speed limit computations), a future warning was indicated. If the predicted acceleration crossed the limit, it indicated a warning message. For each sequence, there were four possible results:

1. True positive. The system projects an excessive acceleration to occur before or when the excessive acceleration actually occurs. A good prediction system would discover this as early as possible.
2. True negative. The system never predicts an excessive acceleration, and there is none.
3. False positive. The system projects an excessive acceleration, but there never is one. This error is serious if it occurs so often that the driver ignores legitimate warnings.
4. False negative. The system never predicts an excessive acceleration, but there is one. This is the most dangerous error. Even a poor prediction system would rarely completely miss a dangerous maneuver, but the warning may come too late to do any good.

Based on hotspot 1, here are the results:

1. True negative. The lion's share of the predictions, 90%.
2. True positive. Excessive acceleration predicted on average 10 seconds before exceeding the limit, giving the driver enough time to react.
3. False positive. Excessive acceleration wrongly predicted to occur after, on average, 26 seconds elapse. The predictive accuracy seems to fall off somewhere between 10 and 26 seconds.

4. False negative. On average, missed dangerous maneuvers occur after 11 seconds of elapsed time. They are usually corrected promptly as the driver gets closer to the dangerous spot.

One final evaluation considered how much data was necessary to make these accurate predictions. Recall that the data was used to estimate three relevant attributes along the curve: curvature, bank, and speed distribution (for the percentile model). First, just using NavTech's commercial map database was considered with no FOT data. It was possible to derive a rough curvature from the shape points using NavTech's recommended algorithm, but there was no way to estimate the bank or the speed distribution. Next a single trace was considered in which a curve fit was used based on a methodology developed by the VSTC that was optimized for this task. The curvature was somewhat better than NavTech's, but the bank estimate was very poor. Even worse, there was only a single sample of the speed distribution, making the percentile model impossible.

Finally, the lower-quality map approach (as described in Task 18 Part II) was used. This produced estimates of all the relevant attributes, but with less precision. As described in Task 18, the centerline accuracy decreased by a factor of four, so a similar reduction in accuracy it was estimated for the other attributes. The results are similar to the full data set with one exception:

1. True negative. Again the majority prediction, with 85% of the predictions.
2. True positive. Again, on average predicted 10 seconds in advance.
3. False positive. Predicted on average only 21 seconds in advance, reflecting a slightly poorer predictive accuracy.
4. False negative. Predicted on average 16 seconds in advance, giving even more time for corrections. This unintuitive result needs more exploration.

If these results bear out under further examination, it appears that only ten or fewer passes are needed to project the speed and lateral acceleration of a vehicle accurately enough to provide warning at least ten seconds in advance of a dangerous maneuver. However, it is noted that the accuracy of the low quality map for Hotspot 2, also produced with ten traces, is twenty times less accurate than the high quality map. So ten traces may not be enough in all cases, if the position accuracy is low.

3.4.8 Conclusions

This investigation has shown that with a map made from ten passes and the percentile speed prediction model, it is possible to provide drivers with enough advance warning to avoid dangerous situations.

It may be possible to predict vehicle speeds even better with a more sophisticated model. For example, a hybrid model that uses acceleration for the first several seconds then switches to the constant percentile model, or perhaps a variable percentile model, where the vehicle's speed percentile changes according to the driver's typical habits.

Finally, it is noted this report describes a safety system that is intended to avoid accidents. It is also possible to repurpose much of this work to a comfort system that advises the driver or controls the vehicle to keep the lateral acceleration of the driver within a “comfort zone” while rounding a curve. This implies a lower, “blue line,” speed curve, perhaps personalized to the g-force preferences of individual drivers, and control algorithms designed to keep the vehicle near the curve as much as possible.

4 Evaluation of the Lane Guidance™ System

This chapter addresses the analysis of the data collected by the Lane Guidance™ system as part of Task 21 of the Field Operational Test (FOT). The goal of this investigation was to understand the performance of the system under different environmental conditions such as rain, snow and night/daytime. Additionally, the data were used to identify characteristics for potential warning scenarios as well as lane change maneuvers in order to better understand the overall system capabilities and performance.

Data collected by the Praxair tractors from November 2000 to June 2001 relevant to the Lane Guidance™ system were analyzed. The results showed that the Lane Guidance™ system performed best when the driver was potentially at the least attentive, during the night and early morning hours with cruise control engaged at highway speeds, during dry conditions.

4.1 Introduction

A commercial vehicle's unexpected deviation from its current lane, often referred to simply as lane departure, can be a manifestation of any number of problems focused on either the vehicle (mechanical or electrical malfunction) or the driver (distraction or drowsiness). Lane departure played a role in approximately 32% of all fatal accidents that involved trucks in 1999 for a total of 1,674 fatalities (TIFA, 1999). This statistic includes vehicle's running off road (8.5%), vehicle's side-swiping each other (10.3%) as well as head-on collisions (13.2%). To address the topic of commercial vehicle lane departure, DaimlerChrysler Research, Freightliner and Odetics developed Lane Guidance™, a commercially available lane departure warning system.

The Roll Advisor and Control (RA&C) Field Operational Test (FOT) as part of the Intelligent Vehicle Initiative (IVI) offered an excellent opportunity to evaluate the Lane Guidance™ System with real world data. In fact, FOT objective number seven as outlined in the original Freightliner proposal, Field Operational Test of the Rollover Stability Advisor (RSA), (Request for Application No: DTFH61-99-X-00003) was "to test the lane tracker system's availability and the reliability of the lane tracker under all weather and road conditions." This was performed as Task 21 of the RA&C FOT and consisted of extracting and evaluating data collected by the Lane Guidance™ System. The goal of this evaluation was to understand the performance of the system under different environmental conditions such as rain, snow and night/daytime. Additionally, the data were used to identify characteristics for potential warning scenarios as well as lane change maneuvers in order to better understand the overall system capabilities and performance.

Data collected by the Praxair tractors from November 2000 to June 2001 relevant to the Lane Guidance™ system were analyzed. The results showed that the Lane Guidance™ system performed best when the driver was potentially at the least attentive:

- during the night and early morning hours,
- with cruise control engaged,
- at highway speeds,

- during dry conditions.

4.2 The Lane Guidance™ System

The Lane Guidance™ system is a safety system intended to prevent unexpected lane departures due to driver inattentiveness or driver drowsiness. The product was developed by DaimlerChrysler Research, Freightliner and Odetics and is an adaptation of the Lane Tracker™ system available in Europe (Bishel et al., 1998). The commercially available Lane Guidance™ system consists of a digital camera mounted near the top of the tractor's windshield, a central processing unit (CPU), two speakers located in the left and right side doors, a status lamp to inform the driver if the system is ready for warning and an on/off switch. The camera mounted on the inside of the windshield of the cab detects the road in front of the vehicle. By means of proprietary image processing algorithms, the lane markings are captured and extracted out of the video image. Based on this information, the position of the vehicle inside the lane is determined. The system continuously predicts the time reserve until the vehicle will leave the lane, referred to as the Time-to-Line-Crossing (TLC). If the predicted time reserve is less than a certain value, for example one second, the driver is warned by an acoustic signal that resembles a rumble-strip noise. The acoustic feedback is directional and is emitted only from the speaker on the side of the vehicle drift. The driver intuitively steers away from the rumble-strip noise and consequently repositions the vehicle in the center of the lane of travel. The system is shown in Figure 4-1 as well as an example of its forward view of the lane markings.



Figure 4-1: The Lane Guidance™ windshield mounted camera and additional CPU (both shown in corner) process forward viewing images of the lane markings to detect if the vehicle is drifting out of the lane of travel

The Lane Guidance™ system used during the RA&C FOT did not have any driver feedback capability, consequently making the system invisible to the drivers. The intention was to simply collect and analyze data produced by the system to better understand the performance of the Lane Guidance™ system in general. Therefore, no conclusions can be made on the impact of the system on driving behavior.

4.3 Data Structure

The analyzed data were collected during both Phase I and Phase II of the RA&C FOT by the six Praxair tractors starting in November 2000. A meaningful use of the tractors' data was possible beginning in February 2001. In the first three months of data collection, some tractors were seldom in operation, thus their data were not statistically valid.

Table 4-1: Lane Tracker Status Bits

Bit:	Description:	Significance:
0	Always 1	1
1	Always 1	2
2	Tracking Right/Warning Available	4
3	Warning on Right	8
4	Tracking Left/Warning Available	16
5	Warning on Left	32
6	System Disable Switch	64
7	Turnsignal active	128

The analysis mainly evaluated the tracker status byte sent from the Lane Guidance™ System. It was recorded every half second (2 Hz) when the tractor was in operation. The status byte was broken down into bits. The tracker status was the combination of the significance values of the bits that were currently active. For example if the system was tracking the right and the left lanes, the tracker status would be 23 (Significance of Bit 0+1+2+4). The status bits were described as shown in Table 4-1:

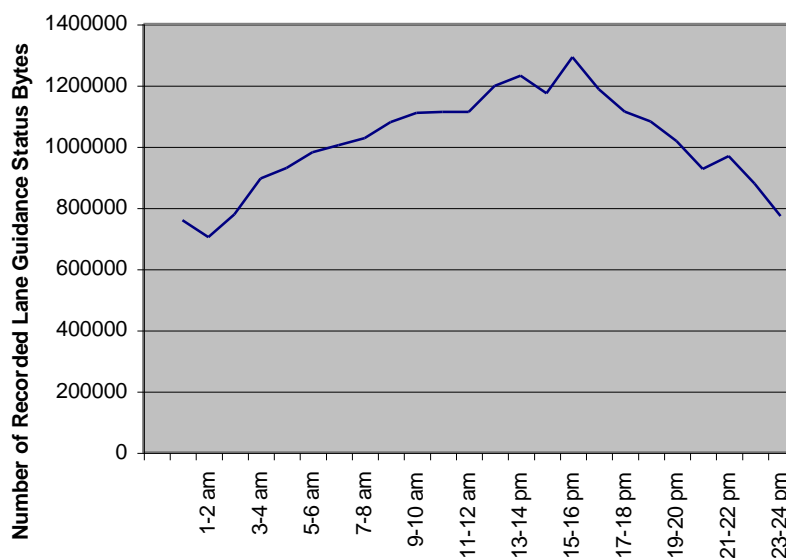


Figure 4-2: Total number of recorded status bytes on an hourly basis for all tractors from February 1, 2001 to May 18, 2001.

Every half-second, a Lane Guidance™ status byte was recorded when the tractors were in operation. This produced between 700,000 and 1,000,000 records an hour for all tractors combined. Figure 4-2 depicts the total number of Lane Guidance™ status byte records on an hourly basis from February 1, 2001 to May 18, 2001. The data illustrate that the tractors were driven more during the day than at night.

4.4 Performance Evaluation

4.4.1 Overall tracking performance

One of the main goals of this study was to quantify how often the Lane Guidance™ System tracked at least one lane during a day. Tracking performance is defined as identifying a lane through tracking at least one series of lane markings (ideally both) on either side of the vehicle and tracing them forward. Table 4-2 gives the percentage of records when tracking at least one lane on a monthly basis for each tractor. It shows that not all tractors were in operation from November 2000 until January 2001. Tractor 4 had a malfunctioning Lane Guidance™ system until March 2001, therefore its data were not evaluated. Taking the tracking performance of tractors 1, 2, 3 and 5 between February 1, 2001 and May 18, 2001, the overall tracking performance was 83.12%. This was calculated based on 17,244,474 tracking event records out of a total of 20,746,290 Lane Guidance™ status byte event records.

Table 4-2: Average Percentage of Tracking Performance per Day Reported on a Monthly Basis

	November 2000	December 2000	January 2001	February 2001	March 2001	April 2001	May 2001
Tractor 1	72.97%	45.31%	80.87%	84.71%	84.03%	83.65%	86.49%
Tractor 2	0.00%	76.31%	79.17%	81.48%	82.14%	84.77%	82.17%
Tractor 3	0.00%	76.93%	83.95%	84.11%	84.51%	82.43%	81.54%
Tractor 4	0.00%	0.00%	82.51%	56.74%	2.68%	84.38%	85.19%
Tractor 5	0.00%	0.00%	0.00%	80.36%	82.05%	82.72%	83.84%

4.4.2 Performance Dependent upon Daytime

Tracking performance was analyzed on an hourly basis because of different sunlight levels throughout the 24-hour day period. Figure 4-3 depicts the accumulated tracking events for tractors 1, 2, 3 and 5 on an hourly basis in February 2001. Figure 4-4 depicts the percentage of tracking performance for all four tractors on an hourly basis in February 2001. These figures together briefly illustrate that tractors were driven more during the day than at night and tracking performance was better at night. Again, tracking performance is defined as identifying a lane through tracking at least one series of lane markings (ideally both) on either side of the vehicle and tracing them forward.

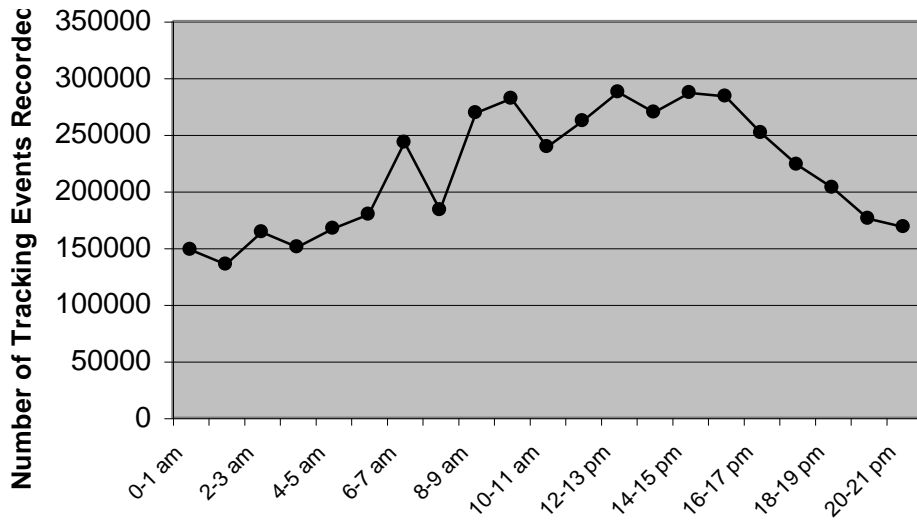


Figure 4-3: Total number of tracking events for all tractors on an hourly basis in February 2001

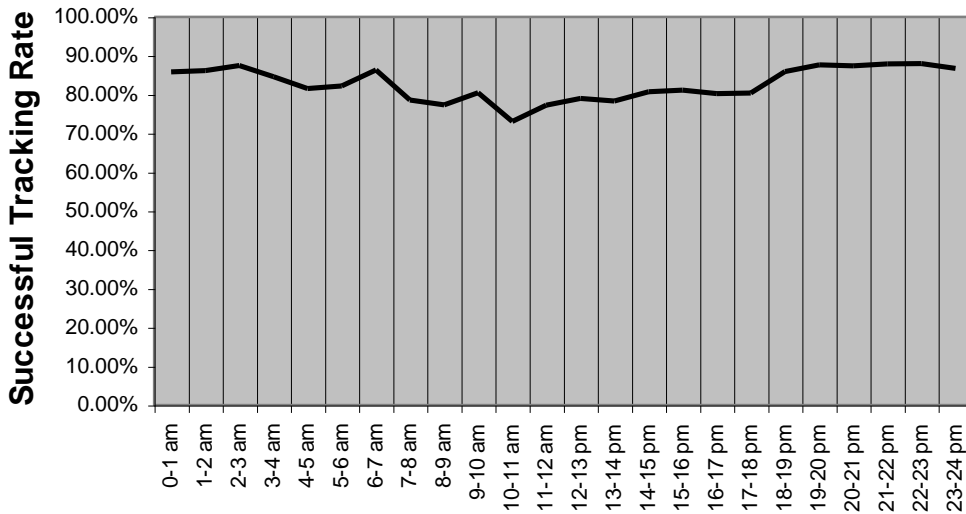


Figure 4-4: Daily average percentage of tracking for tractors 1, 2, 3 and 5 on an hourly basis in February 2001

Similar behavior was observed for the following months in 2001. Recalling from Figure 4-4, the tracking rate during the night is slightly better than during the day. The night period was defined from 10:00 pm to 5:00 am and the day period from 10:00 am to 5:00 pm. The transition times of morning and evening are not as easily defined because of the two different time zones in which the tractors were operated as well as the increasing duration of daylight from February 2001 to May 2001. The difference between night and day period is depicted in Figure 4-5.

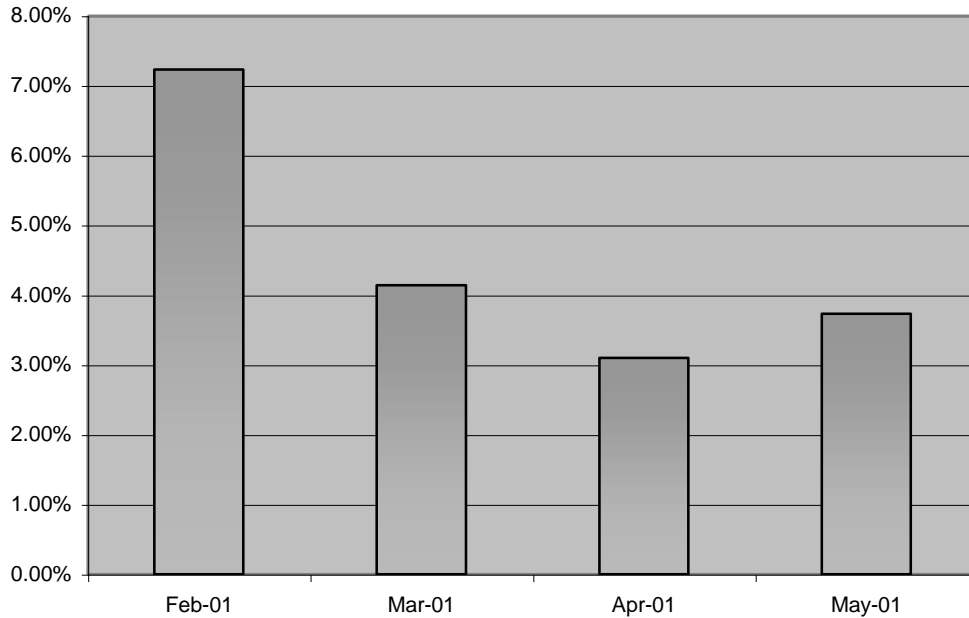


Figure 4-5: Monthly average percentage of improved tracking during night period compared to day period

Figure 4-5 shows that tracking improved as much as 7.23% during the night period compared to the day period. The average tracking improvement during the night period was 4.55%.

Figure 4-6 underlines the difference of night and day period in an absolute sense. It compares the tracking performance in February 2001 and May 2001 for all four studied tractors on an hourly basis. Figure 4-6 clearly shows tracking performance improved around 5:30 pm in February 2001. A similar performance jump was observed around 8:30 p.m. for the May 2001 data. This behavior is attributed to the longer daylight period in May and is consistent with the idea that tracking is better at night compared to tracking during the day.

There are two main reasons for this performance difference. First, during the day there was more traffic than during the night. The driver was forced to make more lane changes whereby losing the tracked lane. Additionally, shadow marks, light reflections and direct sunrays on the camera decrease tracking performance during daylight. At night, the contrast between dark road and white lane marking was significantly better, which led to an improved performance during the night. This is an important finding because the purpose of the Lane Guidance™ System is to warn inattentive drivers. A tired driver is more likely to be an inattentive driver than a driver steering the truck through heavy traffic.

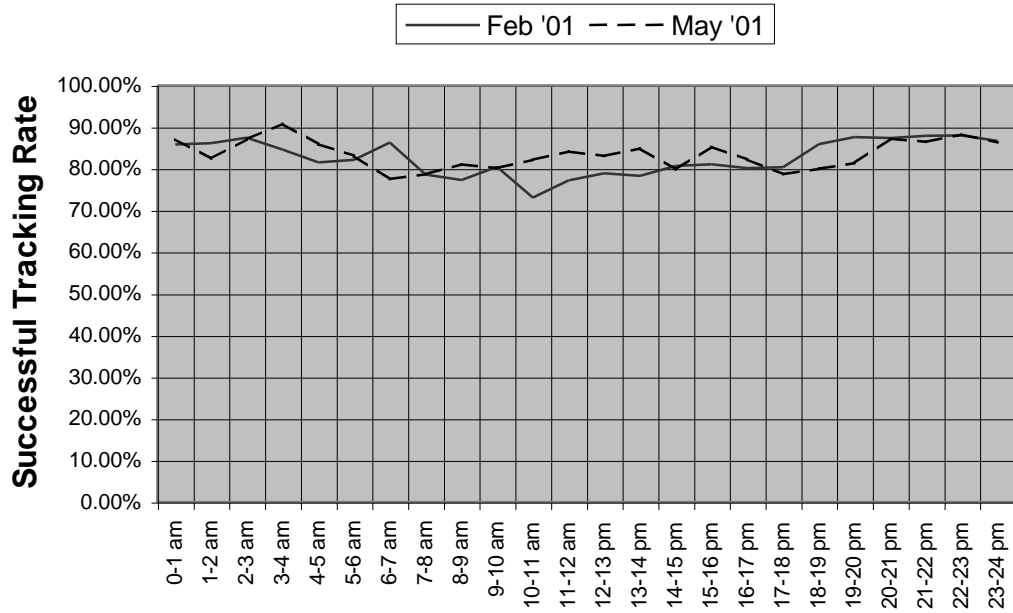


Figure 4-6: Comparison of daily average tracking performance on an hourly basis in February 2001 and May 2001

4.4.3 Performance dependent upon weather conditions

The overall and day/night performance analysis of the Lane Guidance™ System did not differentiate between different weather conditions. However it was expected that rain and snow would degrade the tracking performance. To quantify this hypothesis, four different weather scenarios were defined: dry, wet, slush and snow condition. Dry condition was defined as wipers being off and temperature being above zero degrees Celsius. Wet condition was defined as wipers being on and temperature also being above zero degrees Celsius. Different wiper intensities were not considered because the number of records at several interval steps was too few to be statistically valid. Slush condition was defined as wipers being on and temperature being between zero and minus two degrees Celsius. Snow condition was defined as wipers being on and temperature being below minus two degrees Celsius.

Although there were thousands of records every day, data combinations reflecting slush and snow conditions were rare. Only data sets for tractors 1 and 2 delivered sufficient records to reflect representative winter conditions.

Table 4-3 shows the percentage of tracking performance for tractors 1 and 2 as a function of the defined weather conditions. The data were recorded during the winter months from November 2000 to February 2001.

As hypothesized, the tracking performance depends on weather. It degraded significantly for slush and snow conditions. The minimal deterioration for the rain condition was caused by slight reduction in visibility. However snowfall impacts the visibility significantly more and consequently made it much more difficult to recognize the lane

markings. The extreme case being that the lane markings would be nearly invisible because they were covered with snow. This scenario would result in the image contrast between the road and the markings being too low for consistent recognition.

Table 4-3: Weather-Dependent Tracking Performance for Tractors 1 & 2

Weather Conditions	Tractor 1	Tractor 2
Dry condition	85.85%	84.36%
Wet conditions	82.33%	80.11%
Slush condition	70.40%	72.20%
Snow condition	66.11%	65.29%

4.4.4 Performance dependent upon vehicle speed

The Lane Guidance™ System is intended for class-8 vehicles operating at highway speeds. Therefore, quantifying the tracking performance as a function of vehicle speed is a very valuable and useful measurement of the system.

It was necessary to use the speed data from GPS for this evaluation. The GPS speed was recorded every half second just like the Lane Guidance™ status byte. The data set chosen for this evaluation was for tractor 1 from November 2000 to June 2001. The speed data were clustered in six speed bands. From these speed bands, typical urban and non-urban highway drives could be derived.

Table 4-4: Tracking Performance dependent upon Vehicle Speed in kilometers per hour (kph)

Ground Speed from GPS	Tracking Performance
<20 kph	21.43 %
Between 20 and 40 kph	67.92 %
Between 40 and 60 kph	77.48 %
Between 60 and 80 kph	87.18 %
Between 80 and 100 kph	96.29 %
>100 kph	88.43 %

Table 4-4 shows that the tracking performance is significantly better at high speeds compared to low speeds. The decrease in performance at speeds above 100 kph is attributed to recording errors in the FOT data acquisition system and not the Lane Guidance™ system. Speeds between 80 and 100 kph are typical for driving on highways. The result of 96.29% shows that the Lane Guidance™ System works extremely well in its main area of application.

4.4.5 Performance dependent upon cruise control state

The evaluation of tracking performance dependent upon speed did not take into account the usage of cruise control. Consequently, there was an interest in better understanding if there was a correlation between the usage of cruise control and the usage of the Lane Guidance™ System.

Prior to merging both data sets, the general usage of cruise control was analyzed. The question was how often did the Praxair drivers use cruise control and how was the usage distributed during the 24-hour day period. Because the cruise control state message came randomly, the 24-hour period was divided into eight, three-hour segments. The evaluation considered all tractors from November 2000 to June 2001. Because the combination of 2 Hz Lane Guidance™ status byte and randomly appearing cruise control state message were quite expensive, the merger was done for only tractor 1 over the same period of time.

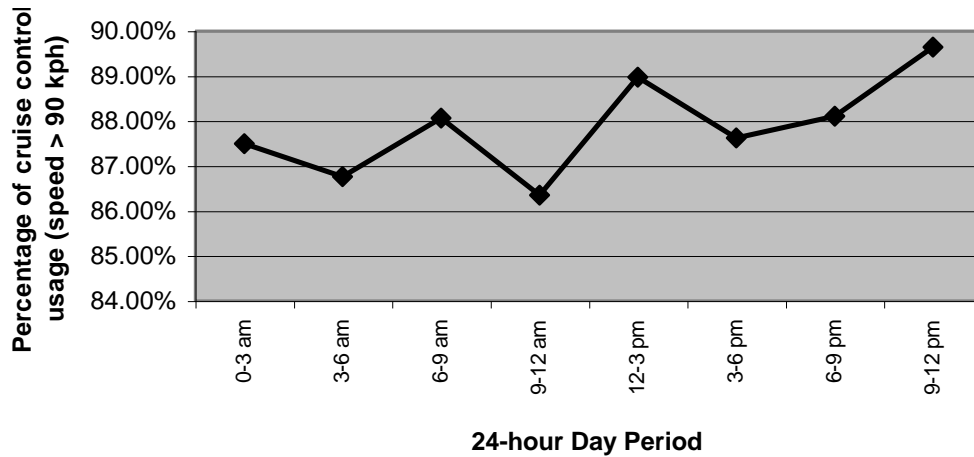


Figure 4-7: Average cruise control usage dependent upon 24-hour day period, only considering Tractor 1 Vehicle Speeds > 90 kph (November 2000 – June 2001)

Figure 4-7 shows that cruise control usage is very high when the vehicle is traveling at speeds above 90 kph. Cruise control use is nearly constant at an average value of 87.87% and consistently used throughout the entire day. Stated differently, the Praxair drivers used cruise control 87.87% of the time that the vehicle was traveling greater than 90 kph.

When driving with cruise control on, the tracking performance was much higher compared to driving without cruise control turned on. For example, the tracking performance of Tractor 1, when driving with cruise control on was 96.92% while it was only 66.26% when driving without cruise control engaged. This also reflects that the cruise control was used often when driving on highways. When it was turned off, it was very likely that the vehicle was driving on local roads or through towns. In these situations, the performance cannot be as high as on highways, because the lane markings tend not to be as consistent or as maintained as on highways.

4.4.6 Performance during lane change maneuvers

Earlier in this chapter, lane tracking was defined as identifying a lane through tracking at least one series of lane markings (ideally both) on either side of the vehicle and tracing them forward. However, there are situations in which the system should stop the forward tracing process and search for a new lane. One example is a typical lane change

maneuver. The characteristics of the maneuver and the ability of the system to find a new lane was investigated.

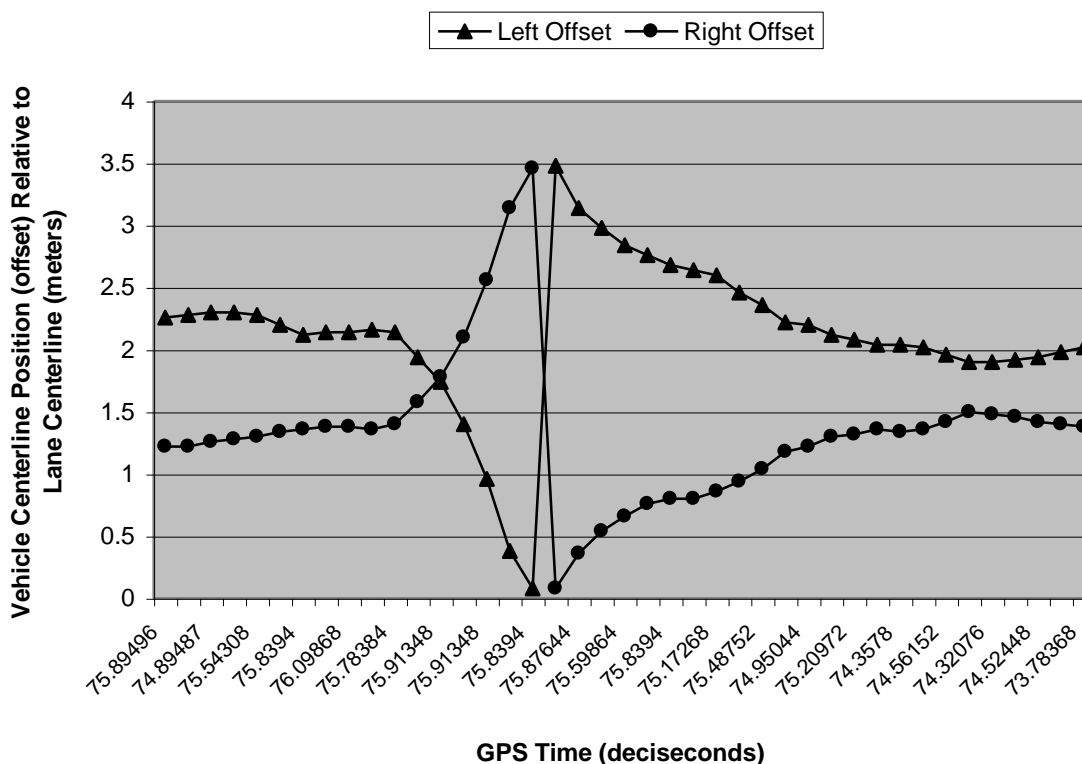


Figure 4-8: Typical Lane Change Maneuver Data History, Tractor 1, Trip 16

In addition to the Lane Guidance™ status byte, the data set also contained the left and right lane offsets measured from the middle of the vehicle. This was a special feature added to the Lane Guidance™ software specifically for the FOT investigation. The data were recorded every half second which was enough to capture and identify the lane change process even at high vehicle speeds. Figure 4-8 contains the data sequence for trip 16, tractor 1 which illustrates the data footprint associated with a typical lane change maneuver.

Figure 4-8 shows a typical data history for a lane change maneuver. The vehicle was traveling slightly to the right of the center of its lane. It then made a lane change to the left as indicated by the left offset decreasing to zero meters and the right offset increasing to approximately 3.5 meters. At that point, the system started to track the new lane markings as shown by the reversal in the left and right offset values. It should be noted that if the vehicle were in the exact middle of the lane, the left and right offset values would be identical in magnitude and located exactly on top of each other. The offset is measured in meters, whereas the horizontal axis is the GPS time measured in deciseconds.

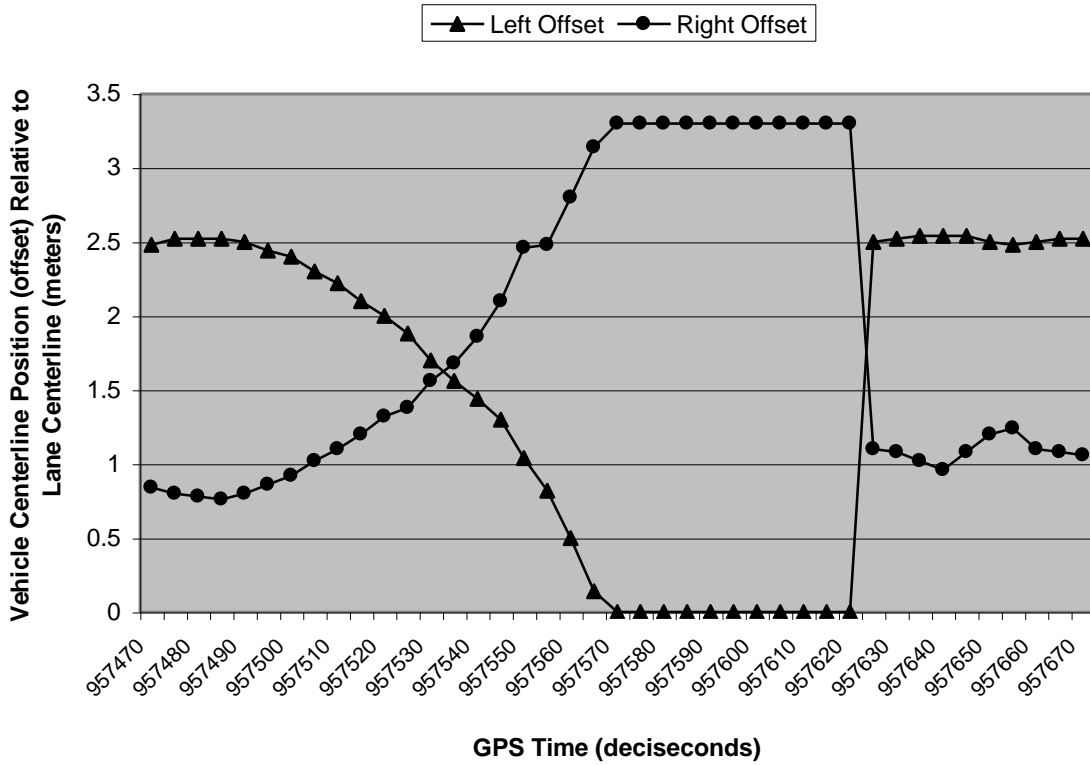


Figure 4-9: Lane Change Maneuver with detection delay, Tractor 1, Trip 552

Figure 4-9 shows a lane change maneuver where the Lane Guidance™ System did not detect the lane markings immediately after the lane change. The tracker status remained in the same state until the system once again started detecting the new right/left lane markings. The tractor was driving at approximately 87 kilometers per hour and made a change from the right to the left lane.

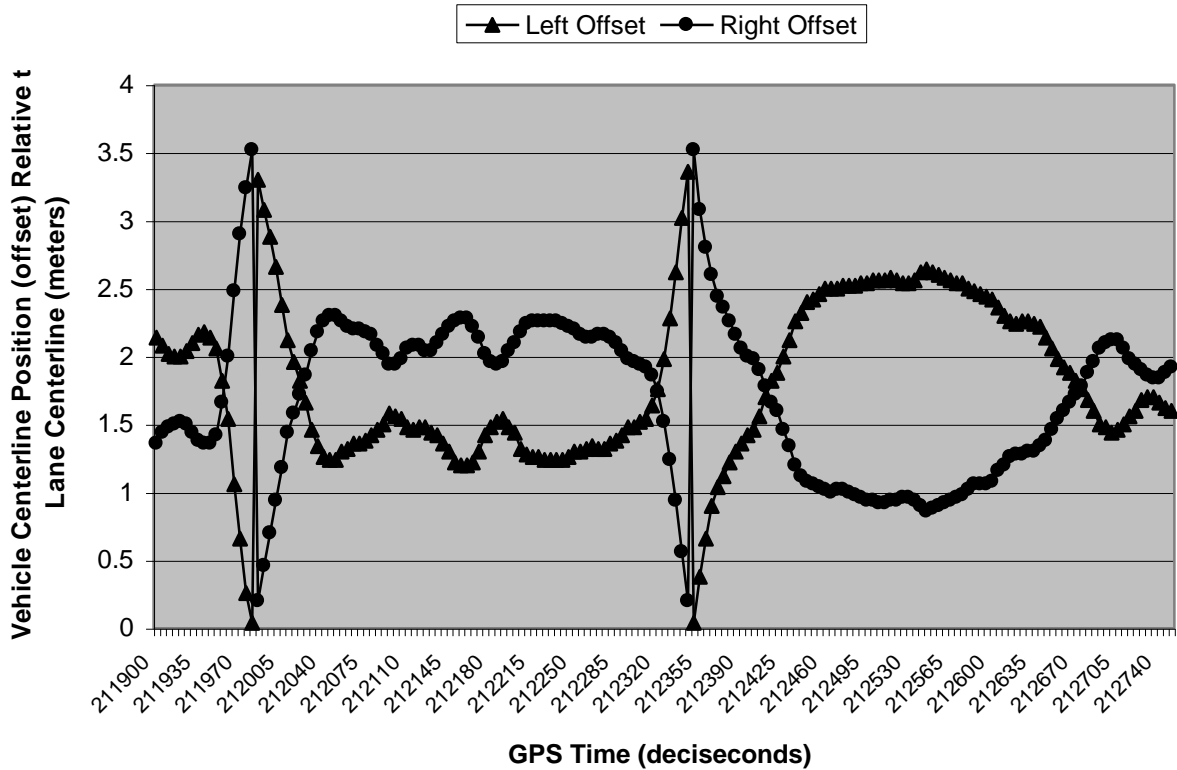


Figure 4-10: Double Lane Change Maneuver, Tractor 3, Trip 43

Figure 4-10 illustrates a tractor performing a double lane change maneuver, most likely to pass another vehicle on a highway, as the vehicle speed was approximately 95 kilometers per hour.

As the previous figures have shown, lane change maneuvers have a characteristic offset trace. Figure 4-8 and Figure 4-10 illustrate that the detection of the new lane was rapid. Bad lane markings however can delay the detection as highlighted in Figure 4-9.

Figure 4-11 is an excellent example of a typical potential lane departure scenario as opposed to a lane change maneuver. This type of maneuver is exactly the type of scenario that the Lane Guidance™ System is intended to identify and stop. During a 33 second interval, the vehicle drifts closer and closer to the right lane edge until the driver realizes it and steers the vehicle over to the left again, back toward the center of the lane. Recall that the system was simply collecting data and did not provide the driver with any feedback. Therefore, it is speculated that if the system had been fully functional and operational, the driver would have reacted earlier to the potentially dangerous lane departure situation.

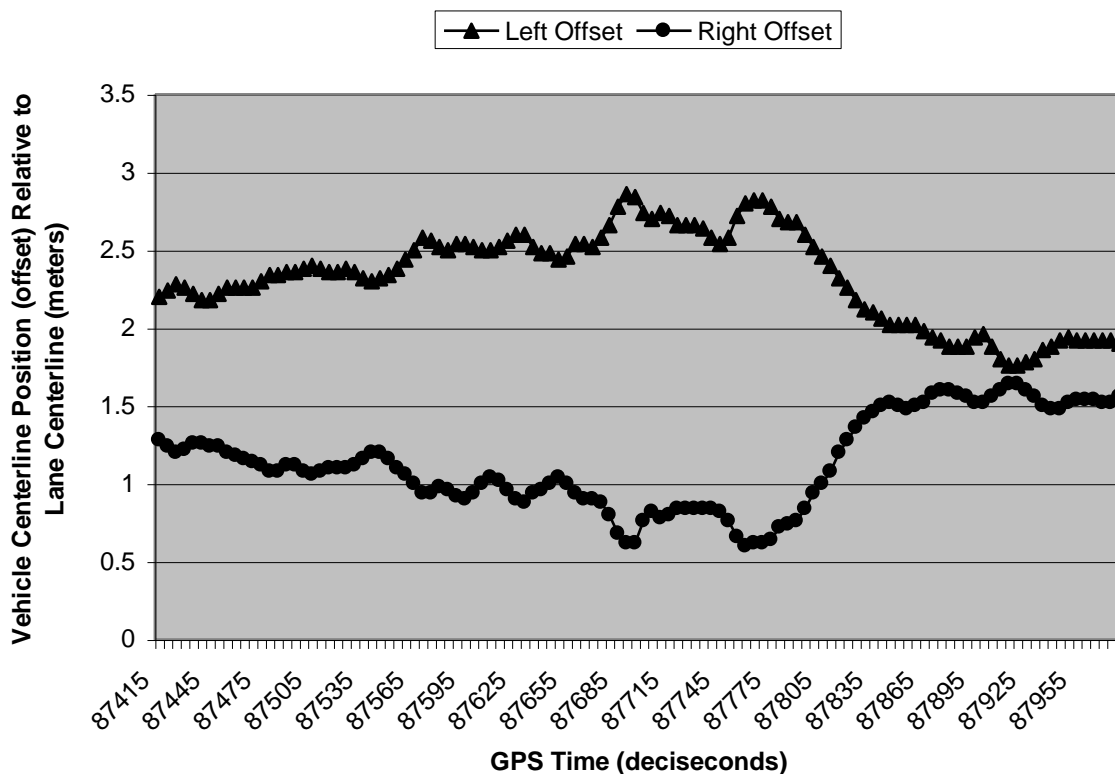


Figure 4-11: Typical Lane Departure Situation, Tractor 1, Trip 135

4.5 Warning Situations

The Lane Guidance™ System is a safety system. Its purpose is to warn inattentive drivers when their vehicle inadvertently or unexpectedly departs from the current lane as defined by the lane markings. A study has been performed to quantify how often potential lane departure situations occurred during the 24-hour day period. The six combinations of the Lane Guidance™ status byte listed in Table 4-5 describe a warning situation.

Table 4-5: Status Byte Combinations describing a Warning Situation

Tracking Left + Warning on Left
Tracking Right + Warning on Right
Tracking Right/Left + Warning on Left
Tracking Right/Left + Warning on Right
Warning on Left
Warning on Right

Figure 4-12 shows the daily average identified warning situations for all tractors, for each hour of the day from February 2001 to June 2001. The peak time for potential lane departures occurred between 4 am and 5 am with a maximum average of 66.9 dangerous situations. During the day, on average less than 30 critical situations took place. In general, the data show that lane departure scenarios were nearly twice as common at

night than during the day and over three times more common in the early morning hours compared to the day. It makes sense that drivers would be drowsier and less attentive at night and during the very early morning hours compared to the daytime. This difference highlights that the Lane Guidance™ system performed well when it was really needed, when the driver was potentially at the least attentive during the night and early morning.

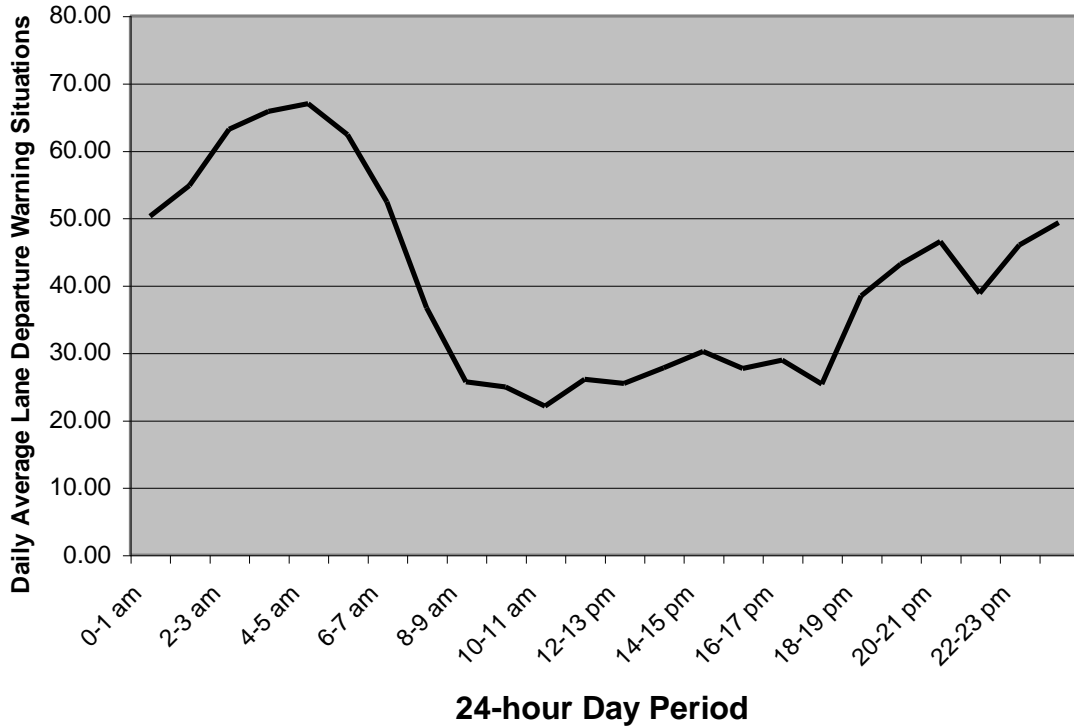


Figure 4-12: Daily average Warning Situations on an hourly basis, all tractors, from February 2001 to June 2001.

4.6 Summary and Conclusions

Task 21 of the FOT required the examination of the Lane Guidance™ System. This was achieved through analyzing the Lane Guidance™ status byte. This byte was recorded more than one million times on average, thus providing statistically valid data.

The general conclusion of the analysis regarding the performance of the Lane Guidance™ system is that the system performed best when the driver was potentially at the least attentive, during the night and early morning hours with cruise control engaged at highway speeds, during dry conditions.

The Lane Guidance™ System was evaluated based on:

- Overall Lane Tracking Performance
- Performance Dependent Upon Time of Day (Daylight)
- Performance Dependent Upon Weather Conditions
- Performance Dependent Upon Vehicle Speed

- Performance Dependent Upon Use of Cruise Control
- Performance During Lane Change Maneuvers
- Warning Situation Performance (no system feedback was made to the driver during the FOT)

The general characteristics of the system were:

- The system performed better at night than during the day
- The system performed better at highway speeds
- The system performed best during cruise control operation when the vehicle speed was greater than 90 kilometers per hour

General results of the analysis showed:

1. The average tracking performance of the Lane Guidance™ system was 83.12% of vehicle operation time.
2. Performance increased at night as much as 7.2% relative to day, with an average night increase of about 4.6%.
3. Weather conditions affected tracking performance:

Dry Condition (Wiper Off, Temp > 0°C)	~ 85%
Wet Condition (Wiper On, Temp > 0°C)	~ 81%
Slush Condition (Wiper On, 0°C > Temp > -2°C)	~ 71%
Slush Condition (Wiper On, Temp < -2°C)	~ 66%
4. Vehicle speed affected tracking performance:
 - Best tracking performance (96.3%) occurred for vehicle speeds in the range of 80 to 100 kph
 - Combination of all operating speeds greater than 60 kph yielded 87.2%
5. Cruise control tracking performance:
 - When vehicle was operating at speeds greater than 90 kph, the cruise control was engaged 87.9% of the time
 - When cruise control was engaged and the vehicle was traveling at speeds greater than 90 kph, the tracking performance was at its peak of 96.9%
6. Potential warning situations (no feedback to driver during FOT):
 - Based on a daily average, over two times more warning situations (potential lane departures) were identified at night compared to during the day and nearly three times more warning situations were identified in the very early morning hours compared to during the day

5 References

- Bishel, R., Coleman, J., Lorenz, R., Mehring, S., "Lane Departure Warning for CVO in the USA," SAE 982779, 1998.
- Ehlbeck, E., Kirn, C., Moellenhoff, J., Korn, A., Rosendahl, H., Ruhnau, G., "Freightliner/MeritorWABCO Roll Advisory and Control System," SAE 2000-01-3507, 2000.
- Evaluation of Prototype Automatic Truck Rollover Warning Systems (ATRWS)*, United States Department of Transportation, Federal Highway Administration, Publication No. FHWA-RD-97-124, January 1998.
- Field Operational Test of the Rollover Stability Advisor (RSA), Volume I – Technical, Staffing and Past/Performance Application*, Request for Application No: DTFH61-99-X-00003, submitted by Freightliner Corporation to the United States Department of Transportation as part of the Intelligent Vehicle Initiative, 1998.
- Gillespie, T.D., *Fundamentals of Vehicle Dynamics*, Society of Automotive Engineers, Warrendale, Pennsylvania, pp. 309-317, 1992.
- Rill, G., *Simulation von Kraftfahrzeugen*, Vieweg Verlag, Braunschweig, Wiesbaden, 1994.
- Sherman, M. and Myers, G., "Vehicle Dynamics Simulation for Handling Optimization of Heavy Trucks", SAE 2000-01-3437, 2000.
- TIFA - Trucks Involved in Fatal Accidents Facts, 1999*, Center for National Truck Statistics, University of Michigan Transportation Research Institute, 1999.
- Tseng, H.E., "Dynamic Estimation of Road Bank Angle," *Vehicle System Dynamics*, Vol. 36, No. 4-5, pp. 307-328, 2001.
- Winkler, C.B., Blower, D., Ervin, R.D., Chalasani, R.M., *Rollover of Heavy Commercial Vehicles*, Society of Automotive Engineers Research Report RR-004, Warrendale, Pennsylvania, p. 28, 2000.
- Wolfe, S., Phone conversation, Road Operations Engineering, Toll Road District, Indiana Department of Transportation, June 2002.

Volume III

VSTC Contribution to the RA&C FOT

Final Report: Field Operational Test for the Roll Stability Advisor and Control System



Appendix

September 25, 2002

Table of Contents

Appendix A Driver Questionnaire..... 1
Appendix B Message Summary and Specifications..... 3
Appendix C Driver’s Manual Insert Pages..... 5
Appendix D FOT Tractor and Semitrailer Characteristics 9
Appendix E Dynamic Rollover Simulation Results..... 10

Appendix A Driver Questionnaire

Name: _____
 Age: _____
 Years Driving with CDL _____

Date: _____
 Vehicle: _____
 Gross Vehicle Wt. Outbound: _____
 Gross Vehicle Wt. Return: _____

Directions: Please indicate the extent to which you agree or disagree with each of the following statements by putting an "X" in the appropriate box.

Statements	Strongly Agree	Agree	Neither Agree or Disagree	Disagree	Strongly Disagree
1. The messages were on the screen long enough to comfortably read them all.					
Comments:					
2. The advisories did not affect my ability to pay attention to the driving task .					
Comments:					
3. The advisories were easy to understand .					
Comments:					
4. The advisories were justified . If you disagree, please provide a detailed description of unjustified occurrences (THIS IS VERY IMPORTANT -Use back of page, if necessary).					
Comments:					
5. I was aware that the messages could be cleared and the tones stopped through use of the message center button labeled with the green diamond .					
Comments:					
6. The system will be valuable in helping drivers to improve their driving performance with regard to rollover risk and braking.					
Comments:					
7. I understood that the advisories were presented about dangerous maneuvers in the immediate past and not warnings about the truck's current situation .					
Comments:					
8. I found the system to be annoying .					
Comments:					

Summary Questions:

1. **Display Times** of the messages were: Too Short Just Right Too Long **(please circle one)**

comment: _____

2. For advisories accompanied by a tone, the **length of the tone** was: Too Short Just Right
Too Long **(please circle one)**

comment: _____

3. How many **different levels** of roll **advisories** do you remember seeing? 1 2 3 **(please circle one)**

comment: _____

4. The **speed reduction values** seemed: Too Low Accurate Too high **(please circle one)**

comment: _____

5. How do you feel about the current **number of levels**?

The **current** number is **optimal** _____

There should be **more** _____

There should be **fewer** _____

comment: _____

6. Did you **notice the printed label** which describes the **/A lamp**? Y N.

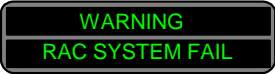










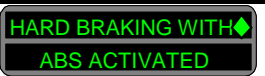
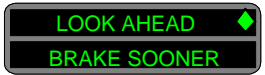
comment: _____

7. Did you refer to the **Driver's Manual Insert**? Y N




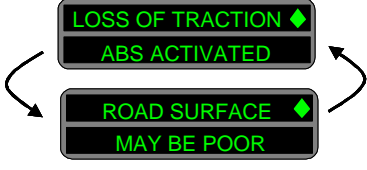


comment: _____

8. **Overall impressions** –

Appendix B Message Summary and Specifications

Message	Message to display	Data Bus Message	Display Time	Buzzer Time
System Fault		136 226 7 54 0 1 1 1 0 0	4 sec	1 sec
RSC		136 226 7 54 0 1 1 2 0 0	1 sec	None
RSA Level 3	  <p>or in metric</p> 	136 226 7 54 0 1 1 3 X 0 X = Speed in MPH	19.6 sec Duty cycle = 1.4s	10 sec
RSA Level 2	  <p>or in metric</p> 	136 226 7 54 0 1 1 4 X 0 X = Speed in MPH	14 sec Duty cycle = 1.4s	5 sec
RSA Level 1	  <p>or in metric</p> 	136 226 7 54 0 1 1 5 X 0 X = Speed in MPH	8.4 sec Duty cycle = 1.4s	0.5 sec
HBED Level 3	 	136 226 7 54 0 1 1 6 0 0	14 sec Duty cycle = 1.4s	0.5 sec

Volume III, Appendix B

Message	Message to display	Data Bus Message	Display Time	Buzzer Time
HBED Level 2	 <p>HARD BRAKING  DETECTED</p> <p>LOOK AHEAD  BRAKE SOONER</p>	136 226 7 54 0 1 1 7 0 0	14 sec Duty cycle = 1.4s	0.5 sec
HBED Level 1	 <p>LOSS OF TRACTION  ABS ACTIVATED</p> <p>ROAD SURFACE  MAY BE POOR</p>	136 226 7 54 0 1 1 8 0 0	14 sec Duty cycle = 1.4s	0.5 SEC

Appendix C Driver's Manual Insert Pages

Roll Advisor and Control System

Our new Freightliner trucks are equipped with an advanced technology driver information and vehicle control system named Roll Advisor and Control (RA&C).

RA&C provides 3 functions – Roll Stability Advisor, Roll Stability Control and Hard Braking Advisor.

Information from this system is provided to the driver via text messages displayed in the dash-mounted Driver Message Center, an audible tone and/or illumination of a dash indicator lamp.

The goal of this new system is to reduce accidents – especially rollover accidents – by assisting you, the driver, to identify high-

risk conditions and reduce vehicle speed appropriately.

The Roll Stability Advisor is an onboard rollover information and training system. It employs a lateral acceleration sensor that monitors rollover risk. Shortly after a curve, lane change or other driving maneuver that results in significant rollover risk, a driver advisory message is displayed in the Driver Message Center. The purpose of this message is to advise that the previous maneuver produced a significant rollover risk. It is important to understand that THIS IS NOT AN ADVANCE WARNING SYSTEM. The system only advises after the driving maneuver is completed.

Roll Advisor and Control System

The Roll Stability Control system automatically reduces engine power and/or applies the engine brake when the acceleration sensor detects that the vehicle is near rollover. The control can intervene even before an advisory message is displayed.

BUT PLEASE NOTE that some maneuvers can produce a rollover so rapidly that neither a driver nor the Roll Stability Control can stop the rollover from occurring. Roll Stability Control will not prevent every rollover and it is NOT a replacement for a driver's good judgment.

The Hard Braking Advisor is an onboard braking information and training system. It utilizes the information from the ABS wheel speed sensors to determine when braking is severe enough to produce lockup at one or more wheels on the tractor and/or very rapid vehicle deceleration. Occurrences of these messages may indicate that the braking behavior was too aggressive for the current road surface conditions. Shortly after either of these conditions occurs, an advisory message is displayed in the Driver Message Center. This system is not a replacement for a driver's good judgment. Sometimes it is necessary to brake hard.

Roll Advisor and Control System

Clearing Messages

An acknowledgement function has been added to the system to allow drivers to clear the screen (and tones, when present). When a green diamond symbol in the upper right corner of the display appears, this indicates that pressing the key with a diamond label will clear the screen and stop the tone. Pressing any key on the keypad should also accomplish this. If a key is not pressed, the message will self-extinguish.

Trip/Leg Totals

A count of Roll Stability and Hard Braking advisories is included with the TRIP and LEG information presented in the Driver Message Center. By pressing the TRIP or LEG keys on the Driver Message Center keypad **twice** you can see the number of these events that have occurred during a TRIP or LEG. Holding the set/reset button while viewing the screen resets the event counters. Again, the goal of the RA&C system is to assist you, the driver, to identify and avoid more of the “high risk” driving situations that can result in accidents.

Roll Advisor and Control System

Manual Insert

Appendix D FOT Tractor and Semitrailer Characteristics

Table D-1: FOT tractors.

FOT Truck	Praxair ID	OEM	Model	Serial #	Notes
1	5552	Freightliner	Century Class S/T	H59663	
2	5551	Freightliner	Century Class S/T	H59662	
3	5553	Freightliner	Century Class S/T	H75154	
4	5549	Freightliner	Century Class S/T	H59660	
5	5548	Freightliner	Century Class S/T	H59659	
6	5550	Freightliner	Century Class S/T	H59661	
7	5547	Freightliner	Century Class S/T	H59658	UMTRI test vehicle

Table D-2: FOT tanker semitrailers.

Praxair ID	OEM	Model	Serial #	Diameter	Straight Length	Tare Weight
				mm	mm	kg
L823	Process Engr.	-	N-04587/C	1955.8	10515.6	8845
L831	LOX Equipment Co.	8500	24075	1930.4	10668.0	6759
L861	LOX Equipment Co.	8500	25160	1930.4	10617.2	7031
L862	LOX Equipment Co.	8500	25161	1930.4	10617.2	7031
L863	LOX Equipment Co.	8500	25162	1930.4	10617.2	7031
L891	LOX Equipment Co.	8500	25168	1930.4	10617.2	6287

* inner pressure vessel

Appendix E Dynamic Rollover Simulation Results

Table E-1: Tractor 1 trip 930 (hotspot 1) dynamic rollover data.

Payload	S_{crit}	K_{crit}	V_{crit}	a_{y,crit,trac}	a_{y,crit,trail}	a_{y,crit,sens}
(%)	m	1/m	kph	g	g	g
0	399.6150	-0.0150	16.3400	-0.4099	-0.4039	-0.4300
10	450.8610	-0.0120	16.5660	-0.4494	-0.4221	-0.4733
20	450.4140	-0.0120	16.0750	-0.4023	-0.4058	-0.4339
30	446.6780	-0.0150	16.0050	-0.4129	-0.3892	-0.4389
40	448.6740	-0.0120	15.5180	-0.3823	-0.3767	-0.4153
50	449.6780	-0.0120	15.0240	-0.3542	-0.3587	-0.3925
60	444.7250	-0.0150	14.9520	-0.3688	-0.3392	-0.4018
70	444.9150	-0.0150	14.4550	-0.3455	-0.3220	-0.3838
80	445.5070	-0.0150	13.9640	-0.3211	-0.3063	-0.3654
90	446.3500	-0.0150	13.4760	-0.2934	-0.2896	-0.3423
100	447.2850	-0.0150	12.9880	-0.2664	-0.2716	-0.3194

Table E-2: Tractor 1 trip 953 (hotspot 1) dynamic rollover data.

Payload	S_{crit}	K_{crit}	V_{crit}	a_{y,crit,trac}	a_{y,crit,trail}	a_{y,crit,sens}
(%)	m	1/m	kph	g	g	g
0	219.4062	-0.0125	15.8364	-0.412	-0.406	-0.4425
10	247.8112	-0.0136	15.6221	-0.4873	-0.4156	-0.5002
20	247.9022	-0.0136	15.6144	-0.4838	-0.4141	-0.4986
30	223.7276	-0.0140	15.7021	-0.4052	-0.3948	-0.4357
40	312.1327	-0.0145	14.3865	-0.4255	-0.3879	-0.4543
50	223.7610	-0.0140	15.1847	-0.3727	-0.3682	-0.4112
60	204.2663	-0.0149	15.5911	-0.3852	-0.3384	-0.4199
70	203.3501	-0.0149	15.1275	-0.3670	-0.3181	-0.4048
80	203.6432	-0.0149	14.5991	-0.3424	-0.3030	-0.3857
90	203.5651	-0.0149	14.0741	-0.3175	-0.2854	-0.3655
100	204.4603	-0.0149	13.4919	-0.2910	-0.2673	-0.3435

Table E-3: Tractor 4 trip 897 (hotspot 1) dynamic rollover data.

Payload	S_{crit}	K_{crit}	V_{crit}	a_{y,crit,trac}	a_{y,crit,trail}	a_{y,crit,sens}
(%)	m	1/m	kph	g	g	g
0	371.4672	-0.0141	16.2823	-0.4155	-0.3943	-0.4229
10	525.0448	-0.0007	20.2720	0.4240	0.3946	0.4527
20	523.8260	-0.0007	20.0543	0.4234	0.3972	0.4563
30	416.3619	-0.0128	15.8536	-0.4084	-0.3889	-0.4325
40	418.9538	-0.0128	15.8356	-0.3858	-0.3939	-0.4218
50	413.2394	-0.0163	15.2914	-0.3840	-0.3561	-0.4116
60	414.3254	-0.0128	14.7999	-0.3658	-0.3406	-0.3981
70	414.5086	-0.0128	14.3034	-0.3418	-0.3224	-0.3791
80	415.5681	-0.0128	14.2805	-0.3360	-0.3238	-0.3816
90	417.4839	-0.0128	13.8046	-0.3007	-0.3090	-0.3552
100	411.3878	-0.0163	13.2603	-0.2905	-0.2728	-0.3392

Table E-4: Tractor 5 trip 862 (hotspot 1) dynamic rollover data.

Payload	S_{crit}	K_{crit}	V_{crit}	a_{y,crit,trac}	a_{y,crit,trail}	a_{y,crit,sens}
(%)	m	1/m	kph	g	g	g
0	507.2619	-0.0007	18.8265	0.4827	0.3477	0.5047
10	403.0325	-0.0128	16.1656	-0.4171	-0.4081	-0.4408
20	401.0134	-0.0128	16.0899	-0.4264	-0.3980	-0.4478
30	508.3549	-0.0007	18.6669	0.4465	0.3860	0.4812
40	401.4879	-0.0128	15.5389	-0.3957	-0.3741	-0.4228
50	403.0077	-0.0128	15.0551	-0.3641	-0.3603	-0.4001
60	404.9681	-0.0128	14.5855	-0.3234	-0.3451	-0.3681
70	406.0706	-0.0128	14.5634	-0.3137	-0.3441	-0.3650
80	399.7614	-0.0128	13.9671	-0.3262	-0.3067	-0.3675
90	401.0124	-0.0128	13.4853	-0.3026	-0.2908	-0.3488
100	402.3059	-0.0128	13.0076	-0.2751	-0.2738	-0.3276

Table E-5: Tractor 5 trip 917 (hotspot 1) dynamic rollover data.

Payload	S_{crit}	K_{crit}	V_{crit}	a_{y,crit,trac}	a_{y,crit,trail}	a_{y,crit,sens}
(%)	m	1/m	kph	g	g	g
0	391.8908	-0.0141	16.5735	-0.4045	-0.4149	-0.4342
10	398.0617	-0.0135	16.6905	-0.3922	-0.4324	-0.4197
20	395.9429	-0.0135	16.5628	-0.3924	-0.4297	-0.4294
30	392.5980	-0.0141	15.9893	-0.3791	-0.3977	-0.4112
40	393.8001	-0.0141	15.9603	-0.3718	-0.3964	-0.4084
50	388.2624	-0.0141	15.3347	-0.3626	-0.3627	-0.3984
60	389.4188	-0.0141	15.3152	-0.3581	-0.3633	-0.3998
70	385.0591	-0.0154	14.7307	-0.3407	-0.3272	-0.3799
80	385.6061	-0.0154	14.2502	-0.3159	-0.3068	-0.3577
90	389.4707	-0.0141	13.8469	-0.2974	-0.2935	-0.3430
100	389.2835	-0.0141	13.3542	-0.2777	-0.2745	-0.3276

Table E-6: Tractor 1 trip 878 (hotspot 2) dynamic rollover data.

Payload	S_{crit}	K_{crit}	V_{crit}	a_{y,crit,trac}	a_{y,crit,trail}	a_{y,crit,sens}
(%)	m	1/m	kph	g	g	g
0	425.6510	0.0001	20.2347	-0.4216	-0.4137	-0.4413
10	460.7252	-0.0000	20.4537	0.4487	0.3913	0.4764
20	455.5411	0.0002	20.7897	-0.4207	-0.4197	-0.4478
30	374.7358	-0.0108	18.8329	-0.3850	-0.4138	-0.4191
40	377.8321	-0.0108	18.5486	-0.3749	-0.3967	-0.4077
50	375.5853	-0.0108	18.0138	-0.3511	-0.3776	-0.3884
60	368.5734	-0.0110	17.3425	-0.3415	-0.3513	-0.3822
70	367.2418	-0.0110	16.8124	-0.3186	-0.3304	-0.3622
80	385.9186	-0.0096	16.7589	-0.3009	-0.3131	-0.3477
90	364.0697	-0.0110	16.0814	-0.2967	-0.2957	-0.3445
100	365.5044	-0.0110	15.5563	-0.2771	-0.2793	-0.3297

Table E-7: Tractor 1 trip 939 (hotspot 2) dynamic rollover data.

Payload	S_{crit}	K_{crit}	V_{crit}	a_{y,crit,trac}	a_{y,crit,trail}	a_{y,crit,sens}
(%)	m	1/m	kph	g	g	g
0	185.8644	0.0124	-8.1215	0.0913	-0.2867	0.1087
10	347.2368	-0.0106	18.9324	-0.3971	-0.4226	-0.4125
20	340.2150	-0.0109	18.8613	-0.4040	-0.4201	-0.4344
30	340.0552	-0.0109	18.3632	-0.3816	-0.3971	-0.4117
40	338.2580	-0.0109	18.3178	-0.3840	-0.3924	-0.4189
50	342.0694	-0.0109	17.8401	-0.3551	-0.3745	-0.3906
60	336.8577	-0.0109	17.2797	-0.3427	-0.3487	-0.3829
70	337.3012	-0.0109	17.1488	-0.3294	-0.3429	-0.3746
80	356.3269	-0.0079	16.6724	-0.2957	-0.3139	-0.3445
90	356.1255	-0.0079	16.3172	-0.2845	-0.2959	-0.3333
100	354.4191	-0.0079	15.8385	-0.2740	-0.2784	-0.3248

Table E-8: Tractor 5 trip 862 (hotspot 2) dynamic rollover data.

Payload	S_{crit}	K_{crit}	V_{crit}	a_{y,crit,trac}	a_{y,crit,trail}	a_{y,crit,sens}
(%)	m	1/m	Kph	G	g	g
0	139.9724	0.0015	11.8917	-0.4276	-0.3832	-0.4336
10	166.5458	0.0065	13.6583	0.4528	0.3678	0.4775
20	191.7524	0.0120	15.5476	-0.4558	-0.4156	-0.4695
30	198.6040	0.0150	16.5250	-0.4476	-0.4069	-0.4654
40	344.0201	-0.0109	18.3754	-0.3798	-0.3945	-0.4152
50	347.1791	-0.0109	17.9854	-0.3562	-0.3771	-0.3910
60	339.6746	-0.0112	17.3669	-0.3496	-0.3468	-0.3882
70	340.1306	-0.0111	16.8984	-0.3308	-0.3290	-0.3722
80	340.2751	-0.0111	16.4270	-0.3115	-0.3121	-0.3569
90	340.4631	-0.0111	15.9340	-0.2929	-0.2955	-0.3424
100	341.8575	-0.0111	15.4345	-0.2681	-0.2780	-0.3213

Table E-9: Tractor 5 trip 939 (hotspot 2) dynamic rollover data.

Payload	S_{crit}	K_{crit}	V_{crit}	a_{y,crit,trac}	a_{y,crit,trail}	a_{y,crit,sens}
(%)	m	1/m	kph	g	g	g
0	284.8190	0.0130	16.1798	0.3875	0.3590	0.4106
10	520.2454	-0.0003	22.0719	0.4416	0.4027	0.4687
20	426.1734	-0.0108	19.0843	-0.3880	-0.4136	-0.4102
30	421.4962	-0.0108	18.9484	-0.3926	-0.4142	-0.4239
40	420.4013	-0.0108	18.4889	-0.3753	-0.3966	-0.4098
50	420.9204	-0.0108	18.0711	-0.3556	-0.3789	-0.3919
60	414.5385	-0.0111	17.4464	-0.3463	-0.3507	-0.3856
70	415.0526	-0.0111	16.9802	-0.3286	-0.3325	-0.3705
80	413.8258	-0.0111	16.7585	-0.3225	-0.3253	-0.3707
90	415.7455	-0.0111	15.9478	-0.2857	-0.2958	-0.3345
100	413.3640	-0.0111	15.4715	-0.2743	-0.2774	-0.3269

Table E-10: Tractor 5 trip 982 (hotspot 2) dynamic rollover data.

Payload	S_{crit}	K_{crit}	V_{crit}	a_{y,crit,trac}	a_{y,crit,trail}	a_{y,crit,sens}
(%)	m	1/m	kph	g	g	g
0	234.2570	0.0122	16.3180	0.3718	0.3701	0.4011
10	365.5141	-0.0110	19.0663	-0.4061	-0.4271	-0.4304
20	362.4538	-0.0110	19.0303	-0.4144	-0.4205	-0.4432
30	361.1919	-0.0110	18.5553	-0.3951	-0.3986	-0.4257
40	363.6537	-0.0110	18.1422	-0.3695	-0.3836	-0.4015
50	365.0464	-0.0110	17.7206	-0.3489	-0.3646	-0.3827
60	361.7822	-0.0110	17.6717	-0.3542	-0.3610	-0.3944
70	363.2787	-0.0110	17.2440	-0.3336	-0.3446	-0.3768
80	363.3319	-0.0110	16.7588	-0.3147	-0.3260	-0.3618
90	358.4178	-0.0110	16.1340	-0.3025	-0.2994	-0.3520
100	358.0715	-0.0113	15.5495	-0.2796	-0.2772	-0.3318